Electrical and structural properties of 8 and 12 hole % yttria stabilized zirconia

J.S. Ross

ELECTRICAL AND STRUCTURAL PROPERTIES

of

8 AND 12 MOLE % YTTRIA STABILIZED ZIRCONIA

by

J.S. ROSS B.Sc.

Presented in candidature for the degree of

Doctor of Philosophy

in the University of Durham

September 1973

ACKNOWLEDGEMENTS

Scientific research is largely teamwork; so it is right that mention be made of some of the other people (and groups) who contributed, directly and indirectly, to the work described in this thesis. I therefore take this opportunity of thanking the following :

The Science Research Council, for the award of a research studentship.

Dr. J.S. Thorp, my Supervisor, for taking an interest in everything from reading dials to writing papers (and a thesis) and above all for his good psychology.

Professor D.A. Wright for holding the department together so that there were departmental facilities to use.

Dr. Abidin Ayper for three years of comradeship and very lively (and useful) scientific debate.

Mr. Frank Spence and his skilled team of technicians principally :

Mr. Ron Waites, who constructed much of the apparatus,

Mr. Colin Savage, because of whom apparatus was where it should be, and working, and Mr. Trevor Harcourt, for cutting and polishing many crystals.

Dr. Ted Nice and Dr. Geof Sturgess, for introducing me to the mysteries of electron spin resonance.

Mr. Mike Farley, for instruction on the ways of ultrasonics.

Many other members of the department, and a few from other departments, who have performed numerous acts of assistance, both remembered and forgotten.

And finally, family and friends who have kept me sane (?) while this work was done.

I must add Mrs. Carol Courts who typed this page quickly before I had time to correct the omission.

Stuart Ross

September 1973

ABSTRACT

Single crystals of 8 and 12 mole % yttria stabilized zirconia (YSZ) have been studied to elucidate the relationship between the presence of point defects in the material and its electrical and mechanical properties, in particular its tendancy to blacken and disintegrate on carrying an electrical current. The thesis introduces the material and its uses and describes how the presence of point defects is explained. X-ray and density measurements confirmed that most of the defects are oxygen vacancies but suggested that cation interstitials are also present. It was found that the crystals turned white due to cracking on heat treatment but did so more rapidly in an oxygen atmosphere than in an argon atmosphere. Up to three types of electron spin resonance line were observed at 35 GHz depending on how the samples had been treated. One of these (for which $g_{//} = 2.003$ and $g_{\perp} = 1.880$) was attributed to an electron trapped in an oxygen vacancy which was associated with a yttrium ion. This complex (minus the electron) had been used to explain the temperature dependence of the conductivity of polycrystalline YSZ. Measurements of the conductivity of single crystal 8 mole % YSZ gave an oxygen vacancy activation energy of 1.2×10^{-19} J and a complex association energy of 1.9×10^{-19} J which were similar to published values for polycrystalline material, but maintaining the sample as a single crystal was found to be difficult. Blackening by current passage was compared in the two compositions, but no difference was observed. Ultrasonic measurements confirmed that blackening was not associated with a phase change. Preliminary relative permittivity measurements gave a value of 32.

CONTENTS

"A WORK OF ART IS NEVER FINISHED, MERELY ABANDONED"

Anon.

A general principle ?

Chapter 1.

Introduction

1.1 The material and its uses.

Yttria stabilized zirconia, (YSZ), is zirconium oxide, (ZrO_2), stabilised in its cubic form by the addition of yttrium oxide, (Y_2O_3). At high temperatures the material is an electrical conductor and this property, coupled with its high melting point and high resistance to chemical attack, makes it a potentially suitable material for high temperature electrodes. In practice however there are shortcomings and the particular difficulties involved in its use for electrodes in magneto-hydrodynamic generators led to the initiation of the present study. Yttria stabilised zirconia is also interesting for other reasons stemming from its wide industrial use as a refractory material. Among these may be mentioned

(a) Refractory textiles which maintain fibrous form at temperatures as high as 2770 K; typical applications listed by the manufacturer include separators and matrices for high temperature fuel cells, insulation space forming, reinforcement of ablative materials, ultra-high temperature filtration, catalyst support and diffusion of combusting gases.

(b) Non-reactive saggers for use in ceramic firing kilns (including those breeding YIG for microwave filters and control).

(c) Nozzles and covers for the tundishes in which molten steel is teemed and from which it is metered in the continuous casting of slabs and billets.

(d) Casting mould linings which will not wet with molten metal and therefore provide free stripping and parting.

(e) Heat storage elements capable of extended mass-flow service to heat gases for simulating jet engine conditions.

(f) Protection tubes for thermocouples and sensors in high-heat zones of kilns or furnaces and muffles for firing systems.

(g) Heat resistant coatings to give protection from erosion by hot gases; the coatings are sprayed by oxy-acetylene flame or plasma jet on, for example, rocket nozzles, combustion chambers, valves, piston heads and other engine parts.

(h) Dissociation cells in which YSZ serves as the electrolyte at 1270 K making for example hydrogen more efficiently from steam or, in nitrogen fixation chambers, to turn atmospheric nitrogen to nitrates.

(i) Burners for either internal or surface supported gas-air combustion and electrical resistance heating elements for laboratory furnaces.

Consequently, it was hoped that a further study of the properties of yttria stabilised zirconia, especially in single crystal form, would provide further understanding of the physical processes on which the applications were based.

1.2 Stabilization

The pure oxide, which occurs naturally as the mineral Baddeleyite (ZrO_2), possesses most of the refractory properties required for these applications. Its melting point is 3000 K, M. Foex, 1967, (1). However it suffers from the major disadvantage of being polymorphic. At room temperature it is monoclinic, Smith and Newkirk, 1965, (2); it becomes tetragonal at about 1400 K - the transformation occurs at about 1200 K on cooling - Duvez, Brown and Odell, 1951, (3) and finally cubic at 2600 K, (1). If the solid is cycled between its monoclinic and tetragonal forms it breaks up. The cubic structure can be stabilised down to room temperature

by the addition of more than 7 mole percent of yttrium oxide, (3). Not only is the stabilised material resistant to damage by temperature cycling but also its electrical conductivity is greater than that of the pure oxide. It is found that the conductivity changes with composition and is highest for just-stabilised compositions, Strickler and Carlson, 1964, (4). This information was used when choosing the compositions for the present study. Zirconia may be stabilised in its cubic form by the addition of oxides other than yttria. Oxides of calcium, magnesium, cerium, dysprosium, lanthanum, neodymium, samarium, europium and ytterbium have been used for this purpose, Kohler and Glushkova, (5). In industrial applications calcia and sometimes magnesia are often used for cheapness but these stabilising agents have the disadvantage that they evaporate slowly at high temperatures limiting the lifetime of the material. YSZ is more stable in this respect. It has been stated, Meadowcroft, 1969, (6), that the price of yttria stabilised zirconia was about £20 per kilogramme whereas calcia stabilised zirconia cost only about £1 per kilogramme.

1.3 Oxygen vacancies

Yttria stabilised zirconia has basically a fluorite structure but does not have the required ratio of the number of cations to the number of anions of 1 : 2. Hence it contains defects. Of these, the oxygen vacancies are of particular interest because it is on them that the electrical conductivity depends; it also seems likely that they have an important part to play in the blackening and disintegration of the material resulting from the passage of electric current. (The existence of oxygen vacancies has been generally accepted since it was proposed by Wagner (7) in 1943). Consequently, relationships between lattice parameter and density are derived in Chapter 2, using three models for the defect structure of

YSZ. Density and lattice parameter measurements were made, as discussed in Chapter 3 in order to make estimations of the vacancy concentrations after various treatments. The occurrence of vacancies in the material also suggested that, if unpaired electrons were trapped in vacancies during electrolysis, useful information might be obtainable from electron spin resonance studies; this proved to be the case and the results are reported in Chapter 4.

1.4 Choice of material and preparation of samples

Since most of the previously reported work on yttria stabilised zirconia had been performed on polycrystalline material, and since in particular complementary electrical conductivity studies on polycrystalline M.H.D. electrodes were being made at this time by Casselton at I.R.D. Newcastle, it was decided to concentrate on the study of single crystal material. This choice had additional advantages in that, from the conductivity point of view, the effects of grain boundaries were avoided and, from the e.s.r. viewpoint, very much more information could be obtained than would have been possible from powders.

It would appear that if M.H.D. electrodes were to be made from YSZ, a low yttria composition - containing just more yttria than the minimum required for stabilisation - should be selected in order to give high conductivity. For these reasons the composition $(Y_2O_3)_{0.083}\cdot(ZrO_2)_{0.917}$ was selected. The properties of this composition were compared with those of one containing more yttria, $(Y_2O_3)_{0.12}\cdot(ZrO_2)_{0.88}$. Single crystals, made by electrofusing mixtures of the pure powdered oxides were obtained from W. & C. Spicer Ltd.. (The purity of the zirconium oxide and resulting crystals used in this manufacturing process had previously been checked by Heffelfinger, Blosser and Henry, 1964, (8)). The single crystals had to

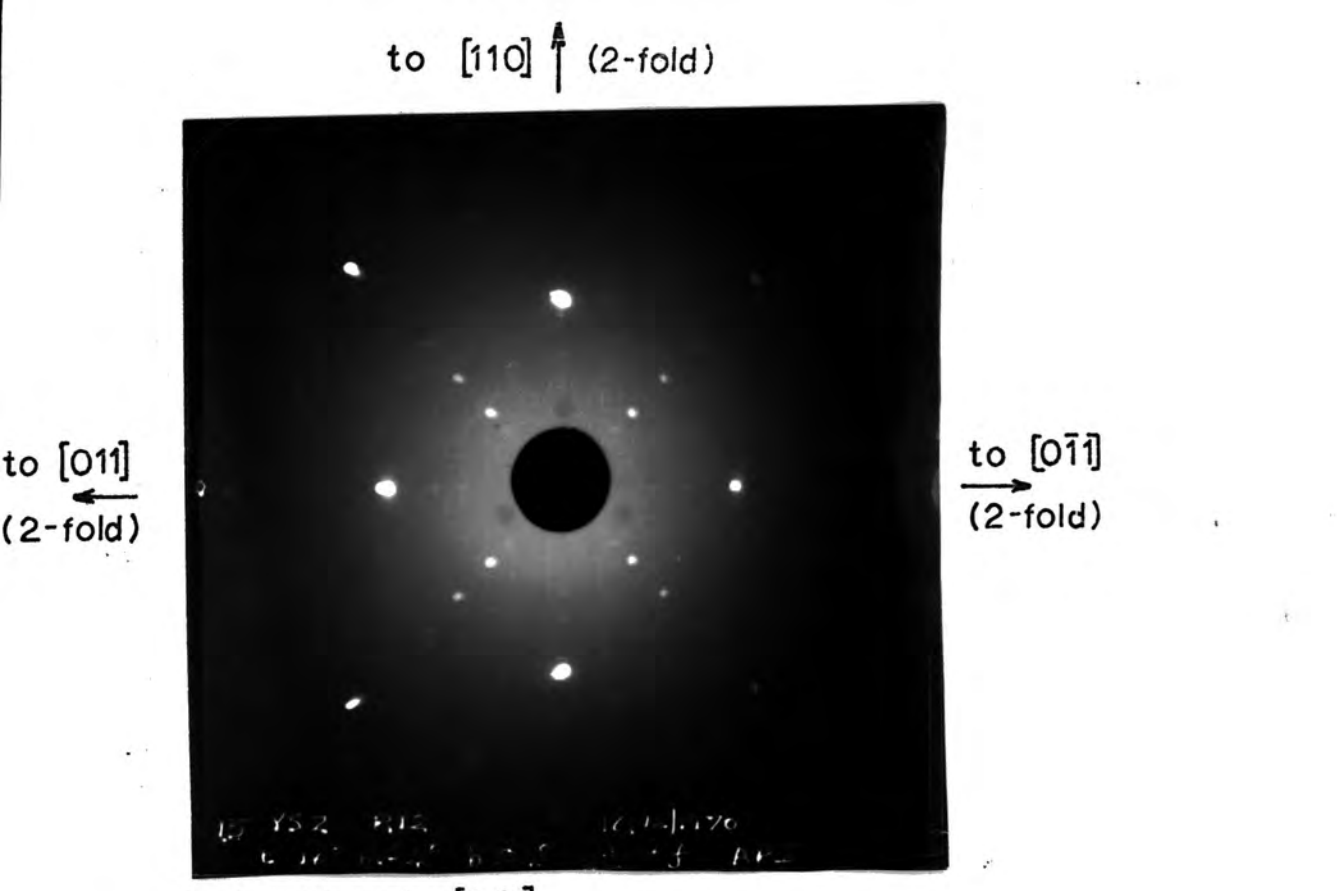

a) 4-fold axis : [001]

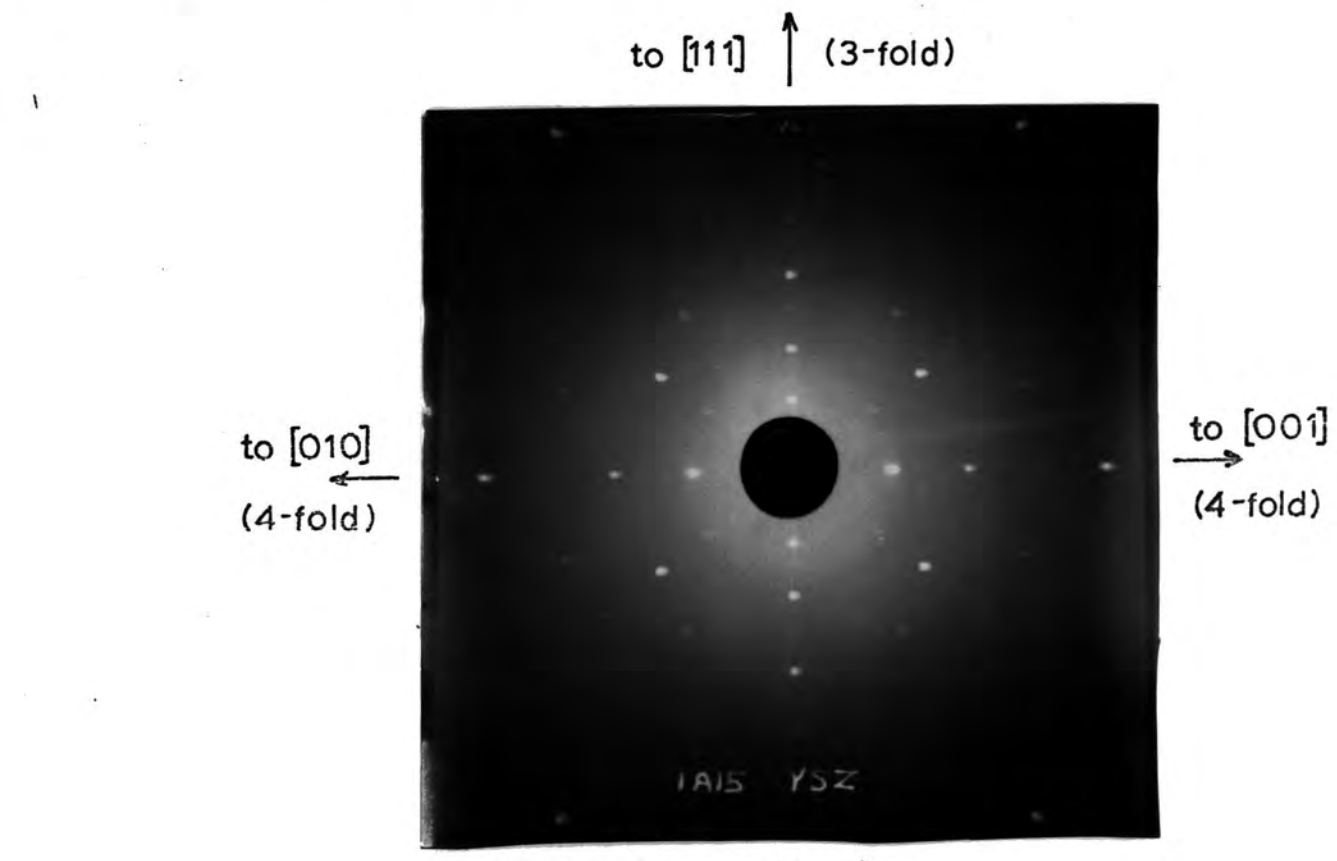

b) 2-fold axis : [01$\bar{1}$]

FIGURE 1.1

X-RAY BACK REFLECTION PHOTOGRAPHS OF SINGLE CRYSTAL YTTRIA STABILIZED ZIRCONIA. (100) PLANE HORIZONTAL.

be chipped or cut out of the solidified melt but many were of quite large size, e.g. 2 cm x 1 cm x 1 cm. They were found to vary considerably in appearance ranging from transparent amber to an almost opaque black. Crystal orientations were determined by X-ray back-reflection methods, (see Figure 1.1); the general absence of evidence of partial Debye-Sherrer rings and in particular the clear shapes of the individual diffraction spots indicated that the single crystals were of fairly high perfection. The crystals were robust and hard and were cut into the shapes required for specimens using diamond wheels without difficulties due to fragmentation or cracking. The visual effects of heat treatment in argon, air and oxygen were investigated, Section 3.2.

1.5 Electrolysis and Current Blackening

If a large enough electric current is passed through a YSZ specimen it turns black, loses its mechanical strength and tends to disintegrate. It is perhaps not surprising that the passage of current should have some effect because the charge carriers are oxygen ions which are removed from the solid (to form gas) at the anode, (for further details see Section 6.2). Unless oxygen ions are produced at the cathode at the same rate their removal must result in a shortage of oxygen ions around the cathode. This would act in a similar way to an excess of metal ions and could lead to the formation of metallic particles.

For the present study current blackened samples were prepared by passing direct current through as-received material in an argon atmosphere at 1070 K using platinum paste contacts to the platinum electrodes. This temperature was low enough to be reached easily with a conventional laboratory furnace yet high enough to make the material sufficiently conducting. Usually the samples were quenched simply by withdrawing the sample holder from the furnace. Further experimental details are given

in section 7.3 but it is worth emphasising here that sample preparation, especially of current blackened material, was by no means straightforward. Apart from the every present risk of fragmentation the current blackening procedure also resulted in the formation of conducting surface layers whose removal had to be ensured before meaningful measurements could be made. The difficulties attendent on the production of sufficiently thin current blackened crystal slices also prevented, during the course of this work, any attempt to examine structural changes by transmission electron microscopy.

1.6 Complementary Work

At the commencement of this research very little was known about the properties of single crystal yttria stabilised zirconia. As already mentioned a programme of electrical conductivity measurements on polycrystalline material had been initiated at I.R.D. Co. Ltd. However, as regards single crystal material, it was simply known from previous Departmental work that after high temperature electrolysis in argon, (a) very heavy optical absorption was observed in the visible, (b) there was a marked tendency for the crystals to disintegrate and (c) that electron spin resonance signals were observable. Consequently two complementary programmes of work were initiated. In the first of these, undertaken by A. Aypar, emphasis was placed on the use of electron spin resonance and of optical methods, primarily optical absorption spectroscopy, to examine the nature of single crystal YSZ with particular reference to current blackened samples; in the course of this work it soon became clear that knowledge of lattice parameters would be desirable and this aspect was included. In the second programme, which is described in this thesis, attention was concentrated on the implications of the defect nature of the material, on the mechanisms of

electrical conductivity and on the structural changes resulting from electrolysis. In view of the close relationship between the two programmes and because of an independent study of the elastic properties of yttria stabilised zirconia made in the Department by members of the Ultrasonics Research Group two sections of the work described were undertaken jointly; these were the electron spin resonance studies (made with A. Aypar) and the ultrasonic studies (made with J.M. Farley).

It may perhaps be mentioned that subsequently a considerable amount of further work on electrolysed yttria stabilised zirconia has been carried out in the Department by H.P. Buckley; this has involved a more detailed appraisal of the optical properties (9) and a study of the dielectric behaviour of the material (10).

Chapter 2.

Structure and Defects

2.1 Phase Diagrams

A phase diagram for the yttria-zirconia system is shown in Figure 2.1. This is basically similar to that (Figure 2.2 a) suggested by Duvez, Brown and Odell (3), but has been modified slightly to take account of more recent measurements. Duvez et al. held samples of the compositions indicated at 2270 K for between two and six hours or at 1650 K for 336 hours and then quenched them. X-ray analysis revealed the presence of the phases shown. In each case the main component is named on the diagram, e.g. "ZrO_2 cubic solid solution" is a single phase solid solution with a cubic structure consisting of a large amount of zirconia (ZrO_2) and a small amount of yttria (Y_2O_3). This solid solution is yttria stabilised zirconia and it was found to have the fluorite (CaF_2) crystal structure.

Thermal expansion measurements were also made. Samples with a low yttria content underwent a sudden contraction at a particular temperature as the temperature rose and a sudden expansion as it fell. This was attributed to a phase change and it was concluded in these cases that the monoclinic phase observed in the quenched samples did not correspond to the temperature before quenching. The phase boundaries marked with short dashes (- - -) were fitted between the experimental points. The phase boundaries marked with long dashes (— —) were tentatively filled in on the basis of the existence of a two-phase region and the lack of any intermediate compounds.

From cooling curves M. Foex (1) found, in agreement with other workers, that pure zirconium oxide had a melting point of 3000 K and that at 2600 K it changed phase. These temperatures are well above the mono-

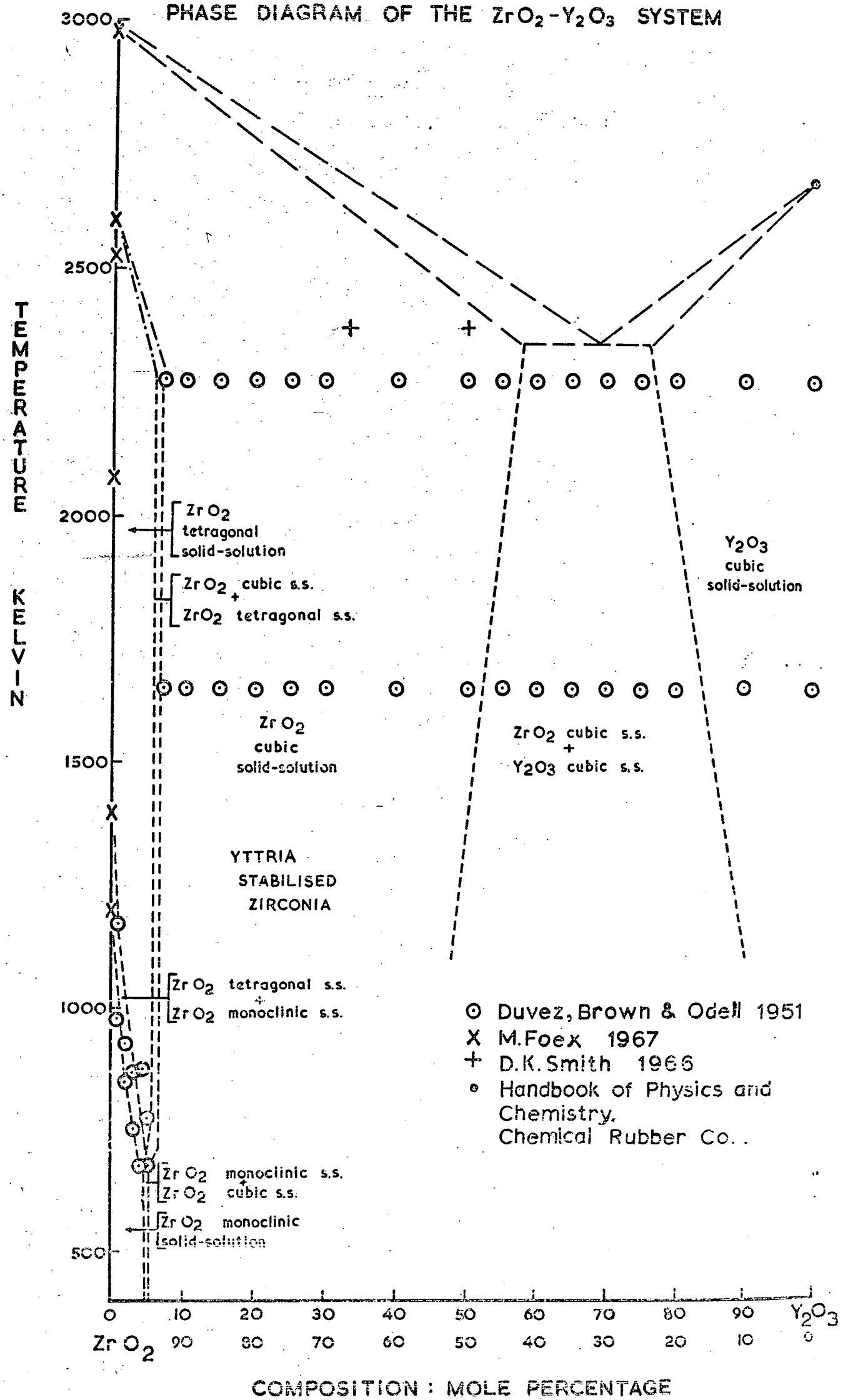
PHASE DIAGRAM OF THE ZrO_2-Y_2O_3 SYSTEM
TEMPERATURE KELVIN
3000
2500
2000
1500
1000
500
ZrO_2 tetragonal solid-solution
ZrO_2 cubic s.s. + ZrO_2 tetragonal s.s.
ZrO_2 cubic solid-solution
Y_2O_3 cubic solid-solution
ZrO_2 cubic s.s. + Y_2O_3 cubic s.s.
YTTRIA STABILISED ZIRCONIA
ZrO_2 tetragonal s.s. + ZrO_2 monoclinic s.s.
ZrO_2 monoclinic s.s. + ZrO_2 cubic s.s.
ZrO_2 monoclinic solid-solution
⊙ Duvez, Brown & Odell 1951
X M.Foex 1967
+ D.K.Smith 1966
• Handbook of Physics and Chemistry. Chemical Rubber Co..
0 10 20 30 40 50 60 70 80 90 Y_2O_3
ZrO_2 90 80 70 60 50 40 30 20 10 0
COMPOSITION : MOLE PERCENTAGE

FIGURE 2·1

PUBLISHED PHASE DIAGRAMS OF THE ZrO_2-Y_2O_3 SYSTEM

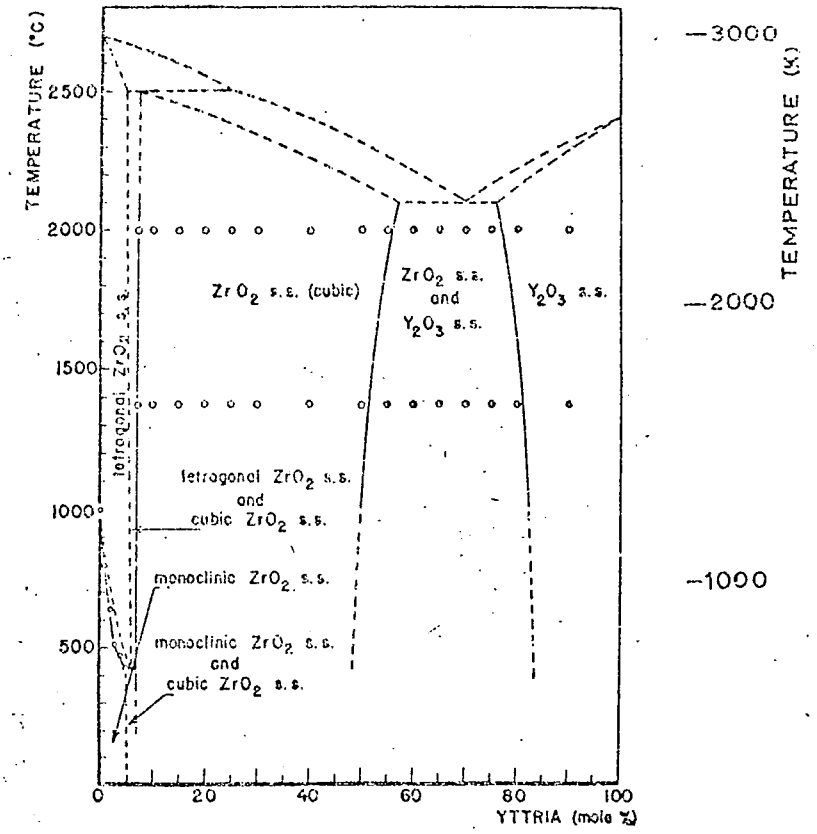

Fig. 6. Tentative phase diagram of the zirconia-yttria system.

a) without a yttrium zirconate ($Y_2O_3.2ZrO_2$) region

by Duvez, Brown & Odell 1951

in the Journal of the Electrochemical Society

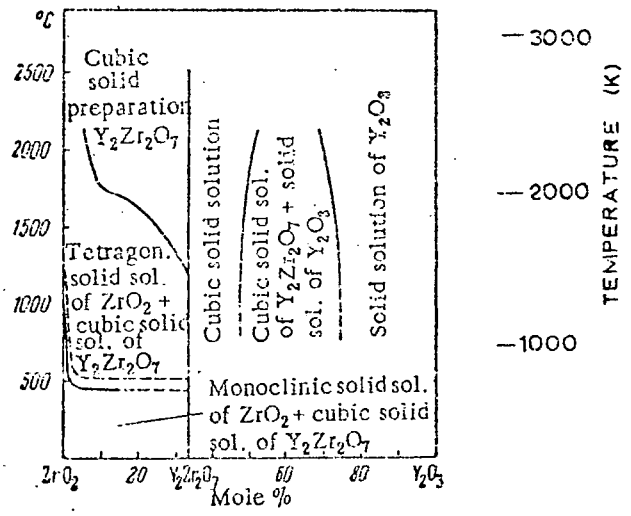

Fig. 6. Diagram of system $Y_2O_3 - ZrO_2$ in solid state (according to Fan' Fu-Kan, Kuznetsov, and Keler)

b) with a yttrium zirconate region

by Fan Fu-Kang, Kuznetov & Keler 1963

in Bulletin of the Academy of Sciences of the U.S.S.R. Division of Chemical Science

FIGURE . 2.2

clinic-tetragonal transition temperature. X-ray powder photographs of the hot oxide confirmed that it had a tetragonal structure at temperatures between 1400 K and 2600 K and showed that at 2600 K its structure became cubic. Foex also found that the addition of other oxides reduced the tetragonal-cubic transition temperature. The additional phase lines marked by chain symbols (— · — · —) have therefore been included in Figure 2.1.

Several binary mixtures of compounds like yttria and zirconia were found to form intermediate compounds; some examples of this are $Ce_2O_3 \cdot 2ZrO_2$, $La_2O_3 \cdot 2ZrO_2$ and $Y_2O_3 \cdot 2TiO_2$. Of these, the compounds containing zirconia had a pyrochlore type of structure. In the yttria-zirconia system however neither Duvez, Brown and Odell, or, Hund (11), 1951 or Roth (12), 1956 found any evidence for the existence of $Y_2O_3 \cdot 2ZrO_2$. An alternative view was proposed by Fan Fu-Kang, Kaznetov and Keler (13), 1963 who claimed to have found extra lines in the X-ray powder patterns of certain compositions in the yttria-zirconia system. They interpreted these as being due to the presence of a $Y_2O_3 \cdot 2ZrO_2$ phase with a pyrochlore structure and drew a very different phase diagram (Figure 2.2 b). As further evidence for the existence of this compound they reported that both density and conductivity measurements, made as functions of composition, showed minima or maxima respectively at the composition corresponding to this formula. In later work D.K. Smith (14), 1966 suggested that yttrium and zirconium were so similar that X-ray diffraction could not satisfactorily distinguish a fluorite structure and a pyrochlore structure. The two elements however have quite different neutron scattering cross-sections. Smith therefore studied samples using neutron diffraction; he prepared two samples with mole ratios 1:1 and 1:2 (Y_2O_3 : ZrO_2), fired them at 2370 K for four hours and furnace cooled them. Both gave X-ray powder patterns characteristic of a fluorite structure. A neutron diff-

raction analysis was made of the 1:2 sample and this showed that a fluorite and not a pyrochlore structure was present. The sample gave the same result after it was heated to 1870 K for fourteen days. Smith attributed the extra lines in the X-ray pattern of Fan Fu-Kang et al. to a combination of the effects of Kβ radiation and the absorption edge of silver. Hence he upheld the phase diagram given in Figure 2.1.

More important for the present study is a knowledge of the smallest yttria concentration required for stabilisation. Duvez, Brown and Odell, (3) believed this to be 7 mole percent; Strickler and Carlson (4) thought it was a little higher at 9 mole percent; (Fan Fu-Kang et al. gave a much higher value). Both the 8.3 mole percent and the 12 mole percent crystals used here gave stable f.c.c. X-ray powder patterns, in agreement with reference (3).

2.2 X-ray unit cell

Yttria stabilised zirconia has a fluorite structure. This is face centred cubic. The cation sites lie on a face centred cubic lattice and the anion sites lie at the centres of the small cubes formed by dividing the (cubic) unit cell into eight sub-units, Figure 2.3.

Several investigators have measured the lattice parameter but since they used different yttria : zirconia compositions a direct comparison of their results is impossible. However, the lattice parameter in the cubic solid solution varies linearly with yttria concentration. Consequently it was possible to estimate the values which would have been obtained for the yttria concentrations used in this work and so attempt an indirect comparison. This is made in Table 2.1 in which, where necessary, the 'a' parameters have been normalised to the 8.3 or 12 mole percent composition by interpolation or extrapolation. The various results appear to be in fairly close agreement.

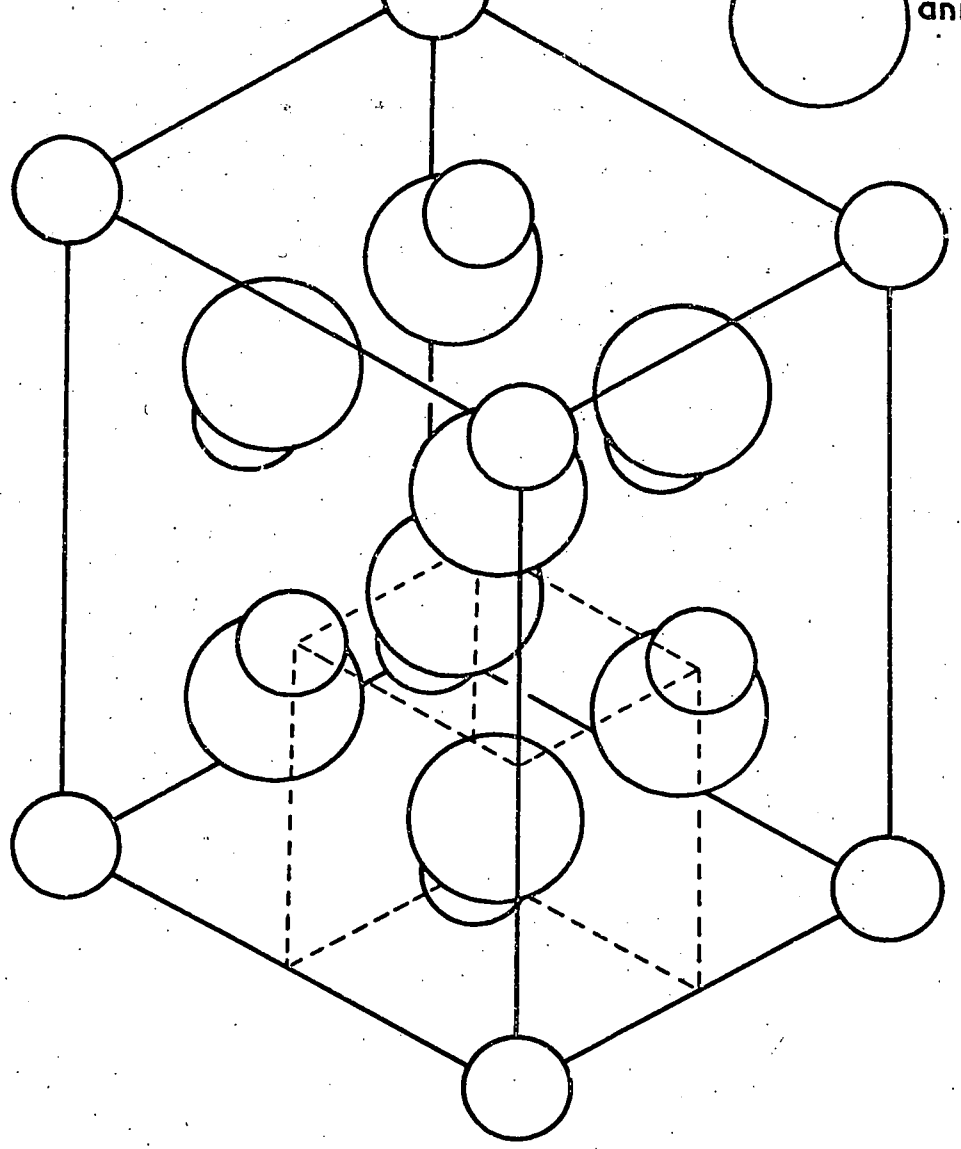

(a)

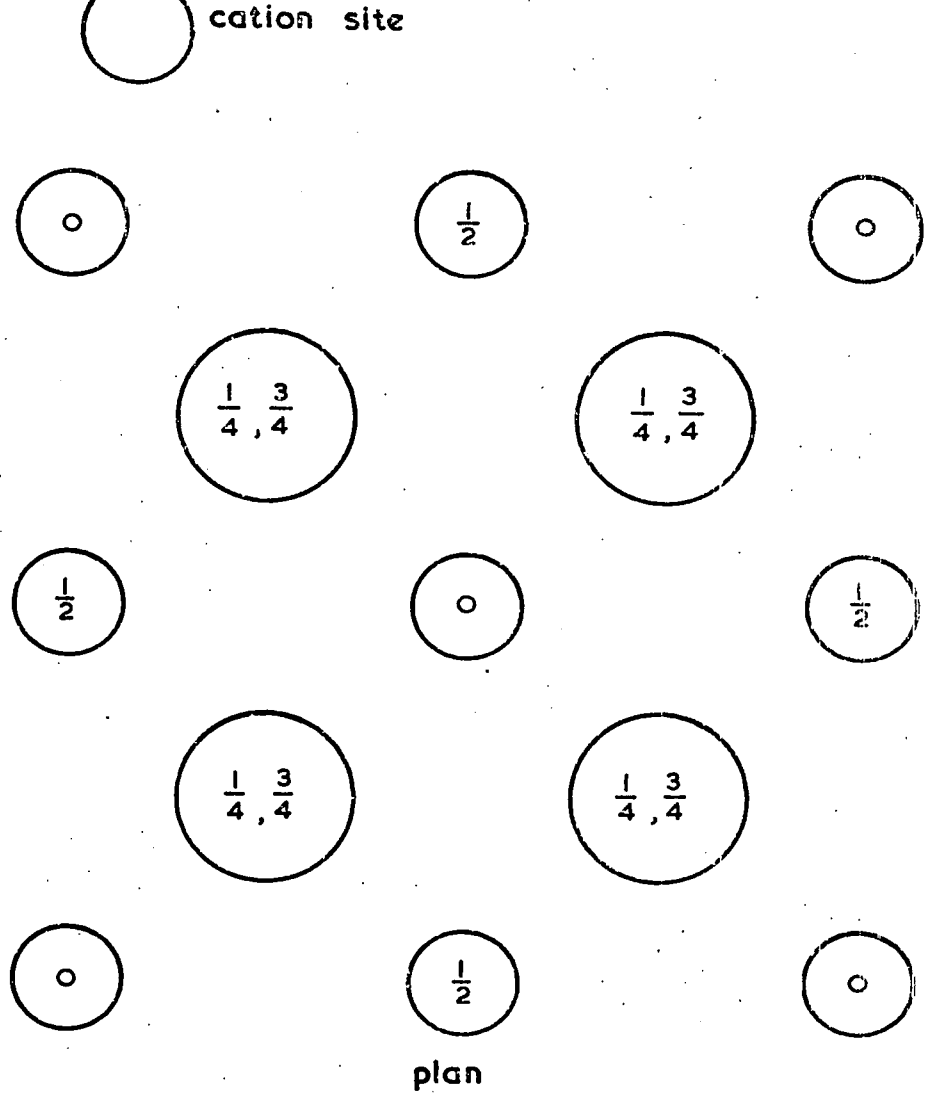

The numbers give the heights of the sites above the base in terms of the lattice parameter.

(b)

Figure 2·3
Unit cell of Calcium Fluoride (Fluorite)

Table 2.1

Comparison of values of lattice parameter obtained for YSZ

Investigator	Lattice Parameter pm		Comments
	8.3 mole %	12 mole %	
Strickler and Carlson (4)	513.9*	515.0*	Polycrystalline
Lefevre (15)	513.7+	514.8*	Polycrystalline
Hund (11)	512.3	513.0*	Polycrystalline
Duvez, Brown and Odell (3)	513.8*	514.0*	Polycrystalline
Pace, Saunders, Sumengen and Thorp (16)	512.76	514.01	Single crystal (powdered)
Aypar and Rose (see also Section 3.3)	513.9	514.8	Single crystal (powdered)

(*, found by interpolation;)

(+, found by extrapolation;)

2.3 Defect Models

2.3.1. General features

In yttria stabilised zirconia there are two oxygen sites to one cation site. Zirconia fits this structure. In yttria, (Y_2O_3), there are one and a half oxygen ions to each cation. Thus fitting yttria into the YSZ structure requires the formation of defects. These may be either oxygen vacancies, or cation interstials, or both. The density of YSZ depends on the defects present. The density and the lattice parameter can be used to calculate the number of atoms in a unit cell. This knowledge can then be used to compare the validity of different defect models. This was attempted by F. Hund in 1951 and he substantiated the proposal, made earlier by C. Wagner in 1943, that oxygen vacancies were present.

This work has been repeated using single crystal material; the X-ray densities and defect concentrations were calculated using the formulae given in the following sections.

2.3.2. "Molecular Weight" and Density

One may define initially that 100 n mole percent YSZ has a formula $(ZrO_2)_{1-n} \cdot (Y_2O_3)_n$. Then the formula contains

$(1-n)$ atoms of zirconium

and $2n$ atoms of yttrium

giving a total of $(1 + n)$ cations. In addition the formula contains $(2 + n)$ oxygen atoms. Thus the mass m of one "formula" is given by

$$m = \frac{(1 - n)\, A_{Zr} + 2nA_Y + (2 + n)\, A_O}{N} \qquad 2.1$$

where A_{Zr}, A_Y and A_O are the atomic weights of zirconium, yttrium and oxygen respectively and N is Avogadro's number.

The density d of 100 n mole percent YSZ can then be expressed as

$$d = \frac{mf}{a^3} \qquad 2.2$$

where f is the average number of formulas in the unit cell and a is the lattice parameter. This relation can be used in two alternative ways. If a value for f is assumed and a is measured it can be used to calculate an X-ray density; conversely, if d and a are both measured experimentally f can be calculated from

$$f = \frac{da^3}{m} \qquad 2.3$$

If f and a are known, then the defect densities can be calculated.

2.3.3. Models which determine f

The value of f, the average number of formulas in the unit cell, is dependent on the nature of the defect model assumed to be operative. There are two simple possible models :-

(a) Oxygen vacancy model

A cubic unit cell contains four cation sites. Here it is assumed that the only defects present are oxygen vacancies and that the cation sites are just filled. Since each "formula" contains (1 + n) cations f is given by

$$f = \frac{4}{(1 + n)} \qquad 2.4$$

(b) Cation interstitial model

The unit cell contains eight oxygen sites. In this model the assumptions are that the only defects present are cation interstitials and that the oxygen sites are just filled.

There are (2 + n) oxygen ions in one "formula" so

$$f = \frac{8}{(2 + n)} \qquad 2.5$$

2.3.4. The Mixture Model

It is possible that yttria stabilised zirconia contains both oxygen vacancies and cation interstitials. (Such a mixture of defects has been observed in calcia stabilised zirconia quenched from 1600°C, Diness and Roy, (17), 1965). In this case f must be calculated from equation 2.3.

It is useful to have expressions for the concentrations of the various types of defect. Since a unit cell contains

(2 + n) f oxygen atoms and 8 oxygen sites

and also

(1 + n) f cations and 4 cation sites

it follows that the concentration of oxygen vacancies C_{OV} is

$$C_{OV} = \frac{8 - \frac{(2 + n)\, da^3}{m}}{a^3}$$

or

$$C_{OV} = \frac{8}{a^3} - \frac{(2 + n)\, d}{m} \qquad 2.6$$

and that the concentration C_I of cation interstitials is

$$C_I = \frac{\frac{(1 + n)\, da^3}{m} - 4}{a^3}$$

or

$$C_I = \frac{(1 + n)\, d}{m} - \frac{4}{a^3} \qquad 2.7$$

It is also worth noting that the concentration of yttrium ions, C_Y, is

$$C_Y = \frac{2nf}{a^3} = \frac{2nd}{m} \qquad 2.8$$

2.3.5. The Effect of Sub-Stoichiometric Oxygen Content

Since the effect of stoichiometry will be considered in Chapter 3 it is worth noting here the effect that a lower oxygen content would have on the above expressions. The general formula for sub-stoichiometric YSZ is

$$Zr_{(1-n)}\ Y_{2n}\ O_{(2+n-x)} \quad \text{instead of} \quad Zr_{(1-n)}\ Y_{2n}\ O_{(2+n)}$$

for stoichiometric material. Allowing for this change equation 2.1 becomes

$$m = \frac{(1-n)\ A_{Zr} + 2nA_Y + (2+n-x)\ A_O}{N} \qquad 2.1a$$

Correspondingly equation 2.5 becomes

$$f = \frac{8}{(2+n-x)} \qquad 2.5a$$

and the oxygen vacancy concentration is

$$C_{Ov} = \frac{8}{a^3} - \frac{(2+n-x)\ d}{m} \qquad 2.6a$$

Although other formulae involve the new value of m the actual change in m will not be great. Thus the main differences will be in the concentration of oxygen vacancies and in the predictions of the cation interstitial model.

2.4 Atomic Radii

For some purposes it is convenient to think of the atoms in a crystal as being hard impenetrable spheres. In this model a crystal containing two species of atoms is represented by two sets of spheres of different diameter. Each atom touches its nearest neighbour atoms of the opposite type. The ratio p of the radii is important since this determines which co-ordination numbers are possible, (the co-ordination number is the

number of nearest neighbours). Of the latter usually the highest is taken. Hence if p is known for the atoms in a compound, the possible structures of that compound can to some extent be predicted.

The problem lies in finding the radii, for these not only depend on the ionic states of the atoms, or the type of co-valent bonding, but also to some extent on the other components present and the co-ordination number, (CN). The ionic radius of a given ion increases by about 4% on going from CN = 4 to CN = 6 and again on going from CN = 6 to CN = 8. If r_a and r_c are the anion and cation radii respectively and a is the lattice parameter it is clear that, for the fluorite structure

$$r_a \leqslant \frac{a}{4} \qquad 2.9$$

It can also be shown that

$$r_c \leqslant \frac{a}{2\sqrt{2}} \qquad 2.10$$

and that $r_a + r_c = \frac{\sqrt{3}}{4} \cdot a$ 2.11

As regards the ratio of the cation and anion radii the co-ordination numbers of eight and four for cations and anions respectively impose the limit

$$\sqrt{3} - 1 \leqslant \frac{r_c}{r_a} \cdot \qquad 2.12$$

In yttria stabilised zirconia, for which the lattice parameter is $a = 514$ pm (Section 2.2), substitution gives

$$128 \text{ pm} \geqslant r_a \geqslant 40 \text{ pm} \qquad 2.13$$

and

$$94 \text{ pm} \leqslant r_c \leqslant 182 \text{ pm} \qquad 2.14$$

When CN = 4 the radius of O^{2-} is 134 pm, which is too large, and the radius of covalent oxygen is 66 pm, which is a suitable value. Similarly the radius of Zr^{4+}, which is 83 pm, is too low. These arguments suggest that the bonding contains a significant amount of co-valency. In addition to this the success of the ionic theory of electrical conductivity applied to YSZ indicates that a large amount of ionic bonding is also present. The radii of Y^{3+} and Zr^{2+}, (96 pm) are within the limits of equation 2.13 and presumably so is that of Zr^{3+} since the same electron shells are occupied in this ion as in Zr^{2+}. The radius of Y^{2+}, (114 pm), indicates that this ion could be present.

It should be emphasised that the limits indicated are not completely rigid; this applies especially in YSZ where, because there are two types of cation with different valencies, the co-ordination numbers are not fixed. Despite this, the main conclusions are

(1) that the bonding is partially covalent and

(2) that the ions Y^{2+}, Y^{3+} and Zr^{2+} would fit into the lattice.

Note : the radii quoted, based on an O^{2-} radius of 140 pm when CN = 6, are taken from Greenwood, (18), modified as indicated above to take account of co-ordination number; see also Azaroff and Brophy, (19).

2.5 Nomenclature

Despite the comments above the ionic notation of Kroger and Vink will be used in the analysis of the low field electrical conductivity and the electron spin resonance data since consideration of the mixed bonding does not provide greater insight in these specific instances. In this notation the effective electrical charge on a site is considered to be the difference between the actual charge and the charge the site would normally have. Superscripts of the type A', A^X and $A^{\cdot}$ indicate a negative, zero and positive effective charge respectively. The normal species to which a site corresponds is shown by a subscript; if the subscript is "i" the site is interstitial.

Using this notation for yttria stabilised zirconia Y^{3+} in a cation site is written as Y'_{Zr} and an oxygen vacancy becomes $V_O^{\cdot\cdot}$. The notation $V_O^{\cdot}$ represents an oxygen vacancy containing one trapped electron. It is quite likely that an oxygen vacancy will be associated with two yttrium ions since this would achieve charge compensation, i.e.

$$2\ Y'_{Zr} + V_O^{\cdot\cdot} \longrightarrow (2\ Y_{Zr}, V_O)^X$$

If only one yttrium ion is associated with the oxygen vacancy the complex would have an effective charge

$$Y'_{Zr} + V_O^{\cdot\cdot} \longrightarrow (Y_{Zr}, V_O)^{\cdot}$$

but if the vacancy trapped an electron the charge would be compensated; this is indicated by the changes

$$V_O^{\cdot\cdot} + e^- \longrightarrow V_O^{\cdot} \quad \text{and} \quad Y'_{Zr} + V_O^{\cdot} \longrightarrow (Y_{Zr}, V_O)^X .$$

These complexes are relevant to the interpretation of the electron spin resonance and electrical conductivity data.

Chapter 3.

Measurement of Density and Lattice Parameter

3.1 Defects

This chapter describes the measurement of density and lattice parameter. The experimentally determined density is compared with the X-ray density for the models described in Section 2.3.3 and the oxygen vacancy model is shown to give the best fit although some cation interstitials also seem to be present. For this reason defect concentrations are calculated using the mixture model formulae given in Section 2.3.4. In making these estimations it is assumed that the mixture is stoichiometric. Evidence is given supporting the correctness of this assumption for the yttria-stabilised zirconia crystals in the as received state. It quickly became apparent however that even simple heat treatments, without electrolysis , caused marked changes in the appearance of the crystals. Consequently these effects were investigated first.

3.2 Effects of Heat Treatment without Electrolysis

3.2.1 Heating in Air or Oxygen

The appearance of the as received crystals varied considerably according to the position in the fused melt from which they were extracted; some, from near the surface, were pale yellow and transparent, the majority amber and transparent and some black and almost opaque. Since the crystals were grown by electrofusion of a powdered mass under reducing conditions it was suggested that the as received crystals were not stoichiometric and hence that this might explain why they were coloured. It was supposed that heating the crystals in air or oxygen would restore the stoichiometry and measurements were made to test this. The treatments

were performed in a variety of ways :

(a) heating in an open silica boat over a bunsen flame;

(b) heating in a furnace with an air atmosphere and

(c) heating in a furnace with open ends through which a stream of oxygen was passed.

Typical observations made are recorded in Table 3.1. The two major conclusions can be summarised as follows :-

(a) The colour of the crystals fades and the crystals turn white.

(b) The crystals fragment, probably from the surface inwards.

It may be noted here that an object appears white because it scatters or reflects light diffusely and does not selectively absorb different colours. Thus a fragmented colourless crystal, sugar for example, will appear white because the random orientations of the surfaces will provide diffuse reflection and any light that passes through a fragment will not be selectively absorbed. Recent measurements by H.P. Buckley have shown that YSZ whitened by heat treatment in oxygen scatters light but absorbs very little of it.

An increase of 1% in the oxygen content of these crystals would give a fractional change in mass of 2.5×10^{-3}. The observed changes in mass due to heat treatment are shown in Table 3.2. Normally there is a fractional gain in mass of less than 10^{-3} (near the experimental sensitivity). This indicates that either the departure from stoichiometry is less than 1% of the oxygen content or that the samples are stable when non-stoichiometric. The latter situation has been encountered with other materials; non-stoichiometric compositions of uranium dioxide, which also has the fluorite structure, are in equilibrium with high or low partial pressures of oxygen at elevated temperatures, (Roberts, 1967, (20)).

Sample	Composition and Heat treatment	Appearance and Comments
S.5	8.3 mole %, as received	Amber, transparent
	Air, 1020 K, 6 hr, furnace	Grey, translucent
	Air, 1120 K, 12 hr, furnace	Grey, translucent
	Air, 1170 K, 12 hr, bunsen burner	White, translucent
S.7	8.3 mole %, as received	Transparent amber cluster of crystals
	Oxygen, 1170 K, 4 hr, furnace	The crystals separated; some turned grey, some white, all were translucent
S.8	12 mole %, as received	Amber, transparent
	Oxygen, 1170 K, 4 hr, furnace	Sample crumbled; pieces were translucent, either grey, white or brown
S.11 (1)	8.3 mole %, as received	Amber, transparent
	Oxygen, 1360 K, 3.5 hr, furnace	Translucent, white with an amber sheen
S.23	8.3 mole %, as received	Transparent, amber; cut into a block with polished and unpolished faces
	Oxygen, heated to 1020 K in 1.5 hr and cooled over 4 hr.	Colour faded White patch in one corner
	Oxygen, 1020 K; held for 1 hr	Surface covered in grey blobs of which there were more on the unpolished than polished faces

Table 3.1

Visual effects of heat treatment in Air and Oxygen

Sample	Composition and Heat treatment	Mass (gram)	Fractional change in mass	Appearance and Comments
R.25	8.3 mole %, as received	8.8516	-	Amber, transparent but containing a black opaque region
	Air, 1070 K, 8.5 hr	8.8516	$<10^{-5}$	Transparent throughout. Pale brown. Split into two, R.25 (a) and R.25 (b)
R.25 (a)	-	6.9044	-	as above
	Oxygen, 1270 K,50 hr	6.9072	$+ 4 \times 10^{-4}$	White, translucent
R.25 (b)	-	1.9471	-	as above
	Oxygen, 1270 K,50 hr	1.9477	$+ 3 \times 10^{-4}$	White, translucent
R.30	12 mole %, as received	2.8126	-	Amber, transparent
	Air, 1070 K, 8.5 hr	2.8035	$- 3 \times 10^{-3}$	Pale brown, transparent
	Oxygen, 1270 K, 50 hr	2.8039	$+ 1.4 \times 10^{-4}$	White, translucent

Table 3.2

Mass changes resulting from heat treatment

3.2.2 Heating in Argon

The electrolysis of yttria stabilized zirconia crystals was, as will be described in detail later (Section 7.3), normally carried out at temperatures near 800°C in an argon atmosphere. For purposes of reference, and to establish the effects of heat treatment alone, observations were made on some single crystal samples heated in argon. The colour of these crystals also faded and the crystals cracked. However, the cracking took place much more slowly than when the atmosphere contained oxygen. Polishing the faces of the crystal also retarded the cracking. The similarity of these results to those of the previous section tends to confirm the conclusion that these effects are not due to oxygen being taken up.

3.3 Lattice Parameters

In collaboration with A. Ayper lattice parameter measurements were made by conventional X-ray powder analysis. The X-ray photographs were obtained with a 114 mm Debye - Sherrer powder camera mounted on a standard Phillips diffraction unit. All the photographs were taken with copper $K\alpha$ radiation using a nickel filter. Many specimens were examined after a variety of treatments e.g. in the as received state, after heat treatment in air, oxygen or argon and after high temperature electrolysis in argon. Figure 3.1 shows the type of powder photograph obtained; generally speaking the diffraction lines were sharp and the overall clarity of the films sufficiently high to enable accurate measurements of the line positions to be made. The lattice parameters were calculated using a computer programme which gave a least squares fit for a Nelson - Riley extrapolation. Some of the results are given in Table 3.3. The main conclusions from this study were

(a) That all the lines observed could be indexed on the basis of a

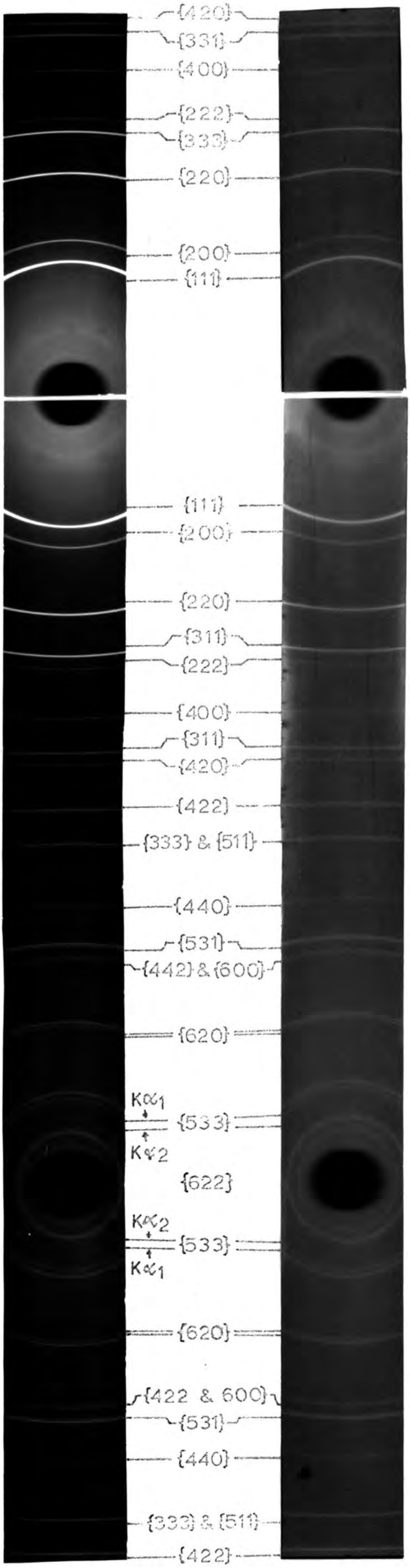

FIGURE 3.1
X-RAY POWDER PHOTOGRAPHS OF
YTTRIA STABILIZED ZIRCONIA.

Sample	Lattice Parameter (pm)	Treatment
8.3 mol per cent yttria crystals		
S.10	513.92 ± 0.08	As received
1 A2 (2)	513.9 ± 0.2	As received
1 A3	513.7 ± 0.1	As received
S7 (1)	514.0 ± 0.2	Heated in oxygen, 1230 K, 4 hr
S7 (2)	514.0 ± 0.1	Heated in oxygen, 1230 K, 4 hr
1 A14 j	514.0 ± 0.1	Current blackened, 1 A/$_{cm}2$, 1070 K, 35 hr, (in argon)
1 A14 h	513.96 ± 0.08	Current blackened, 5 A/$_{cm}2$, 1070 K, 15 min, (in argon)
S5	513.8	Heated in air, (1170 K, 6 hr), then current blackened at 1070 K
S2 (1)	513.8 ± 0.1	Heated in air (800°C, 6 hr), then in vacuum (1.5 x 10-4 torr) at 2470 K for 2.5 hr
12 mole per cent yttria crystals		
2 A1	514.8 ± 0.1	As received
S9 (1)	514.8 ± 0.1	Heated in oxygen, 1360 K, 3.5 hr
S12	514.9 ± 0.1	Heated in air (800°C, 6 hr) then in vacuum (1.5 x 10-4 torr) at 2470 K
S91A	514.9 ± 0.2	Current blackened, .6 A/$_{cm}2$, 1070 K, 3 hr

Table 3.3

Lattice parameter measurements

cubic fluorite structure.

(b) That there was a slight increase in lattice parameter, from 513.9 pm to 514.8 pm, on increasing the yttria content from 8.3 mole % to 12 mole %.

and

(c) that, for a given yttria concentration, there appeared to be no significant changes in lattice parameter resulting from either the various heat treatments or from electrolysis.

Values of X-ray density were calculated from this data for both the oxygen vacancy model and the cation interstitial model. Figures 3.2 and 3.3 show the results for the two yttria concentrations; the X-ray densities are indicated by the horizontal lines and the effect of a $\pm$ 0.5 mol % error in n, the assumed yttria content, is also shown. (The abbreviation "m/o" is used for "mol %").

3.4 Density of single crystal YSZ

Direct measurements of density were made on as received samples, on some whitened by heat treatment in air or oxygen, and on others blackened by current passage in argon. The densities were measured by comparing the weights of the samples in air and when submerged in distilled water. Since the upthrust due to air was negligible the simple formula

$$d_s = \frac{m_a d_w}{(m_a - m_w)} \qquad 3.1$$

was used; in this relation d_s and d_w are the densities of the sample and water respectively, m_a is the mass of the sample found by weighing in air and m_w is the apparent mass found by weighing in water. Corrections were made for the variation of the density of water with temperature and for the volume of suspending wire submerged. The choice of this method was

DENSITY OF 12 m/o YSZ

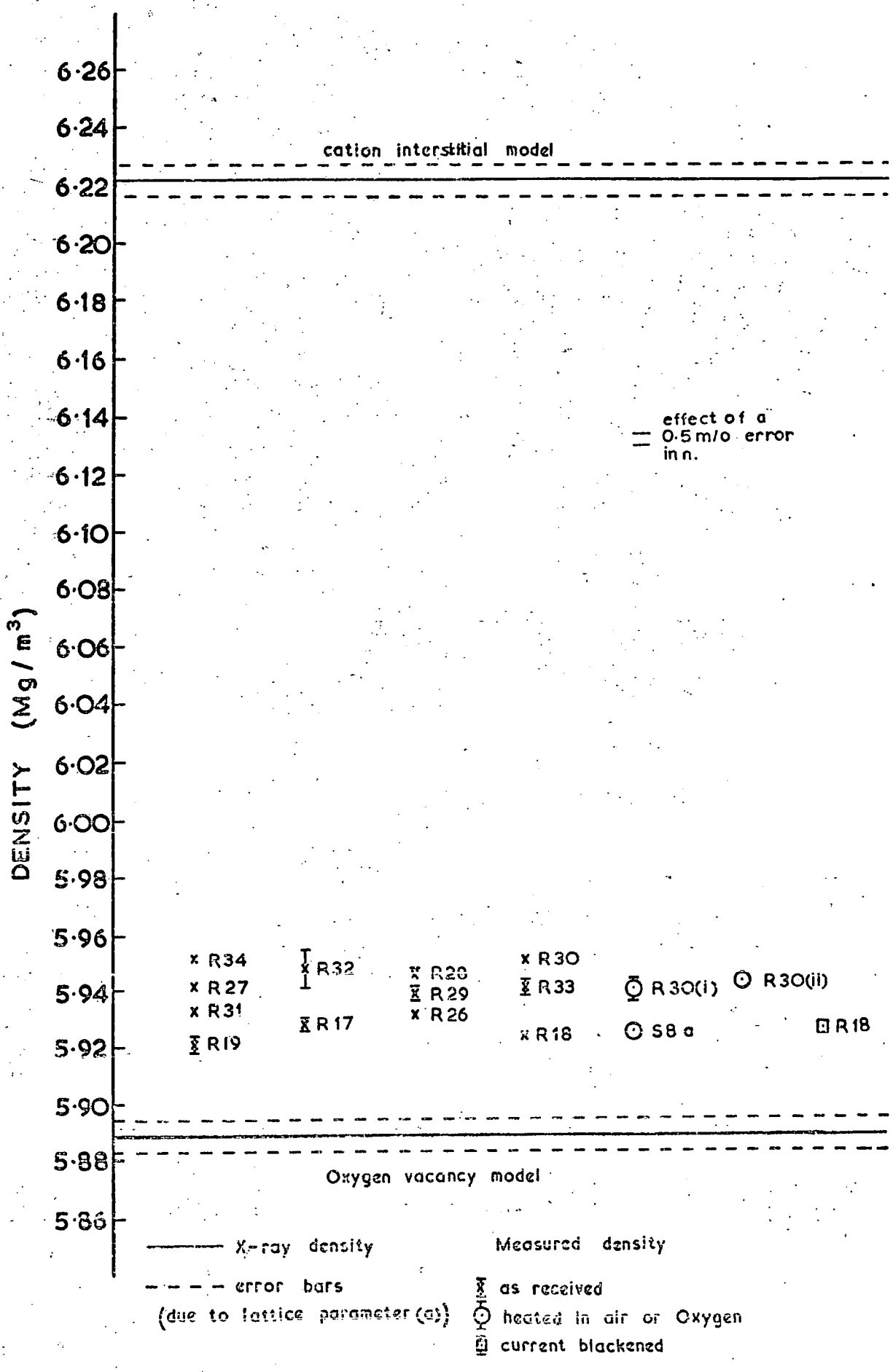

FIGURE 3.2

DENSITY OF 8·3 m/o YSZ

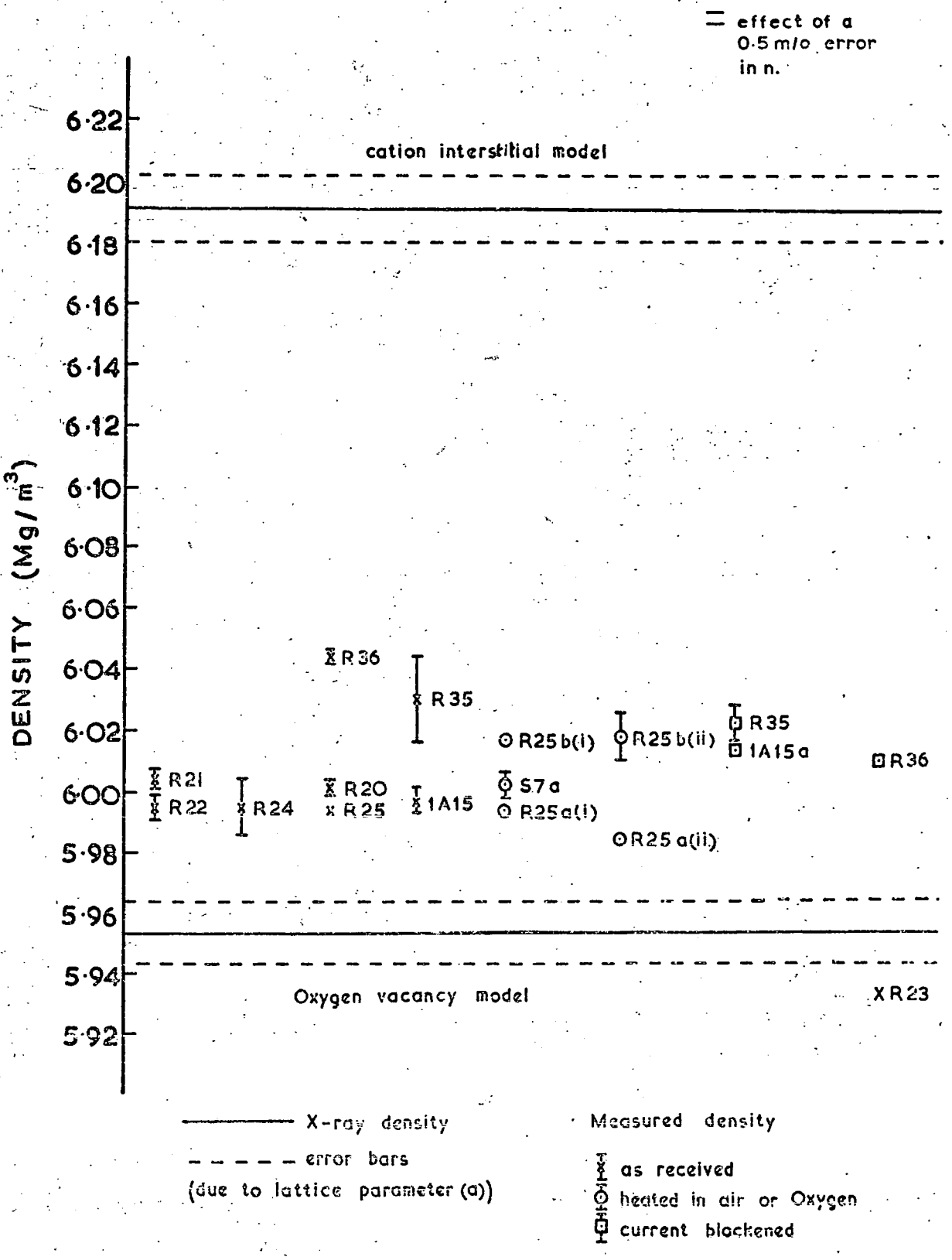

FIGURE 3·3

dictated by the facts that the density of yttria stabilized zirconia, (about 6×10^3 kg/m^3) was too great for the application of flotation methods and that a determination from the weight of a rectangular block of precise dimensions would have involved laborious crystal polishing and, furthermore, not have been applicable to treated samples which tended to fragment. The samples used for the measurements were carefully selected; they were picked or cut so as to be homogeneous and free from bubbles or powder which had incompletely fused. Their masses ranged from about 1.5g to 8.8g which resulted in the apparent changes in mass (from 0.2g to 1.5g) being measurable to a nominal accuracy of 0.2 mg. The reproducibility was checked by repeating the measuremants on every crystal twice.

The results of the density measurements are shown in Figures 3.2 and 3.3. When the measured densities are compared with the X-ray densities it can be seen that they approximately fit the oxygen vacancy model; there is however a relatively small but significant deviation which indicates that some cation interstitials are also present. The scatter of results is a little greater than their reproducibility and probably reflects a real variation. (It seems likely that R.23 was really a 12 mol % yttria sample). The densities of the treated samples, including both those blackened by electrolysis and whitened by heating in air or oxygen, fall within this scatter. Consequently, it appears that the considerable visual changes in appearance shown by the samples examined are not associated with a gain or loss of more than 1% of the oxygen.

3.5 Defect Concentrations

The concentrations of oxygen vacancies and cation interstitials, given in Tables 3.4 and 3.5, were calculated from the lattice parameters given in Table 3.3 and the measured densities shown in Figures 3.2 and

In this table the densities quoted are the maximum and minimum measured and a typical density.

Measured Density ($Mg\ m^{-3}$) or ($g.\ cm^{-3}$)	Oxygen Vacancy Concentration ($\times 10^{27}\ m^{-3}$) or ($\times 19^{21}\ cm^{-3}$)	Cation Interstitial Concentration ($\times 10^{27}\ m^{-3}$) or ($\times 10^{21}\ cm^{-3}$)
5.982	2.0	0.15
6.000	1.8	0.20
6.044	1.5	0.50
Oxygen Vacancy Model	2.3	0

Table 3.4

Defect concentrations in 8.3 mol percent YSZ; (yttrium ion concentration $4.6 \times 10^{27}\ m^{-3}$, $a = 513.9$ pm)

In this table the densities quoted are the maximum and minimum measured and a typical density.

Measured Density ($Mg\ m^{-3}$) or ($g.\ cm^{-3}$)	Oxygen Vacancy Concentration ($\times 10^{27}\ m^{-3}$) or ($\times 10^{21}\ cm^{-3}$)	Cation Interstitial Concentration ($\times 10^{27}\ m^{-3}$) or ($\times 10^{21}\ cm^{-3}$)
5.918	2.9	0.1
5.935	2.7	0.2
5.554	2.5	0.3
Oxygen Vacancy Model	3.14	0

Table 3.5

Defect concentrations in 12 mol percent YSZ; (yttrium ion concentration $6.3 \times 10^{27}\ m^{-3}$, a = 514.8 pm)

3.3 using the mixture model formulae quoted in Section 2.3.4. For each composition the minimum and maximum measured densities have been tabulated, together with a more representative typical value.

A change of about 10^{26} oxygen vacancies per cubic metre (10^{20} vacancies cm^{-3}) should be detectable as a density change which could be quite reliably measured; in yttria stabilized zirconia this would represent a 5% change in the oxygen vacancy concentration. In the experimental work however a much greater absolute error than this arises. Two factors contribute to this. The error due to uncertainties in the lattice parameter (a) in itself amounts to $\pm$ 15%. Furthermore, the exact yttria concentrations are unknown and a change of $\pm$ 0.5 mol % in the value of the mole fraction of yttria (n) used in the calculation would also change the value of the oxygen vacancy concentration derived by $\pm$ 15%. The effect of these uncertainties on the calculated value of the cation interstitial concentration is greater and these values are barely reliable to one significant figure. This shows how accurately the density and lattice parameter must be measured to obtain worthwhile estimates of defect concentrations. Finally, the whole of the analysis made above assumes that the valency difference between the two cations is by far the most important source of defects. This assumption is not unreasonable. The concentration of thermally produced oxygen vacancies, even at 1200 K, would only reach the values mentioned above if the energy required to produce one vacancy was about 6×10^{-20} J (0.4 eV); this seems unrealistically low and hence thermal production of vacancies appears unlikely.

Chapter 4.

Electron Spin Resonance

4.1 Introduction

It is not unreasonable to suppose that when an electric current is passed through Yttria stabilized Zirconia some of the oxygen vacancies will trap an electron. The result will be an F-centre. More significantly, as mentioned in Section 2.5, a vacancy might either have four zirconium ions as its nearest neighbours or have one or more of these replaced by yttrium. Electron spin resonance provides a means of detecting unpaired electrons and determining their environment. This allows the "vacancy-trap" theory for ionic conduction in YSZ (see Chapter 6) to be tested by enabling the traps to be detected. The theory postulates that an oxygen vacancy surrounded by zirconium ions will be free to move at elevated temperatures, but that one 'trapped' by a yttrium ion, to form a 'complex', will not. The present study was intended to continue at 35.5 GHz work started by Mr. Boon at 9.3 GHz, but prematurely terminated.

4.2 Experimental Details

Oriented samples were investigated after various treatments. Some were studied in the as received state, some were examined after current blackening and others after being heated in argon, air or oxygen without having current passed through them. Most of the samples were cleaved from $(1\ mm)^2$ rods. The as received material was very strong, and to cleave it it was necessary to apply a sharp blow to a knife laid across the rod. Usually cleavage occurred in the $\{100\}$ planes but cleavage in the $\{110\}$ planes was quite common. Rods were blackened by the passage of currents between 10 and 250 mA, for times ranging from 3 min. to 1 h. (More details of the blackening procedure are given in Section 7.3). Blackened samples were very friable and had a silvery highly conducting surface layer. The surface layer was

removed by dipping the sample into hot phosphoric acid (typically for 5 s at 200°C). The removal of the layer was indicated by appearance, by the high value of the surface resistance and especially by the reduced effect of the sample on the cavity damping. Etching was repeated until there was no further improvement. For comparison purposes some samples were prepared under the same conditions of atmosphere and temperature but without passing current.

A cavity spectrometer employing phase sensitive detection at 160 kHz was used. The coupling and tuning of the cavity were adjustable. A ruby sample (with which the cavity Q-factor was $\lesssim$ 2000) was used to estimate the spectrometer sensitivity. From this it was deduced that the spectrometer could detect 10^{13} spins per millitesla line width at room temperature, working under normal conditions with a power level of 11 mW and a time constant of 1 second. The introduction of yttria stabilized zirconia samples into the cavity effected the coupling. Furthermore current blackened samples degraded the cavity Q-factor seriously making spectra difficult to observe. Accordingly the sample volume was chosen, at about $(1\ \text{mm})^3$, to give a sufficient number of spins in the sample while retaining an adequate Q-factor. With as received samples Q $\lesssim$ 900. Rough estimates of the number of ESR centres in YSZ samples were made by assuming that

$$\text{number of centres} \propto \frac{hw}{Q}$$

where h is the height of the (derivative) ESR lines, w is their width and Q is the Q-factor of the loaded cavity.

An EMI R5146 Klystron provided the microwave power and the phase sensitive detection system consisted of Brookdeal units 421, 450 and 411. Most measurements were made at 290 K and some at 77 K.

The magnetic field was produced by a Newport Instruments Magnet type D with a type C225 power supply which contained a type A slow sweep

unit. The controlling (sawtooth) voltage of the latter was connected to the X-input of a Moseley 7035A (Hewlett-Packard) X-Y recorder. The range control of the X amplifier was set to (1 to 10) V/in and the set zero was adjusted to make the sweep end at 9.5 inches. The vernier gain then positioned the start of the sweep at 0 inches. These settings did not have to be changed when the sweep time or sweep amplitude was changed. The field and the sweep were calibrated using a Newport (proton and Lithium resonance) magnetometer type P, mark II. The frequency of the magnetometer (or strictly its sub-harmonics) was measured using a Marconi Instruments Precision Hetrodyne Wavemeter TF 783. Even with the probe carefully positioned in the centre of the field the Lithium signal was too small; so phase sensitive detection was used with 50 Hz modulation. Thus calibration marks were drawn directly onto a series of traces produced by the sweep unit. For even the greatest sweep amplitude ("100%") a graph of magnetic field against "X" on the recorder was almost linear. The resonant field of each ESR line was found from the sweep calibration and the position of a DPPH marker.

Samples were changed by unscrewing the base of the cavity, and since the sample stood on a post fitted to the base this process rotated the sample. In order to orient the sample in the field the orientation of the sample with respect to an external scale was first found using a travelling microscope. A cross-wire was alined with the direction of travel, a side of the sample was alined with the cross-wire and the positions on both sides of the scale where the cross-wire crossed the scale were found. The base was screwed into the correct position and locked. A nylon thread was drawn taut between two fixed hooks to act as a datum line and the orientation of the scale with respect to the datum line was found. (Again readings were taken on both sides of the scale). Since the orientation of the magnet when its pole pieces were parallel to the datum line was known,

the orientation of the field with respect to the crystal could be calculated. (See Appendix 3).

For tuning, the Klystron mode could be displayed on an oscilloscope by applying the timebase of the oscilloscope (via an attenuator) to the Klystron reflector. (The signal from the microwave crystal was amplified with a Solartron D.C. decade amplifier). Usually the cavity absorption appeared as a large dip in the mode but when the cavity contained a heavily blackened sample the absorption could flatten the Klystron mode. Then care had to be taken that the wrong cavity mode was not selected.

4.3 Results

Spectra were seen in all samples. They were characterized by three types of line of different shape, intensity and variation with polar angle. Similarly treated 8.3 and 12 mole % YSZ samples gave similar spectra.

The lines from the as received samples were deduced to be of two types, which will be referred to as type-A and type-B (Figure 4.1). The two lines labelled "A" here,seen when the magnetic field lay in the (100) plane, were believed to be due to one type of site because of their similarity in shape and intensity and especially because of the variation of their resonant field with polar angle (Figure 4.2). (The position of the type -A line shownin Figure 4.2 is not the correct one for the calculation of g-value and hence does not correspond to the calculated g-values (Figure 4.4).) The peak to peak width of an A-type line varied according to the field value at which it occurred; from 20 mT at 1.35 T to 8 mT at 1.30 T in the (100) plane reducing further to 5 mT at 1.26 T in the (111) plane. In the (111) plane three apparently symmetrical lines were clearly seen near this range of g-values and a fourth was just detectable. Over a matter of months crystals kept at room temperature lost their type -A lines.

The single type -B line was asymmetrical and of higher intensity.

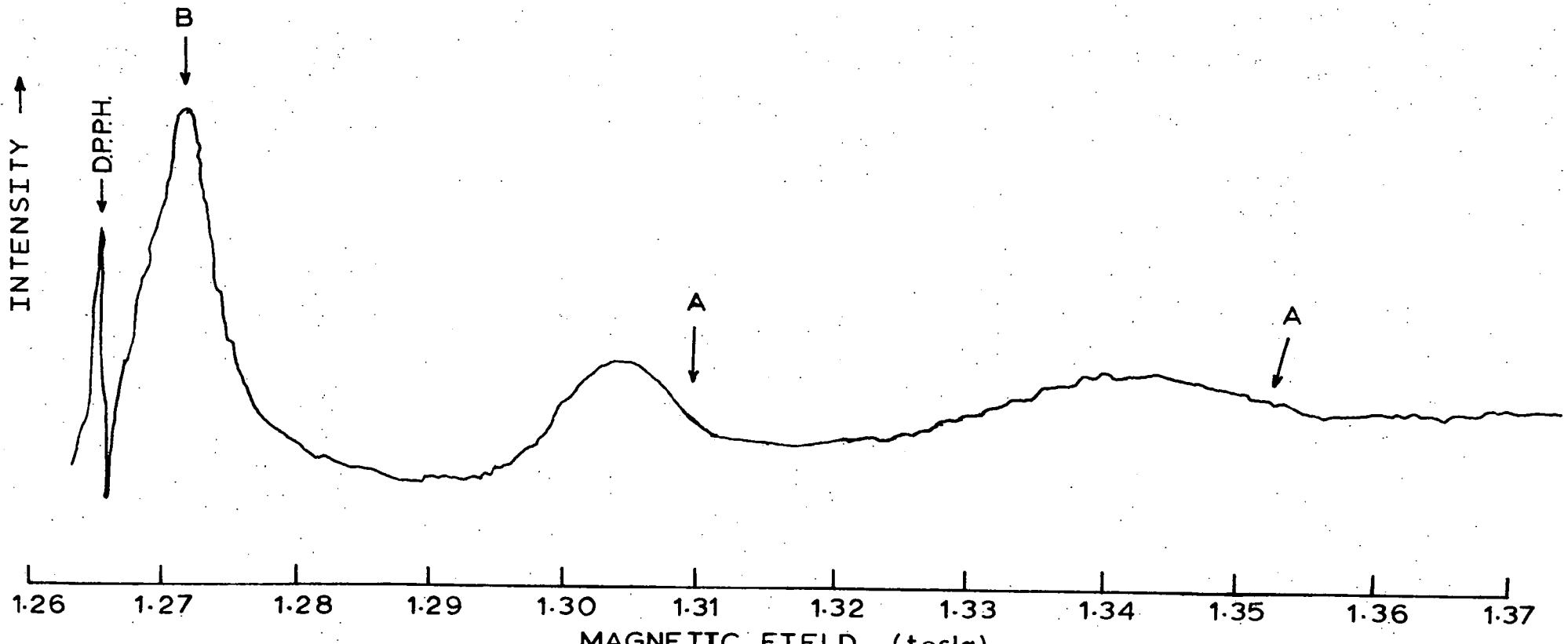

FIGURE 4.1

Spectra observed in as received 8·3 mole % yttria stabilized zirconia.
Magnetic field 16° from [100] direction in (001) plane.
35·5 GHz. 290 K.

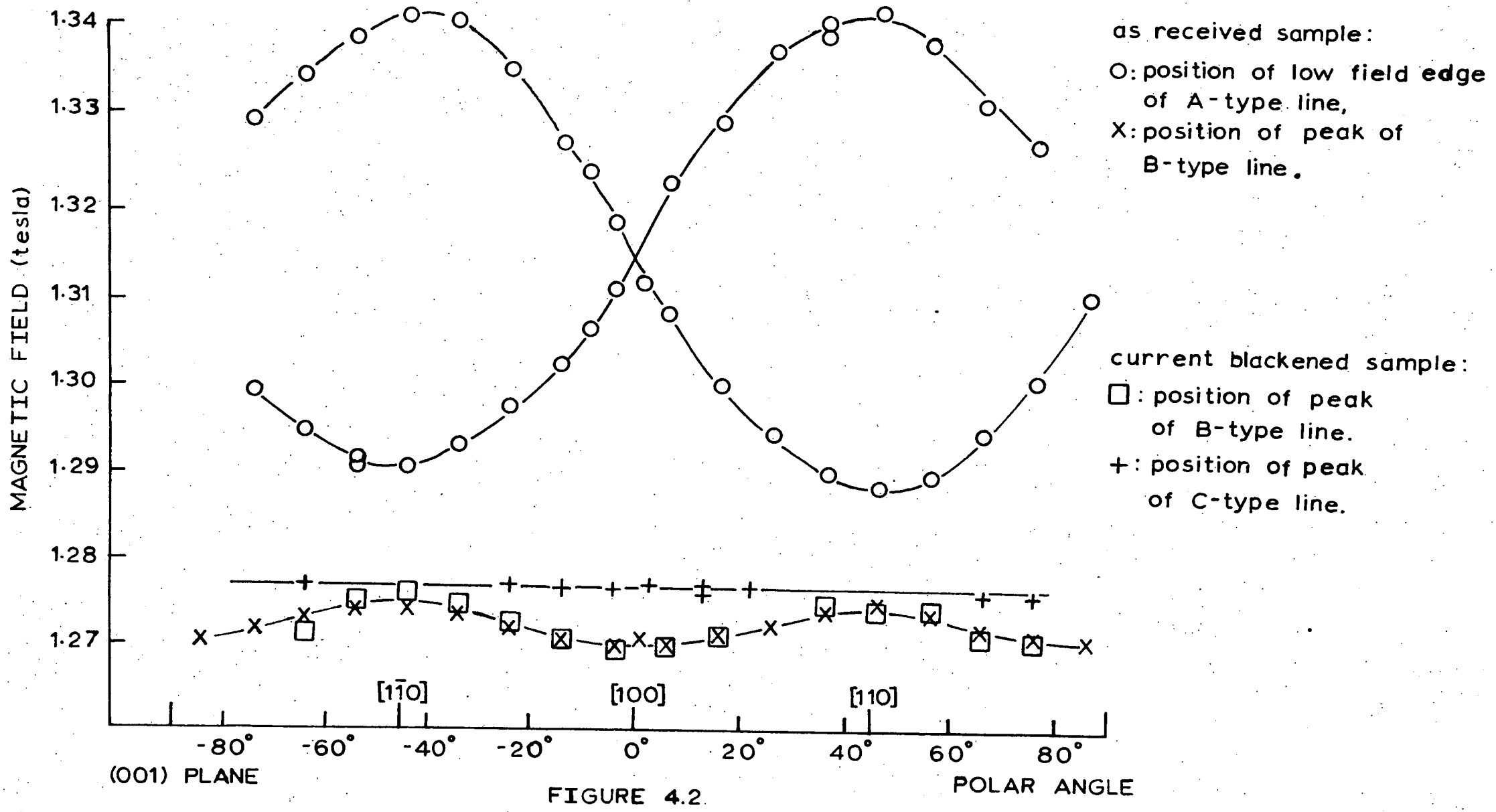

FIGURE 4.2

Variation with polar angle of line peak positions in as received and current blackened YSZ.

Its slightly anisotropic behaviour and the change in the width with polar angle were observed. The g-values varied from 1.990 along the <110> directions to 1.997 along the <100> directions. The linewidth in the <100> directions was 6 mT and it increased asymmetrically to about 10 mT in the <110> directions.

In samples which were heat treated without current passage no type -A lines were observed, but the type -B line seemed unchanged. The ESR spectrum appeared to be independent of the atmosphere (air, Oxygen or Argon) used for the heat treatment. Current blackened samples exhibited both type -A and type -B and also an additional peak (designated type -C) close to the type -B line (Figure 4.3). The type -C line was isotropic and so at some polar angles was obscured by the type -B line. The variations with polar angle of the resonance field values for the type -A, -B and -C lines are given in Figure 4.2. There was some indication that the intensity of the type -C line increased with increasing current density. The position of the peak of the type -C line corresponded to a g-value of 1.986.

The information is summarized in Table 4.1. Only samples known to exibit type -A lines before treatment were used.

Preliminary measurements have been made at lower temperatures on as received 8.3 mole % YSZ samples. The spectra recorded at 77 K were similar to those obtained at 290 K and no extra lines were seen. With current blackened material the type -C line was also present down to 148 K, the lowest temperature at which measurements were made. The relative intensities of the type -A, -B and -C lines were approximately the same at room temperature and low temperature.

4.4 Discussion

4.4.1 Type -A lines

The results shown in Figure 4.2 suggest that each type -A site must

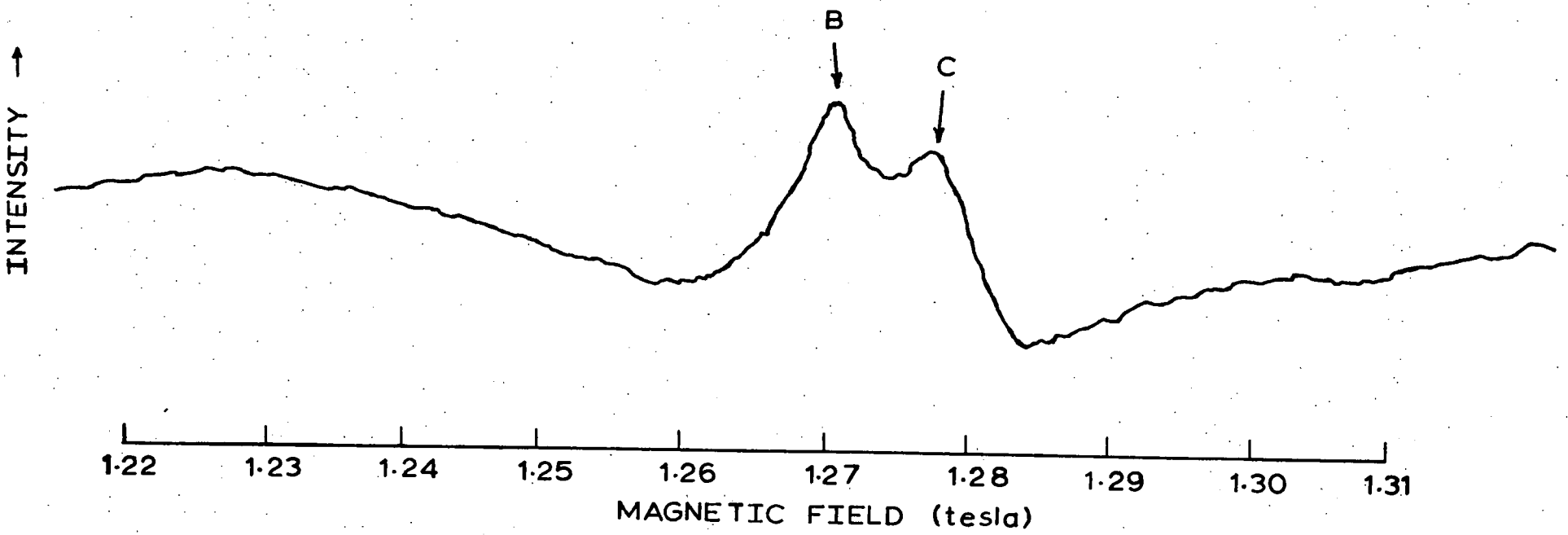

FIGURE 4.3

Spectra observed in current blackened 8.3 mole % yttria stabilized zirconia. Magnetic field 5° from the [100] direction in the (001) plane. 35.5 GHz. 290 K.

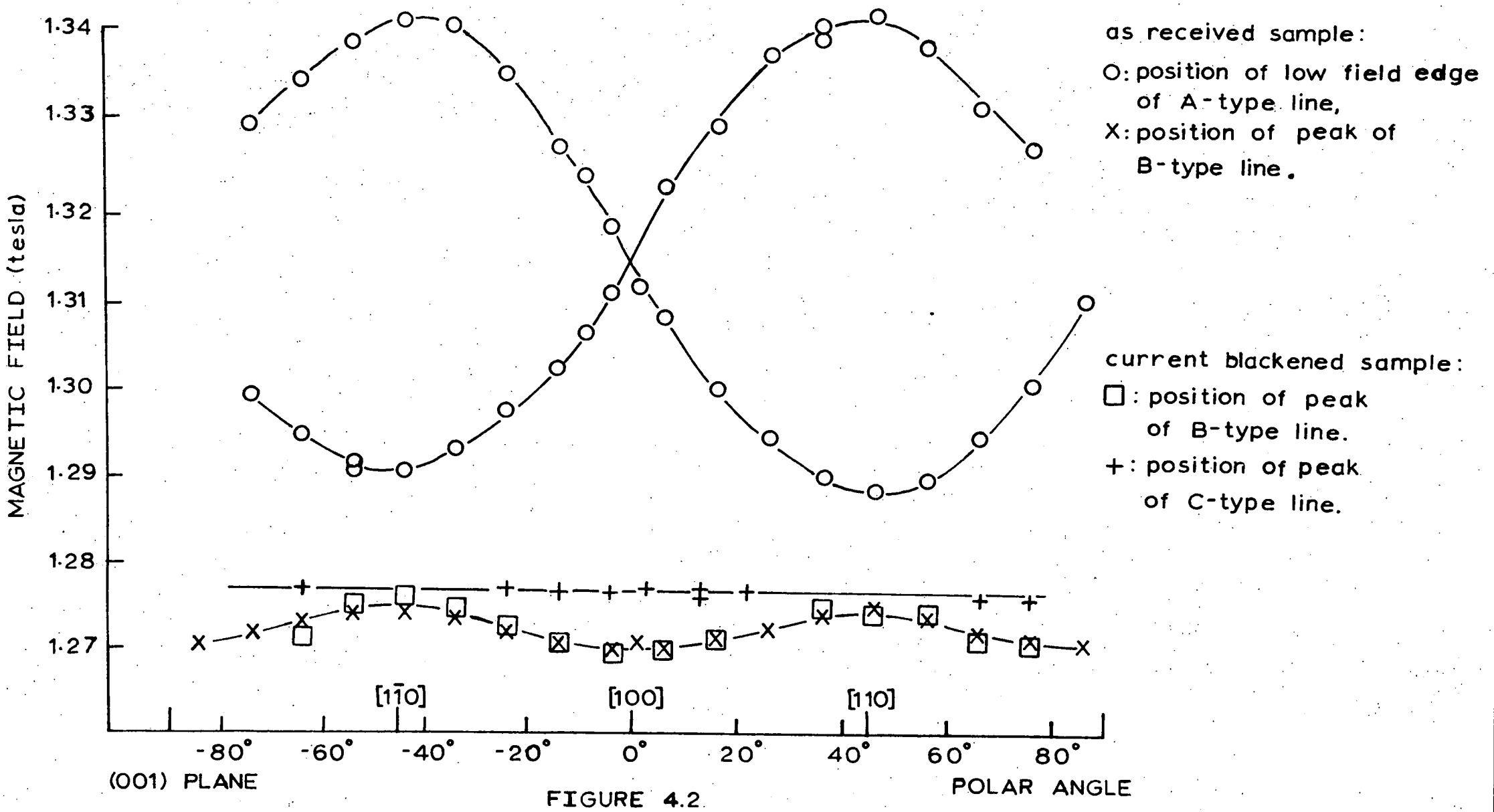

FIGURE 4.2

Variation with polar angle of line peak positions in as received and current blackened YSZ.

	Description of Sample	Type of line present (room temperature)	Result of Treatment (compared with 1)
1	As received (new)	A, B	Reference standard (type -A and type -B present)
2	As received (old)	B	Type -A not present
3	Heated in argon without current passage	B	Type -A not present
4	Current blackened (while heating in argon)	A, B, C	N.B. Type A is present
5	Heated in air or oxygen without current passage	B	Type -A not present
6	As (5) subsequently heated in vacuum at 1100°C for 3.5 h	B	Faint trace of Type -A lines

Table 4.1

Summary of electron spin resonance observed in yttria stabilized zirconia

have a principal axis along one of the ⟨111⟩ directions. This would mean that there were four alternative A-type sites corresponding to the four three-fold axes. Thus, for certain orientations of the magnetic field four type -A lines should be seen. Observations in the (111) plane supported this deduction. The intensities of the lines indicated that all four sites were occupied by roughly equal populations. The g-values of a given site was a maximum parallel to one of the ⟨111⟩ directions and a minimum (1.880 ± 0.002) perpendicular to it. The maximum g-value, calculated from the values observed in the {100} planes (see Appendix 4) was (2.003 ± 0.002); but direct observation, which was much hampered by the presence of the type -B line, suggested a lower value (2.000 ± 0.003).

The 'complex' $(Y_{Zr} \cdot V_O)^x$ (See Section 2.5) provides a possible model for this centre. This consists of two associated point defects. The first is a trapped electron in an oxygen vacancy which provides a free spin on an oxygen site. The other is a yttrium ion on one of the nearest neighbour zirconium sites. If the remaining three nearest zirconium sites were occupied by zirconium ions this would give the required axial symmetry. The electron paramagnetic resonance properties of F-centres in alkali halides, received by Markham (21) show g-values between 1.987 and 2.0029 with line-widths of more than 5 mT. The correspondence between these results and the behaviour of the type -A lines (coupled with their time and temperature dependence) supports the assignment of the line to this complex.

To explain the temperature variation of the conductivity of unblackened YSZ, Caillet (22) has proposed a model based on "free" and "trapped" oxygen vacancies. The vacancies were trapped by forming a complex with either one or two Y^{3+} ions. The model suggested here corresponds to Caillet's first "trapped" vacancy with the addition of an electron. With regard to blackened YSZ, Casselton (23) postulated that the onset of current blackening and an enhanced conductivity is accompanied by the injection of

electrons from the cathode. Using the model suggested this would be consistant with the re-appearance of type -A lines after current blackening since the complexes would act as electron traps.

The density of type -A centres in as received material was about 10^{24} m^{-3}; which implied that only 1 oxygen vacancy in 10^3 gave rise to a type -A centre (see Tables 3.4 and 3.5). However this ratio (f_a) is not the fraction of the oxygen vacancies which were trapped (f_t) since $f_a = f_t f_{te}$, where f_{te} is the fraction of the trapped vacancies which had trapped one electron. In blackened material f_{te} might approach unity, but unfortunately blackened material caused too much cavity damping to allow any estimate of the density of centres.

4.4.2 Type -B line

The type -B line was seen in all samples irrespective of treatment. The symmetry of the variation of resonance field with polar angle showed that the most likely location for this defect centre would be a cation site. The normal occupants of these sites, Zr^{4+} and Y^{3+} are diamagnetic and consequently would give no spin resonance spectra. The defect has not yet been positively identified.

A possible explanation may be the valency changes of the cations. Ionization energy considerations indicate that the ions most likely to be formed would be Zr^{3+} and Y^{2+}. This may apply in the reducing conditions created during crystal growth by electrofusion. If the type -B centre is due to one of these, it is however surprising that the centre is not destroyed by heating in oxygen. No resonance data on Zr^{3+} has been reported in the literature. However O'Connor (24) has reported electron spin resonance of Y^{2+} in CaF_2 at 4.2 K and quotes a g-value of 1.994 ± 0.005. This is similar to the mean g-value, (1.993), found for the type -B line. The observed intensity of the type -B line corresponded to a spin density of about 10^{24}

m^{-3}. On the assumption that Y^{2+} was responsible this would indicate that about 1 in 10^4 yttrium ions had changed their valency state.

An alternative possibility, that the type -B line might be due to an impurity, cannot be excluded although optical spectrographic analysis showed that the only major impurities present were hafnium (about 2.2%), titanium (300 ppm), calcium (100 ppm) and tantalum (300 ppm).

4.4.3 Type -C lines

The type -C lines only appeared after current passage. The line was isotropic, with g = 1.986 and its intensity (like those of the type -A and type -B lines) was not strongly dependent on temperature over the range studied.

A possible model for this site is an F-centre consisting of an oxygen vacancy with a trapped electron surrounded by a tetrahedron of zirconium ions. In as received material the existance of such a site would be more unlikely than the complex used to explain the type -A lines. The oxygen vacancies occur because yttrium is substituted for zirconium (approximately one vacancy is produced for two yttrium ions, see Section 2.3), and the cation tetrahedra in which yttrium is not substituted for zirconium would not be expected to have an associated vacancy. During current passage the applied potential may cause migration of vacancies and the injection of electrons. An electron trapped in a vacancy still associated with a yttrium ion would produce a type -A centre, but if the vacancy had broken free of its yttrium ion (and was therefore surrounded by zirconium ions) the centre would be type -C. Thus a type -C centre would be one of Caillet's "free" vacancies plus an electron.

Chapter 5.

Ultrasonic, optical and dielectric measurements

5.1 Ultrasonics

5.1.1 Aim

Solid material phase changes are usually associated with changes in the elastic constants and velocity of sound. It was hoped that comparison of these properties of yttria stabilized zirconia, before and after blackening, would reveal whether blackening was tending to cause de-stabilization (i.e. phase changes). These techniques had already been used by Pace et al. (16) 1969 to compare the elastic constants of as received 8.3 and 12 mole percent yttria stabilized zirconia. The present work was intended to extend the earlier work so as to compare as received and current blackened material. In the course of the present work some errors in the identification of acoustic modes made in the previous work were corrected.

5.1.2 Theory of the ultrasonics measurements

As the strains induced by ultrasonic waves are only of the order of 10^{-7}, Hooke's Law is valid and each stress component σ_{ij} can be considered as a linear homogeneous function of the strain components ϵ_{kl} :

$$\sigma_{ij} = C_{ijkl}\,\epsilon_{kl} \quad (i, j, k = 1, 2, 3) \qquad 5.1$$

where the connecting components are the elastic stiffnesses or moduli C_{ijkl}. The usual matrix notation giving these constants as C_{ij} is achieved by replacing 11 by 1, 22 by 2, 33 by 3, 23 by 4, 13 by 5 and 12 by 6. Symmetry in cubic crystals reduces the 6 x 6 array for C_{ijkl} in equation 5.1; so that only three independent elastic constants, C_{11}, C_{12} and C_{44}, remain. These can be determined from the velocities of three waves. Three suitable modes are propagated in the [110] direction with velocities (V) and particle displacements (q) as follows :

$$\rho V_1^2 = (C_{11} + C_{12} + 2C_{44})/2 = C_n \qquad 5.2\ a$$

q along [110] , longitudinal,

$$\rho V_{S001}^2 = C_{44}; \qquad 5.2\ b$$

q along [001] , shear,

$$\rho V_{S1\bar{1}0}^2 = (C_{11} - C_{12})/2 = C'; \qquad 5.2\ c$$

q along $[1\bar{1}0]$, shear,

where ρ is the density of the sample. The three constants C_n, C_{44} and C' can also be used to define the three independent stiffnesses and have direct physical significance. For the [110] direction a normal stress σ_n, as applied through the longitudinal sound wave inserted into the (110) face, produces a strain ϵ_n parallel to [110] and σ_n/ϵ_n is C_n. For shear waves propagating down the [110] direction, two physical situations occur; first, for atoms vibrating in the [001] direction the ratio of shear stress to shear strain is C_{44}; second, for forces parallel to $[1\bar{1}0]$, the ratio is C'.

Another simple deformation is a pure volume dilation without shear, expressed as the bulk modulus K, the measure of stiffness to volume dilation. This is given by :

$$K = -V\frac{dP}{dV} = \frac{C_{11} + 2C_{12}}{3} \qquad 5.3$$

where P is pressure and V is volume.

The elastic properties of a solid can also be expressed in terms of the elastic compliances S_{ijkl} defined by

$$\epsilon_{ij} = S_{ijkl}\,\sigma_{kl}. \qquad 5.4$$

In this relation S_{ijkl} is the reciprocal tensor of C_{ijkl}. The compliances of cubic crystals are given by :

$$S_{11} = \frac{-(C_{11} + C_{12})}{(C_{11} + 2C_{12})(C_{12} - C_{11})} \quad ; \qquad 5.5\ a$$

$$S_{12} = \frac{C_{12}}{(C_{11} + 2C_{12})(C_{12} - C_{11})} \quad ; \qquad 5.5\ b$$

$$S_{44} = \frac{1}{C_{44}} \qquad 5.5\ c$$

5.1.3 Experimental Techniques

An as-grown crystal, oriented by the symmetry of X-ray back-reflection Laue photographs to $\pm \frac{1}{2}^{o}$, was cut with a diamond wheel and polished to yield a sample 10 mm x 8 mm x 4.76 mm thick with faces (parallel to within 3 x 10^{-5} radians) perpendicular to the [110] axis and edges parallel to the $[1\bar{1}0]$ direction. This high degree of parallelism of faces was in order to keep the echoes reflecting to and fro in the same region. To achieve this finish the crystal was polished on a Logitech high precision polishing machine and the flatness achieved was checked using interferometric techniques using an optical flat as a reference standard.

Quartz X- and Y- cut transducers, 5 mm in diameter, were used to generate the ultrasound at carrier frequencies of around both 15 MHz and 45 MHz. "Nonaq" stop-cock grease formed a satisfactory transducer-to-specimen bond from about 283 to 77 K. The transducer was pressed on a spot of the grease and was moved round the surface of the sample until it stuck, indicating that the bond was thin enough. The pressure was applied through a small pad of cotton wool. To excite each of the shear modes, the vibration direction (x-axis) of a Y-cut transducer

was very carefully aligned parallel to each of the requisite particle displacement directions, in turn. After measurements had been made on the crystal in the as-grown state, it was blackened by passing a current of 1.00 A between faces (of area $\simeq$ 40 mm^2) cut parallel to the (001) planes, in an Argon atmosphere at 800°C for 10 minutes. This treatment was sufficient to produce marked visual blackening without causing fragmentation. The measurements of the variation of ultrasonic wave transit times with temperature, made using the pulse superposition technique, were then repeated.

The sample was placed in the sample-holder shown in Figure 5.1. This whole apparatus was enclosed in a conventional cyrostat system for working with liquid nitrogen. Further temperature control was provided by the electrical heater. The temperature was measured using a copper-constantan thermocouple, which was glued to the sample with low temperature glue to provide good thermal contact. Electrical contact to the outer electrode on the transducer was via silver dag painted onto the surface of the crystal.

The method illustrated is the arrangement for the "single ended technique"; in other words, the same transducer injects pulses of ultrasound into the sample (under the influence of an r.f. electrical signal) and detects the echoes (producing an electrical signal). A T-R junction is needed to protect the receiver by directing most of the driving signal into the transducer and shielding the receiver, while allowing signal from the transducer to reach the receiver. The pulse superposition technique requires echoes from many different driving pulses to superpose. For this reason it works best for materials which do not strongly absorb or scatter ultrasound; so that each echo train contains many echoes. YSZ is not ideal in this respect, but never-the-less changes (due to temperature variations) of less than 0.1% in the time taken for sound to travel through the sample are

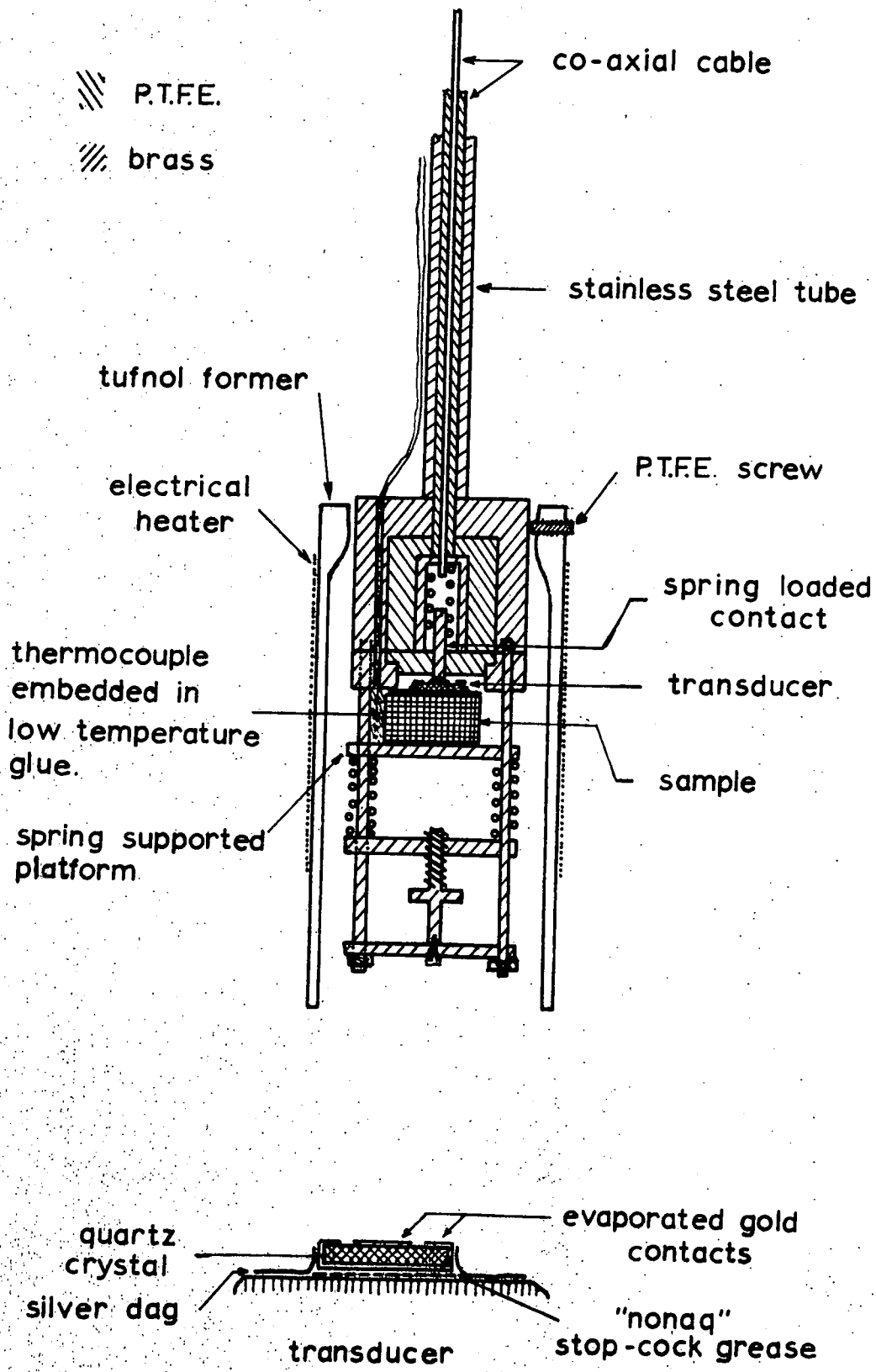

FIGURE 5.1
ULTRASONIC SAMPLE HOLDER

measurable.

This accuracy is achieved by measuring the frequency (ν_p) at which driving pulses must be repeated in order to synchronize these pulses with the echoes. To a first approximation, synchronization is achieved when, in the time between pulses, the ultrasound travels from the top to the bottom of the sample and back, p times, where p is an integer. When the wave is reflected off a surface it normally undergoes a phase change (which depends on the relative acoustic impedances of the bonding material and the crystal and the thickness of the bond), and this may also effect the synchronization. However this involves a timing error of less than half the periodic time of the carrier wave, per reflection, probably considerably less. A final difficulty is that partial synchronization is achieved if the pulses are n carrier wavelengths out of step, where n is an integer.

The circuit used is shown in Figure 5.2. The frequency synthesiser produced a frequency which was selected by decade knobs. This determined the frequency at which the pulse generator operated and hence the repetition frequency of the r.f. pulses from the oscillator. The carrier frequency produced by the oscillator and the working frequency of the pre-amplifier were together tuned to a resonant frequency of the transducer by trial and error. This maximised the detected signal. The envelopes of the pulses were displayed on the oscilloscope, which was supplied by a calibrated, variable delay in the triggering to sweep 'A'. Gate A provided an output while sweep A was sweeping, and this supressed the driving ultrasonic pulses in this period. Thus the driving pulses were periodically cut off so that the resulting echo pattern could be observed without interference. The pulse repetition frequency was adjusted to maximise the height of the echoes, which indicated that the driving pulses and echoes were synchronized.

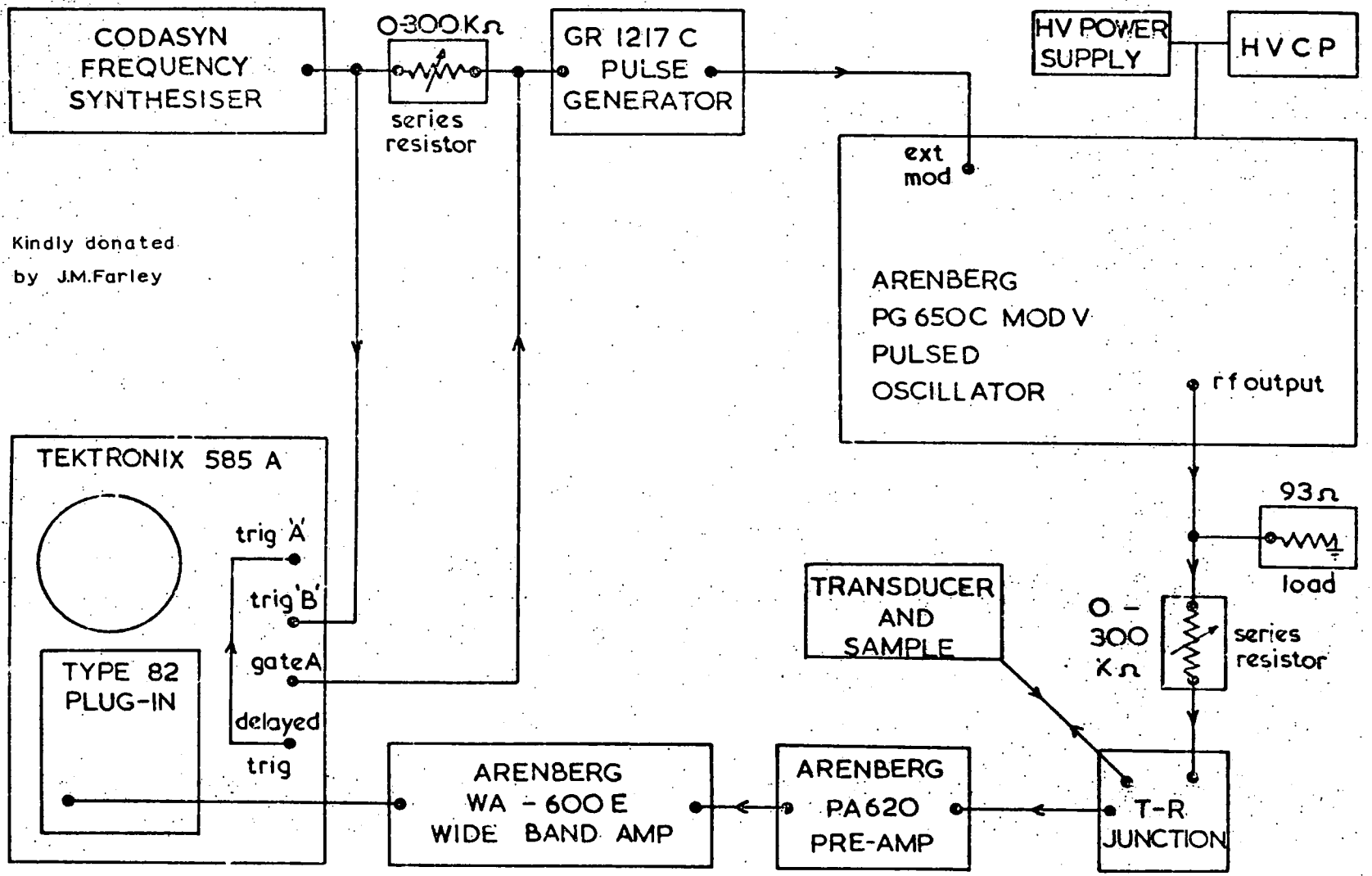

BLOCK DIAGRAM OF PULSE SUPERPOSITION EQUIPMENT.

FIGURE 5.2

In practise a series of maxima were observed (corresponding to n = 0, 1, 2 etc). These were equally spaced, the spacing being inversely proportional to the carrier frequency. Selecting the correct maximum (n = 0) was troublesome and for this reason the low carrier frequency was preferred. To identify the maximum, the echoes from a single pulse were observed by turning down the pulse repetition frequency. The variable delay was used to measure the time lapse (Δ) between two echoes, which were as widely separated as possible. This was compared with the corresponding time lapse (t) for each of the maximised echo patterns. In a good set of maxima the difference ($t - \Delta$) changed by a constant amount on going from any maximum to the next, and for one maximum ($t - \Delta$) was almost zero. The later maximum was taken to be the correct one. The value of p was deduced from the measured magnitude of Δ since approximately,

$$p \simeq \frac{1}{\nu_p \Delta} . \qquad 5.6a$$

More accurately :

$$p \Delta = \frac{1}{\nu_p} - \frac{n}{\nu_c} + \frac{p\theta}{\nu_c} \qquad 5.7$$

where ν_p is the pulse repetition frequency, ν_c is the carrier frequency and θ is the phase change (in wavelengths) when the wave is reflected. Since n was supposed to be zero and measuring θ would have been an involved operation it was assumed that

$$p \nu_p = 1/\Delta \qquad 5.6b$$

For this reason the velocity (V) of sound was calculated from

$$V = 2 p \nu_p d \qquad 5.8$$

However the variation of transit time with temperature can be found to greater accuracy than the transit time itself; if the properties of the bond

do not change. Using equation 5.7 it can be shown that; since $\frac{\nu_p}{\nu_c}$ is small :

$$\frac{\Delta(0^\circ C)}{\Delta(T^\circ C)} \simeq \frac{\nu_p(T^\circ C)}{\nu_p(0^\circ C)} \left(1 + \frac{\phi\, p}{\nu_c}\left(\nu_p(T^\circ C) - \nu_p(0^\circ C)\right)\right) \qquad 5.9a$$

$$= \frac{\nu_p(T^\circ C)}{\nu_p(0^\circ C)} (1 + \epsilon) \qquad 5.9b$$

where $\phi = \theta - \frac{n}{p}$ and $\epsilon = \frac{\phi\, p}{\nu_c}\left(\nu_p(T^\circ C) - \nu_p(0^\circ C)\right)$.

Note that transit time depends on wave velocity and sample thickness and that both are effected by temperature.

5.1.4 Results and Discussion

The velocities of the ultrasound in 8.3 mole % YSZ at $0^\circ C$ were calculated as :

$V_1 = 7.05$, $V_{S001} = 3.05$, $V_{S1\bar{1}0} = 5.02$

(units km/s, accuracy $\pm$ 1%).

To this accuracy the values were the same before and after blackening. It is worth noting that in the worst cases : failure to make $n = 0$ would result in an error of 1.7 n % (for $V_{S1\bar{1}0}$), and the error due to θ is 5θ % (for V_1) (N.B. $\theta \leq \frac{1}{2}$).

Comparison with the data published by Pace et. al. shows that the modes designated fast and slow were incorrectly identified and must be interchanged. (This was confirmed by Pace on consulting his experimental log book). When this alteration is made, the velocities from the previous and present work agree to within the experimental error of $\pm$ 1%. The corrected values of the elastic constants, using the measured density of 6.00×10^3 kg/m^3 are listed in table 5.1.

Elastic - stiffness constants ($\times 10^{11}$ Nm^{-2})		Elastic - compliance constants ($\times 10^{-12}$ m^2N^{-1})	
C_{11}	3.94	S_{11}	2.78
C_{12}	0.91	S_{12}	-0.52
C_{44}	0.56	S_{44}	18.1
Bulk modulus K: $\frac{C_{11} + 2C_{12}}{3} = 1.9 \times 10^{11}$ Nm^{-2}		Anisotropy ratio: $\frac{2C_{44}}{C_{11} - C_{12}} = 0.37$	
Cauchy relation $\frac{C_{12}}{C_{44}} = 1.6$			

Table 5.1

Elastic constant data for 8.3 mole % YSZ.

If the inter-atomic forces are central then the Cauchy relation ($C_{12} = C_{44}$) should hold. The fact that it does not is further evidence that YSZ is not purely ionic.

A comparison of results before and after blackening is made in Figure 5.3. The ratio of the pulse repetition frequencies is almost the reciprocal of the ratio of the transit times, and the latter depends only on the sample. Quantitatively : $\epsilon < 0.04\ \phi\ \%$ (see equation 5.9) and ϕ is probably less than one. Within the experimental error the velocities and their temperature dependence are unaltered. Hence the elastic constants in the as received and blackened states, and thus the lattice stabilities, are the same. This correlates with X-ray evidence that the lattice parameter remains unaltered after blackening at low current densities. In the blackened crystal there was a marked deterioration of echo quality and some intermediate echoes also appeared : the blackened crystal shows the characteristics expected in an inhomogeneous material.

5.2 Optical Scattering

5.2.1 Introduction

The experiment described below was a development of one devised by Dr. D.F. Crabtree to search for evidence for the formation of metallic particles in electrolysed yttria stabilized zirconia.

Since yttria stabilized zirconia (at least in its as grown state) is an ionic conductor, the passage of current through a sample is likely to result in electrolysis. In that event the metal need not necessarily be deposited on the cathode, for, if a number of oxygen vacancies coagulated as they travelled towards the cathode the result would be the formation of a small metallic particle at that position. Although the particle would have a positive charge this could be neutralised if electrons were injected into the solid from the cathode. The high field that this would require

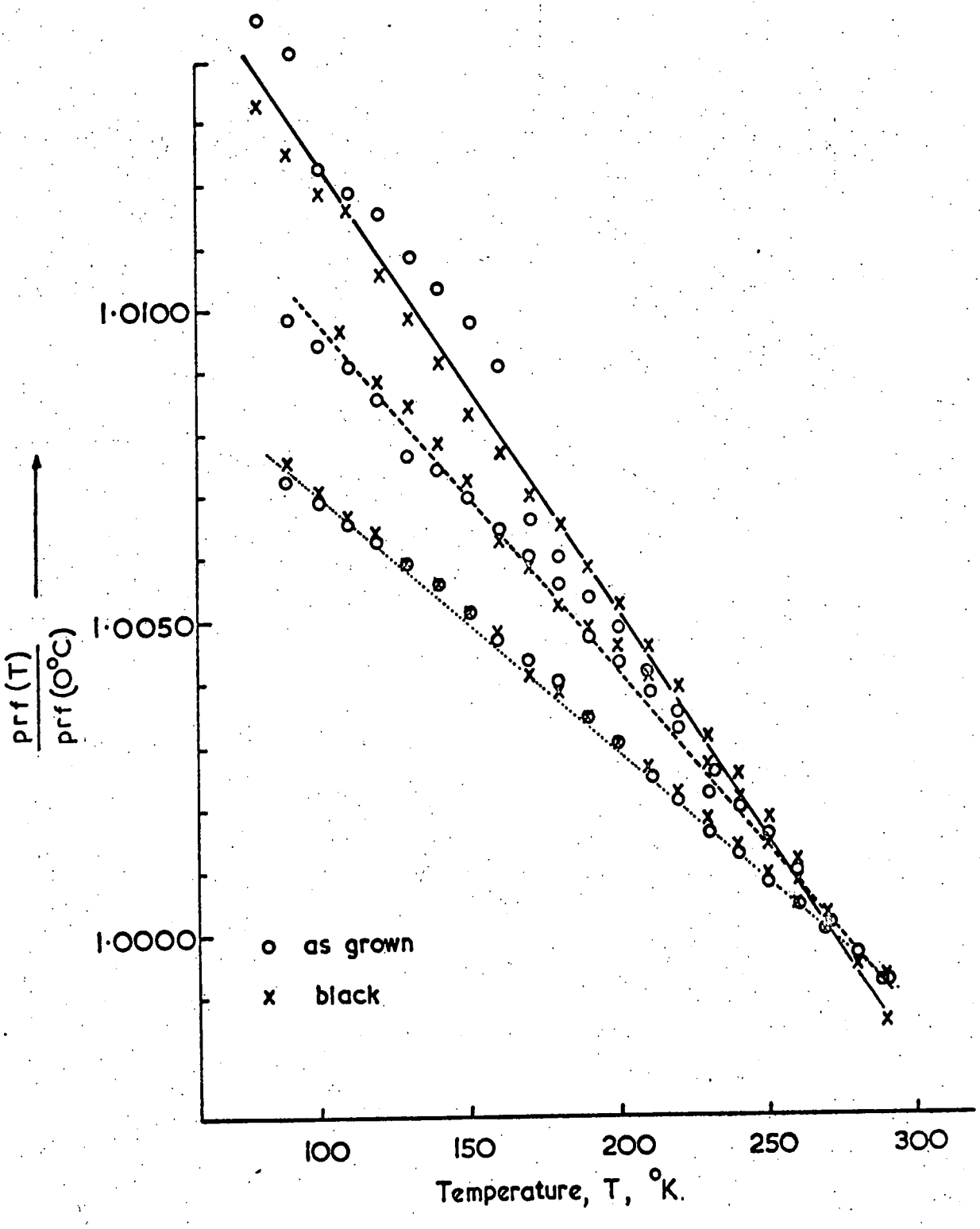

Comparison of temperature dependencies in as grown and current blackened 8 mole percent YSZ single crystals.

ey : open circles, as grown ; crosses, blackened. Full line, shear mode with q along [001]. Chain line, shear mode with q along [1$\bar{1}$0]. Dotted line, longitudinal mode. q is the polarization vector.

FIGURE 5.3

is believed to exist while current blackening is taking place. A collection of such particles, having a different refractive index from the matrix, would give rise to optical scattering. The scattered intensity might either be independent of the wavelength of the light or inversely proportional to its fourth power, depending on the size of the particles relative to the wavelength. The intermediate case, where the dimensions of the particles are similar to the wavelength, was considered, for spherical particles, by Mie. He concluded that scattered intensity, as a function of wavelength, would have a maximum. (See Born & Wolf (25))

5.2.2 Experimental

As a guide to deciding what really were the effects resulting from electrolysis, investigations were made of optical scattering from as received samples and samples whitened by heat treatment as well as from current blackened samples. The samples were cut into rectangular blocks (approximate dimensions = 10 mm x 5 mm x 5 mm). Light from a D 285 Hilger and Watts spectrometer was focussed into one side of the sample. The beam was viewed through a side perpendicular to the first using a Vickers M12a metallurgical microscope to observe the scattered light. The sides of the sample through which the incident light entered and the scattered light left were polished. The microscope had a camera attachment on which a photomultiplier was mounted instead of a camera. Depending on the position of a lever either the area under observation could be viewed or the light could be directed to an exposure-meter. While the photomultiplier was in use the lever was left in its latter position to minimise stray light. The arrangement is shown in figure 5.4. Great care was taken to exclude stray light. To avoid recording light reflected from the surfaces, rather than that scattered in the bulk of the crystal, the incident beam and the area observed were both kept away from the edge of

photograph of the apparatus

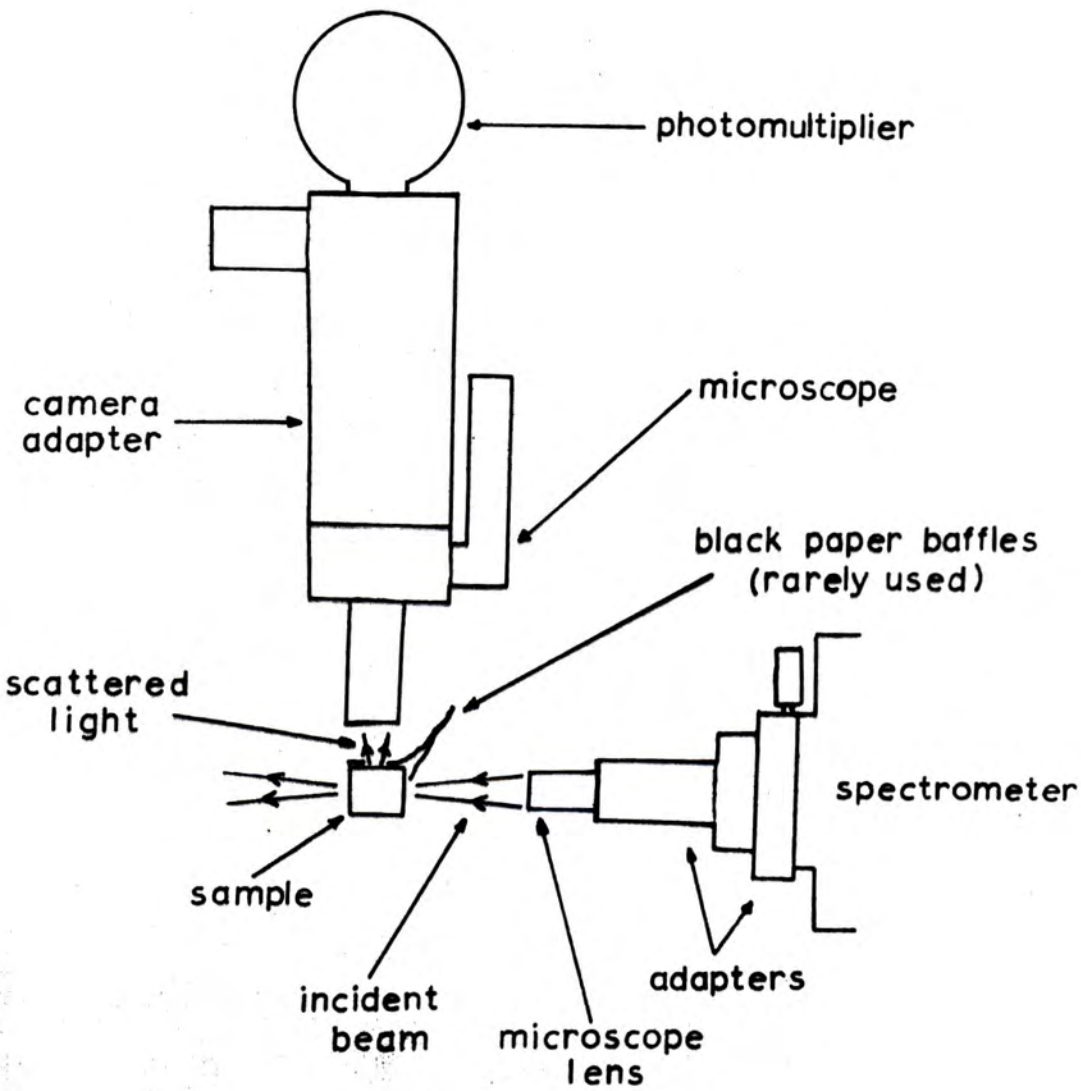

OPTICAL SCATTERING APPARATUS
FIGURE 5.4

the crystal. To find the position of the area under observation it was only necessary to switch on the lamp in the microscope, which illuminated the area in question. The field iris was adjusted so that the illumination just filled the field of view. The lamp was switched off before any measurements were made. This procedure appeared to be successful, for attempts to improve on it by using black paper baffles did not result in any improvement. In some cases, where the sample had been badly cracked by the treatment it had undergone, bright spots were seen under the microscope, where light had been channeled through the cracks. Such spots were avoided when making scattering measurements.

The photomultiplier current due to scattered light was found as a function of wavelength. The current was measured with a galvanometer.

The calibration was usually checked, before and after each run by attaching the photo-multiplier directly to the spectrometer (with the slits at a set width). That the effect of the microscope on the calibration was negligible ($< 20\%$) was shown in two ways. In the first the sample was replaced by a mirror which reflected the light straight into the microscope. In the second the microscope was laid horizontally so that the light entered it directly.

The intensity of the light falling on the photomultiplier was controlled by the widths of the slits on the spectrometer. For each sample these widths were set at different values (these were noted); so that the photomultiplier current remained within a reasonable range. It was found that, as expected, the photomultiplier current was proportional to the exit slit width.

5.2.3 Results and Discussion

The results are shown in figure 5.5. The "relative scattering" has been calculated from the formula :

OPTICAL SCATTERING IN YTTRIA STABILIZED ZIRCONIA

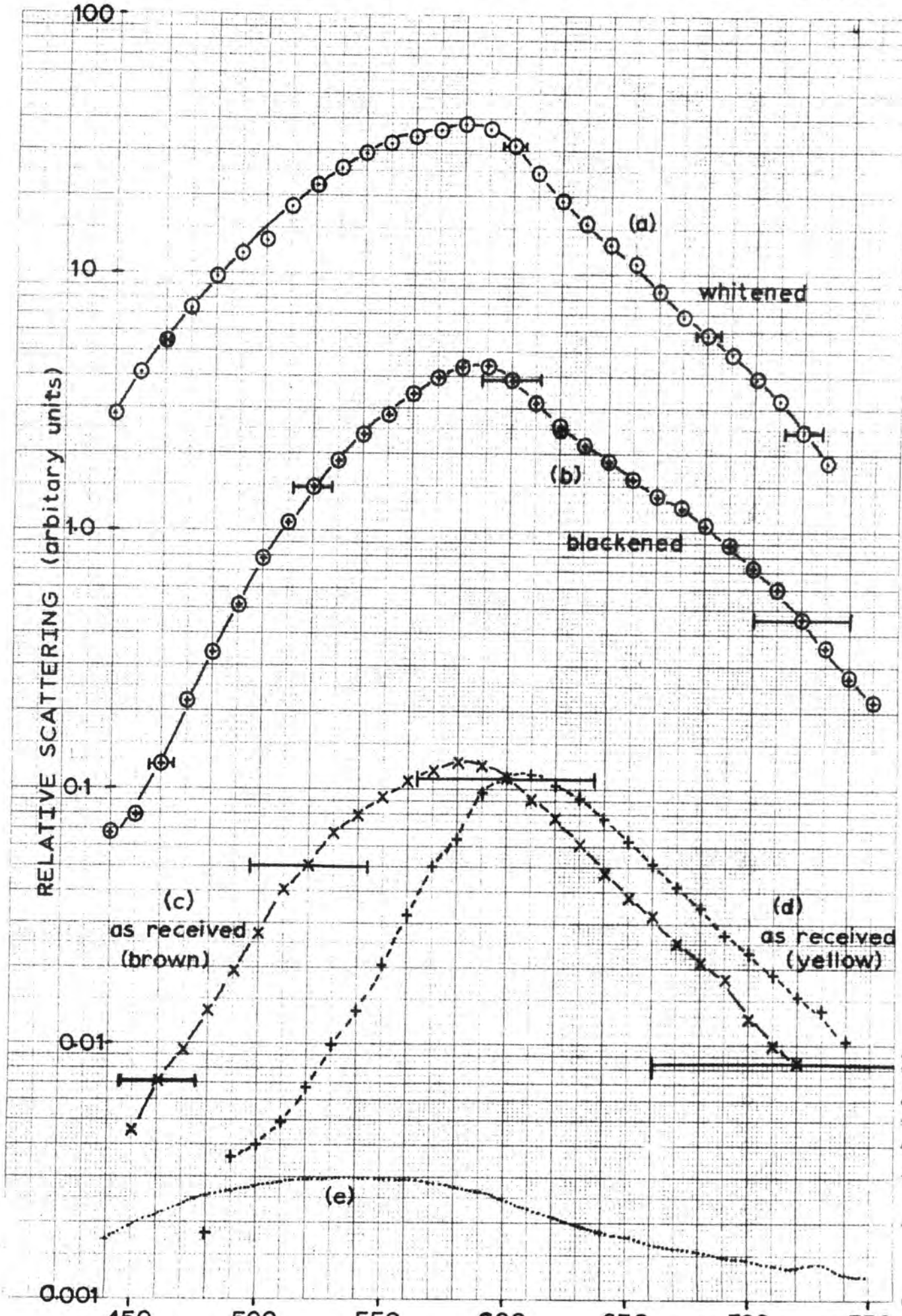

FIGURE 5.5

$$\text{"relative scattering"} = \frac{g}{g_o w_i w_e}, \qquad 5.10$$

where w_i and w_e are respectively the entrance and exit slit widths on the spectrometer, while the intensity of the scattered light was being measured, g is the galvanometer deflection due to scattered light at the wavelength in question and g_o is the corresponding calibration deflection. g_o is a function of wavelength (λ) which includes the effects of the lamp, the spectrometer and the photomultiplier. Since the calibration curves found did not greatly differ from each other an average curve was used.

Provided that loss of beam intensity in the sample (due to either scattering or absorption) is not serious "relative scattering" as defined above should provide a true comparison of scattering from different samples. It is worth noting that the scattered light recorded was always less than 1% of the incident light.

The as received crystals scattered least light, so for them the slits were opened widest, which gave the spectrometer a wide pass-band. This resulted in the larger error-bars on the curves for as received samples and the smaller ones on the whitened samples.

Curves (a), (b) and (c) all peak at 585 nm and have the same shape. Since they are for a sample whitened by heating in oxygen (S7), a current blackened sample (DFC1) and a brown as received sample (S19 ii), respectively, the scattering is obviously not due to metallic particles. The scattering curve (d) obtained for a yellow as received crystal (S19 iii) was reproducibly different from the others and this indicates that the curves were not merely due to the apparatus. The shape of the calibration curve (e), shown for comparison, is completely different from that of the scattering curves. Curve (b) would probably fall nearer curve (a) if optical absorption in the blackened sample was corrected for.

If the curves were due to Mie scattering, then they would indicate

that both heating in oxygen and current blackening produced an increase in number of these centres without changing the size of the centres. This seems highly unlikely. One thing that is common to both whitened and blackened samples is that both are considerably cracked; so it would seem, not surprisingly, that more cracked samples scattered more light. Why micro-cracks should lead to a maximum scattered intensity at such a definite and unchangeable wavelength is, however, obscure. It might possibly be some multiple scattering effect.

More recent measurements have been made by Mrs. H.P. Buckley using an integrating sphere (9). These indicate that whitened samples scatter light, but absorb little, that the reverse is true of blackened samples and that as received samples give both low scattering and low absorption. However the scattering curves obtained are considerably different to those recorded above.

5.3 Dielectric Measurements

This section describes how and why preliminary measurements of the relative permittivity of Yttria stabilized Zirconia were made and outlines attempts to measure loss in the material. During the ESR studies of YSZ it became obvious that current blackening made the material more lossy The Q-factor of the cavity was decreased much more by a blackened sample than by an as received sample. This suggested that dielectric conductivity might be a useful parameter for degree of blackening. The concept of dielectric conductivity (σ_d) is one way of representing the sum of all loss mechanisms in the material (26) Mr. F. Gfeller had just suceeded in measuring the conductivity of a block of germanium, which just fitted into number 22 wave guide (3.56 mm x 7.11 mm), by measuring the fractions of microwave power which the block reflected and transmitted. This seemed an easier way of measuring dielectric conductivity than using a cavity method.

The method also avoided the need to produce thin, uncracked and robust samples of blackened YSZ, such as would be needed to make parallel plate capacitors. Mr. F. Gfeller's method required the relative permittivity of the sample to be known and found the conductivity by iteration (see Appendix 5). It appeared to be feasible to start with an approximation for relative permittivity (ϵ'_r) and iterate to find two unknowns (ϵ'_r and σ_d). (The measurements described below were intended to provide the first approximation). The method had some success with germanium but the results for YSZ indicated that multiple reflections in the sample were significant. When the computer program which performed the iterations was modified to take account of this, convergence was obtained. However the results for both as received and blackened YSZ were unreliable.

The relative permittivity of as received YSZ was measured at 1 kHz using thin parallel sided slices of the material. Circular silver electrodes were deposited on both sides of the slices, taking care that the electrodes were directly opposite each other. The capacitance (C) of the arrangement was measured using a Wayne-Kerr bridge. The thickness (d) of the slice was measured in several places using a micrometer, and the lengths of two mutually perpendicular diameters of the electrodes were found using a travelling microscope. The results are given in Table 5.2. These are not only scattered but are also high compared with values found by other investigators. Harrop and Wanklyn (42) quote a value of 22 $\pm$ 3 for the relative permittivity of pure zirconia (in agreement with other authors) and 27 $\pm$ 4 for polycrystalline Magnesia stabilized Zirconia. The scatter of results might be explained by the presence of stray capacitance, for although when this was measured it appeared to be less than 0.1 pF, the results do fit a straight line of the type $C = Co + \epsilon A/d$ rather well. If A is the area of the electrodes and ϵ is the permittivity, a best straight line fit makes Co, (the stray capacitance) 0.8 pF. This also gives an 'average' relative permittivity for Yttria stabilized Zirconia of 32.

However these measurements can only be regarded as being preliminary. Since they were made Mrs. H.P. Buckley has used more involved methods to find the dielectric constant and loss tangent of both as received and blackened YSZ (10).

Sample	thickness (mm)	electrode diameter (mm)	capacitance (pF)	relative permittivity
R8	0.96 to 0.92	6.5 6.57 6.65 6.61 9.38 9.36	10.5 10.4 10.9 10.6 20.0 20.0	33.7 32.6 33.4 32.8 30.8 30.9
R6	0.275	9.33 6.66 9.6	58 36.4 72.6	26.4 32.5 30.6
R4	1.37	9.31 6.63 9.33	16.6 8.7 16.2	37.8 39.1 36.8
R7	1.54	9.32 6.69 9.39	15.4 8.6 15.4	39.4 42.6 38.8
R38a R38b R38c R38d	0.09 0.47 0.63 0.41	6.63 6.6 6.6 6.59	118 21.3 16.2 24.1	34.8 33.1 33.7 33.4

Table 5.2

Dielectric measurements on Yttria stabilized Zirconia

Chapter 6.

Low Field Conductivity

6.1 The term "low field" is taken here to indicate conditions for which blackening does not occur. This will later be found to mean that the oxygen supply is sufficient to cope with the current densities used. The chapter will describe how the high temperature conductivity of YSZ came to be explained in terms of movement of oxygen vacancies, and how the detailed variation of conductivity with temperature led to the idea of 'trapped' vacancies,or complexes. The chapter ends by describing an experiment in which the temperature variation of conductivity of single crystal YSZ was measured.

6.2 Previous Work and Theory

The conducting properties of YSZ have long been used in a type of lamp called the Nerst glower. It was in order to explain the conduction mechanism and evolution of oxygen in these devices that Wagner invoked the idea of oxygen vacancies.

At high temperatures the oxygen vacancies are mobile. Since they are effectively positively charged they will tend to migrate to the cathode when an electric field is applied. Thus the YSZ is electrically conducting. Provided a supply of oxygen can get through, or along the surfaces of, the electrodes, a closed cycle will be set up. Vacancies will be created at the anode (liberating oxygen) and filled at the cathode. The electrode processes can be represented by the equation :

$$2\,V_O^{\cdot\cdot} + O_2\,(gas) + 4e^- \underset{\text{at anode}}{\overset{\text{at cathode}}{\rightleftharpoons}} 2O_O^X \qquad 6.1$$

The conductivity (σ) due to a fixed concentration of vacancies at absolute temperature (T) is given by the equation :

$$\sigma T = A e^{-E/kT} \qquad 6.2$$

where A is a constant, E is an activation energy and k is Boltzmann's constant. It seemed reasonable to suppose that in YSZ the vacancy concentration depended only on the Yttria concentration and so, for a given sample, was fixed. Various authors (e.g. D.W. Strickler and W.G. Carlson 1965 (4), A.M. Antony 1965 (27), D.B. Meadowcraft 1969 (6) and J.E. Bauerle & J. Hrizo 1969 (28) have made measurements of the conductivity of YSZ as a function of temperature and composition. A.C. methods were usually used to avoid the effects of electrolysis. R.E.W. Casselton, who was working in loose colloboration with our group, has made such studies (29) and the results of the experiment described in Section 6.3 of this thesis has been published with his work (R.E.W. Casselton, J.S. Thorp and D.A. Wright 1969 (30)). A more detailed and comprehensive survey of conductivity measurements can be found in Casselton's thesis, Chapter 8 (P.85). Most of the measurements were made on polycrystalline samples; only Casselton's group and ours seemed to have used single crystals, but no significant difference has been observed between the two types of samples.

There was widespread agreement that :

1. experimental fits to equation 6.2 were obtained, under low field conditions,
2. at any given temperature the conductivity variation with composition was such that the conductivity was a maximum when the yttria concentration was a minimum for stabilization. (Since the vacancy concentration increases with increasing Yttria concentration this result is surprising. It is due to an increase in activation energy with Yttria concentration. It has been tentatively suggested that this could be caused by either strain

produced by the size difference of the two cations, or by the vacancies either clustering or becoming ordered. The precise mechanism is not understood).

The transport number of the Oxygen ions (i.e. the fraction of the total current they carry) was found to be very close to unity (31 , 32).

However close inspection of the graphed results revealed a curvature about five times greater than that due to the normal practice of plotting $\ln \sigma$ against $\frac{1}{T}$ instead of $\ln (\sigma T)$ against $\frac{1}{T}$. Bauerle and Hrizo made precision measurements (0.3%) on a stable sample of YSZ and fitted the resulting curve to the equation :

$$\frac{\rho}{T} = A_1 e^{E_1/kT} + A_2 e^{E_2/kT} \qquad 6.3$$

within experimental accuracy. (ρ is resistivity). They stated two possible interpretations of this equation :

(a) that the vacancies could be trapped (probably by the Yttrium ions),

(b) that the grains (their sample was polycrystalline) were coated in a thin layer of yttria enriched material (thickness 50 nm).

Since Casselton made similar observations on single crystal material he concentrated only on the first interpretation.*1 He analysed his graphs of $\ln \sigma$ against $\frac{1}{T}$ (T = 820 K to 1720 K), into three straight line regions, which suggested the existence of two types of trap. These he explained by assuming that an Oxygen vacancy could be associated with one or two Yttrium ions to form complexes $(Y_{Zr}, Vo)^{\cdot}$ or $(2Y_{Zr}, Vo)^{x}$ respectively (see Section 2.5), as postulated by Caillat et al. 1968 (22).*2 He used this model to formulate a semi-quantitative theory of conductivity and found it more successful than either a trap free or a single

trap model. It did not explain the decrease in conductivity with increasing Yttria concentration. To sum up :

(1) low field electrical conductivity in YSZ is almost entirely due to Oxygen vacancy migration,

(2) the vacancies can be trapped, probably by the Yttrium "ions" and probably in more ways than one, to form such complexes as $(Y_{Zr}, V_o)^{\circ}$ and $(2Y_{Zr}, V_O)^{x}$.

*1 However it should be noted that by the time he had completed his normal procedure of "restoring the crystals to stoichiometry" by heating in air the crystals were extensively cracked.

*2 These authors had rejected the complex $(Y_{Zr}, V_O)^{x}$ because an electron-hole contribution to the conduction was anticipated but not observed. However Casselton and Scott 1967 (33) found that under d.c. conditions, when the ambient gas flow was opposed to the direction of flow of the Oxygen vacancies and when the temperature was above 1100 K there was a small dependence of conductivity on Oxygen partial pressure. This dependence was consistent with a hole contribution to conductivity.

6.3 An experiment to measure the temperature variation of conductivity of a single crystal of $(Y_2O_3)_{0.917}$ $(ZrO_2)_{0.083}$

This experiment was originally intended to obtain measurements for comparison with those of Bauerle and Hrizo made on a polycrystalline sample. In particular single crystal measurements should be able to distinguish between the two interpretations since only their interpretation a) would apply for single crystals. (See equation 6.3 and surrounding explanation). It rather degenerated into an investigation of the difficulties involved. Preventing the single crystal breaking up was a major problem. If single crystal YSZ is heated in air or oxygen it breaks up ("whitens" see Section 3.2.1) although it will pass an electric current without "blackening". If instead it is heated in an inert atmosphere the fragmentation is slowed (Section 3.2.2). However if then an electric current is passed through it, it "blackens". This changes its conductivity and also causes fragmentation. In this experiment a compromise was adopted. The experiment was performed in the blackening apparatus (Figure 6.1(a)) with the argon flowing but with the rubber tube R not connected, so as to allow air into the apparatus. Thus the atmosphere was an air-argon mixture. The samples used for this experiment and the early blackening experiments were 10 mm x 5 mm x 5 mm blocks. Current electrodes of Platinum foil were attached to the small faces using Platinum paste, which was then baked at 1070 K. Similarly Platinum voltage electrodes were pasted into shallow grooves cut 2.5 mm from these faces. The samples were held by clamping between the current electrodes as shown in Figure 6.1(b). Current was measured with a scalamp Galvanometer or an Avometer as appropriate and voltage with a Phillips GM 6020 valve voltmeter. The temperature was read from the temperature controller which used a single Pt - 13% RhPt thermocouple close to the sample. The controller was calibrated using a similar

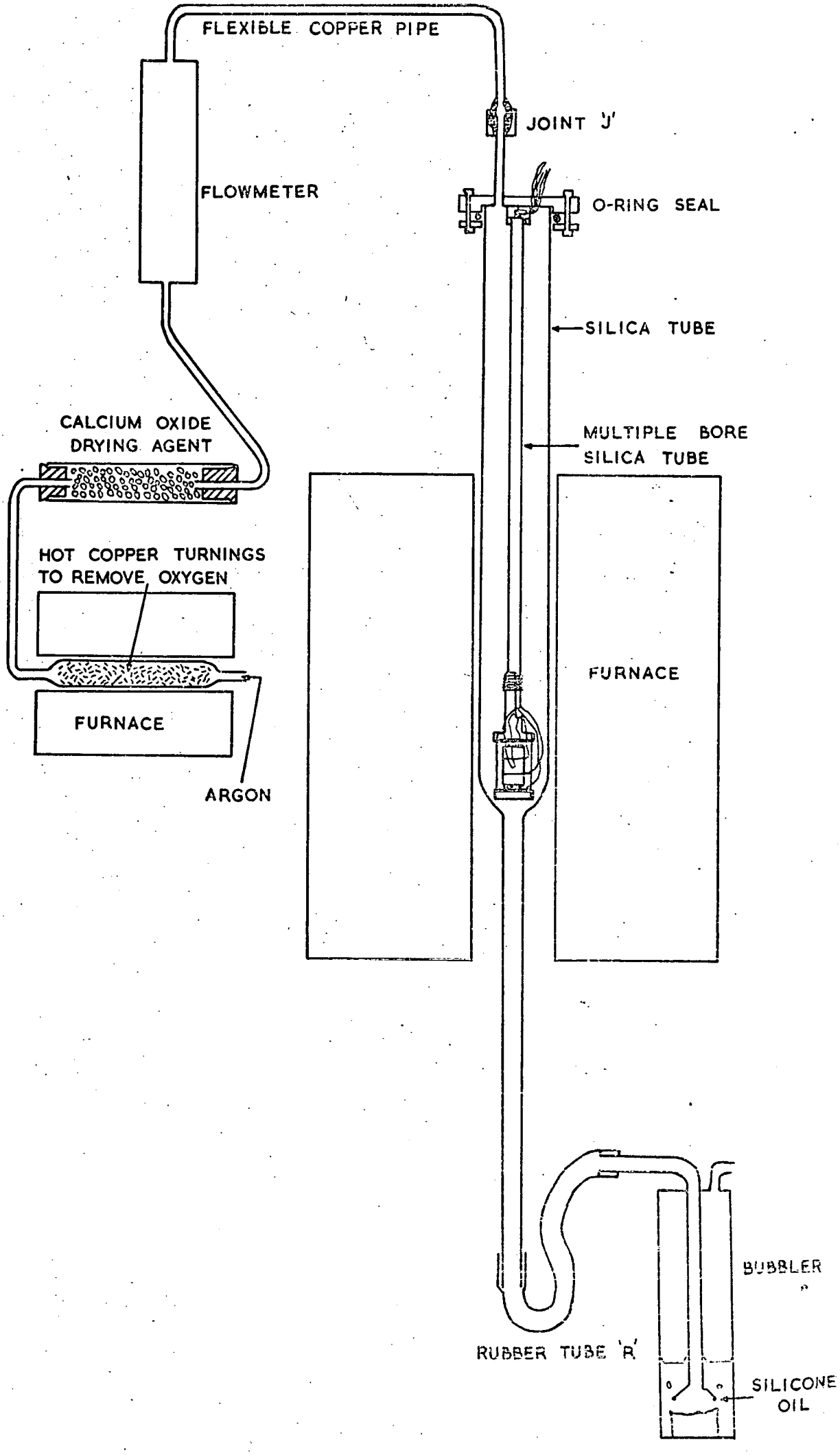

FIG. 61a Apparatus for high temperature electrolysis ; general arrangement.

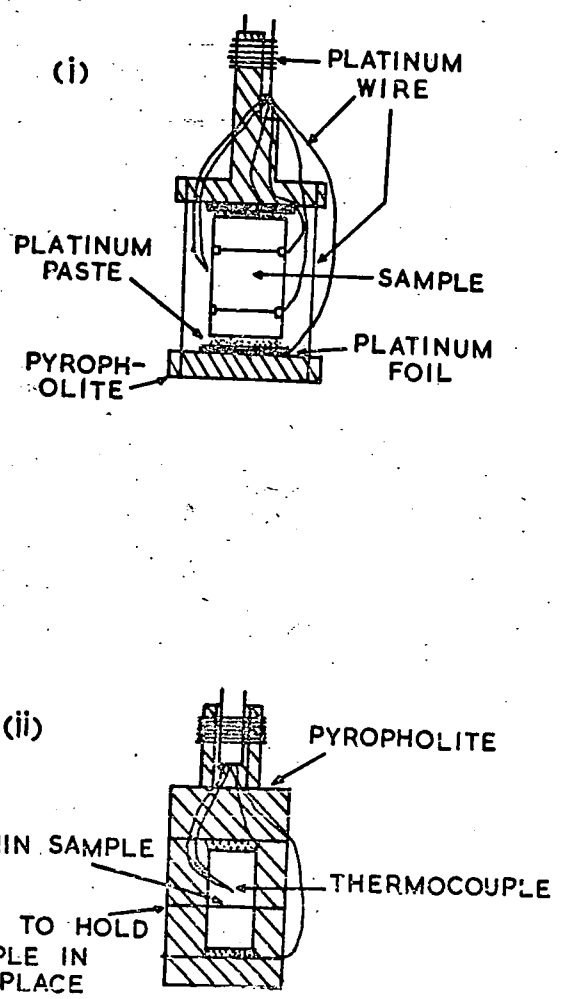

FIG. 6.1b Apparatus for high temperature electrolysis; detail of sample holders.

thermocouple.

As a precaution against thermoelectric voltages and to show that blackening was not occurring, the potential difference between the voltage probe was measured as a function of current through the sample for each temperature. The resistance was taken from the slope of the graph of voltage against current. The stages of recovery from the polarization effects associated with the onset of blackening are shown in Figure 6.2. The current voltage plot was initially linear, region A1 on Figure 6.2. Departure of the graph from a straight line had been found to indicate the onset of blackening (A2). The onset of blackening did not necessarily signify the end of the useful life of the crystal. The crystal could recover if left at a high temperature with the current off (A3), provided the blackening had not gone too far. Curves B and C indicate the behaviour after partial recovery. The sample was then left for over four hours without current passage before its resistance was measured (Curve D). The slope of this line (55 Ω) agreed closely with that of the initial run (slope 57 Ω) indicating that recovery was complete).

As is also shown in this figure, pick-up from the furnace was a serious problem, particularly when the furnace was switching in its temperature control cycle. Before a current was passed voltage was detected. The two points numbered "-1" (i.e. one minute before the start) in the diagram show the voltage detected with no current when the furnace was on and off. That there should be a voltage anything like as big as 64 mV with the furnace off is highly disturbing. The problem proved highly resistant to numerous re-arrangements of earthing and shielding. Finally attempts to solve it were abandoned, on the grounds that provided all measurements were made with the furnace either on or off consistant values of resistance were obtained. Referring again to Figure 6.2, in run A1

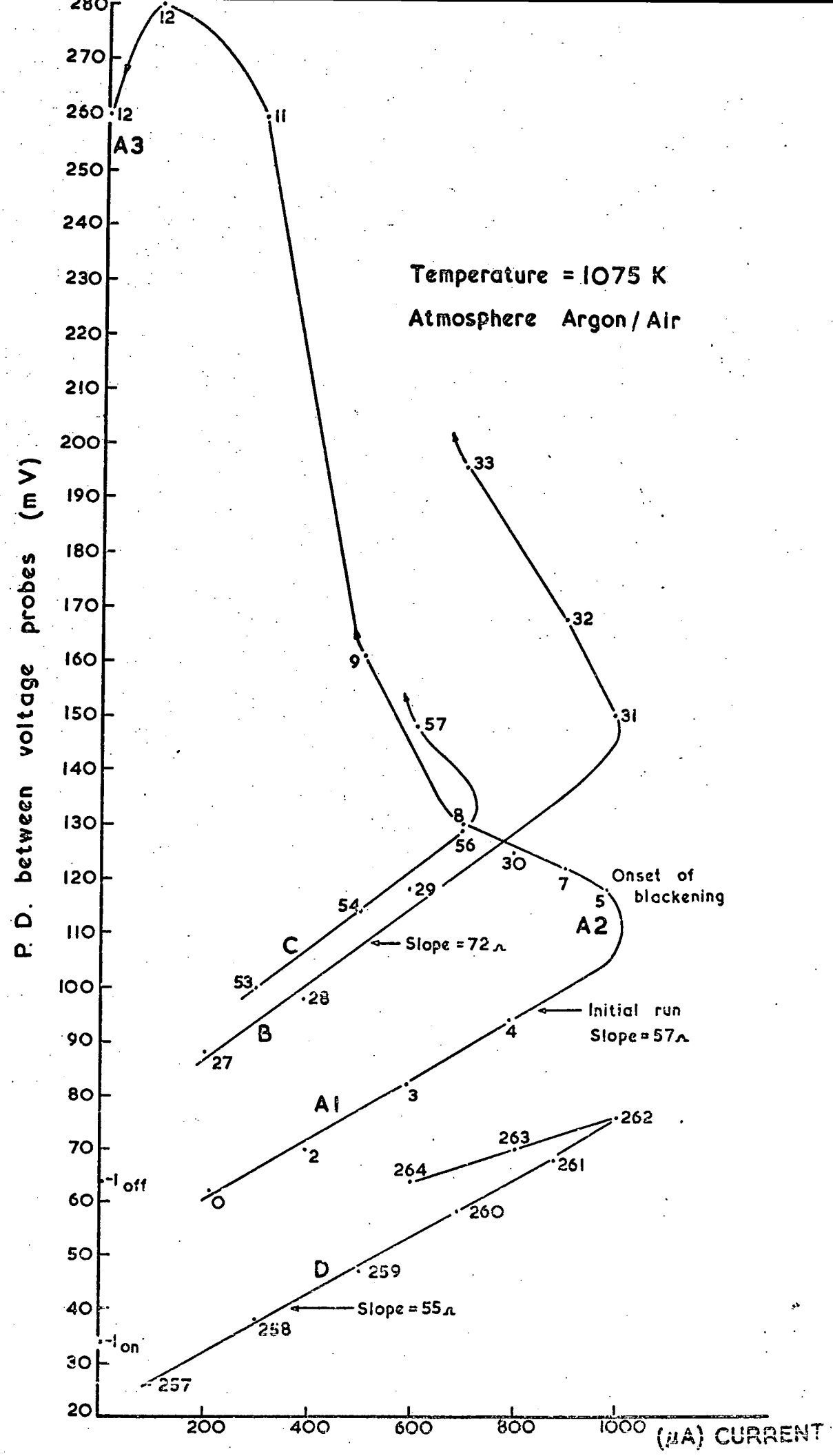

FIG. 6.2 Recovery of a YSZ crystal from the polarization effects associated with the onset of blackening.

(The numbers beside the points indicate the time in minutes since the first current was passed)

all readings were taken with the furnace on, in run D all readings were taken with the furnace off. It should be emphasised that the example given in Figure 6.2 is an extreme one. Normally observation of the point numbered "7" would have led to the immediate switching off of the current. Figure 6.3 shows a typical run for finding the resistance at one temperature. The resistance of the sample was measured as the temperature was raised in steps of roughly 100 K from 725 K to 1175 K. The maximum current used was 100 μA. The sample was then examined and found to be intact but just showing the grey tinge which appears at the start of "whitening". The process was then repeated using currents up to 1 mA. (The larger currents, which increased the probability that blackening would occur, were used in an attempt to improve the signal to noise ratio). The sample was finally blackened by a current of 7 mA.

The resistivity temperature behaviour is shown in Figure 6.4. These will subsequently be taken at face value even though the methods used to obtain them make this a little dangerous. In particular, of the results on the left the top ones may be doubtful because the signal to noise ratio is low and the bottom ones (for which the signal noise ratio is much higher) because blackening may be beginning.

The experimental points were fitted to equation 6.3 by adjusting the parameters A_1, A_2, E_1, E_2 by computer to minimise $\sum_i (\ln y_i - \ln r_i)^2$ where the y_i are experimental values of $\frac{\rho}{T}$ and the r_i are the corresponding values calculated from equation 6.3. (Program DAP 13P). Quite good first approximations were found using the tangents to the ends of the graph. The best fit was obtained when :

$$A_1 = 1.25 \times 10^{-7}\ \Omega mK^{-1}, \quad E_1 = 1.16 \times 10^{-19}\ J$$

$$A_2 = 1.58 \times 10^{-14}\ \Omega mK^{-1}, \quad E_2 = 3.09 \times 10^{-19}\ J$$

(If only the highest results for $1/T = 8.5 \times 10^{-4}\ K^{-1}$ and

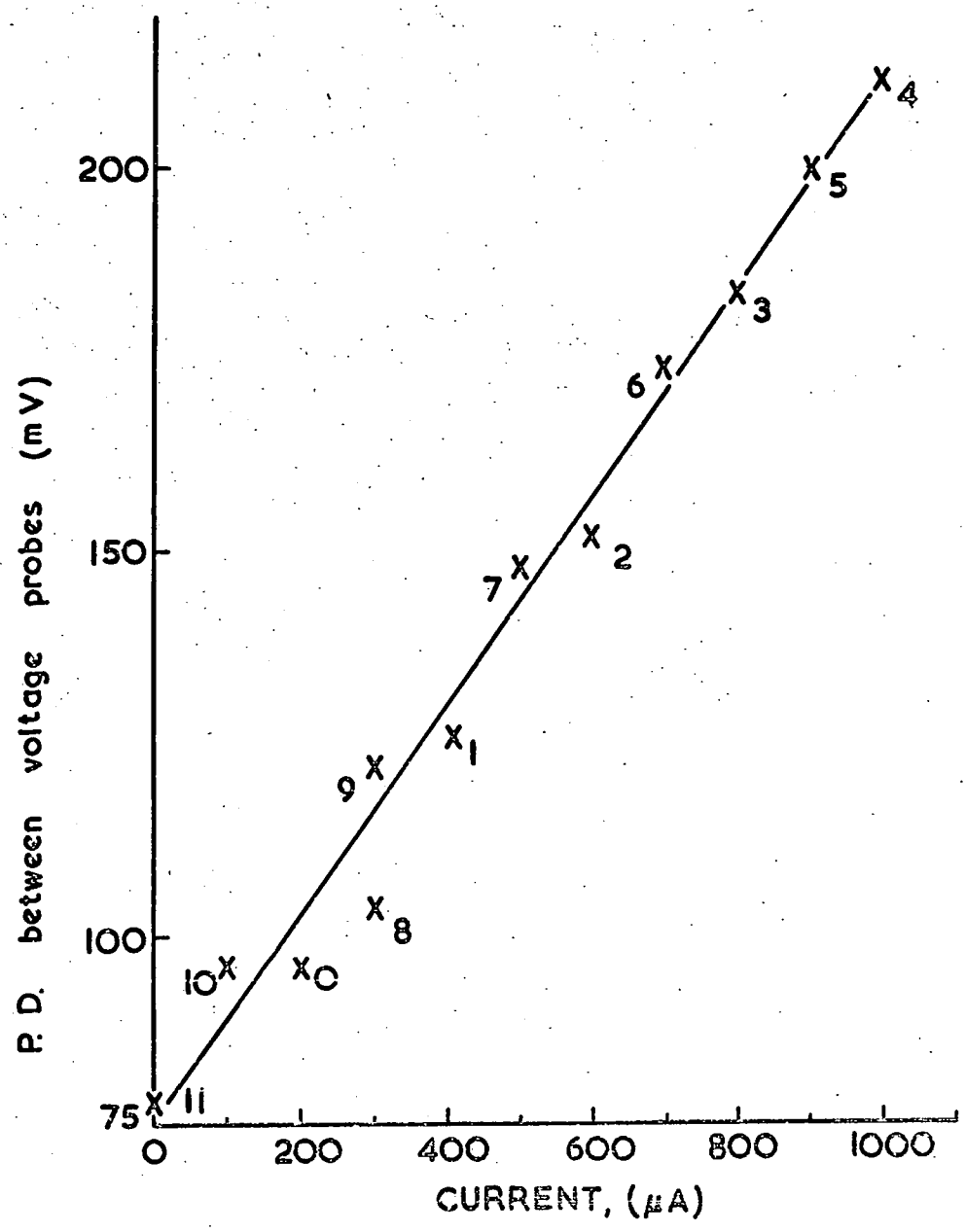

FIG. 6·3 Resistance determination of single crystal YSZ at 980 K. Atmosphere - argon / air.

(The numbers beside the points indicate the time in minutes since the current was first passed)

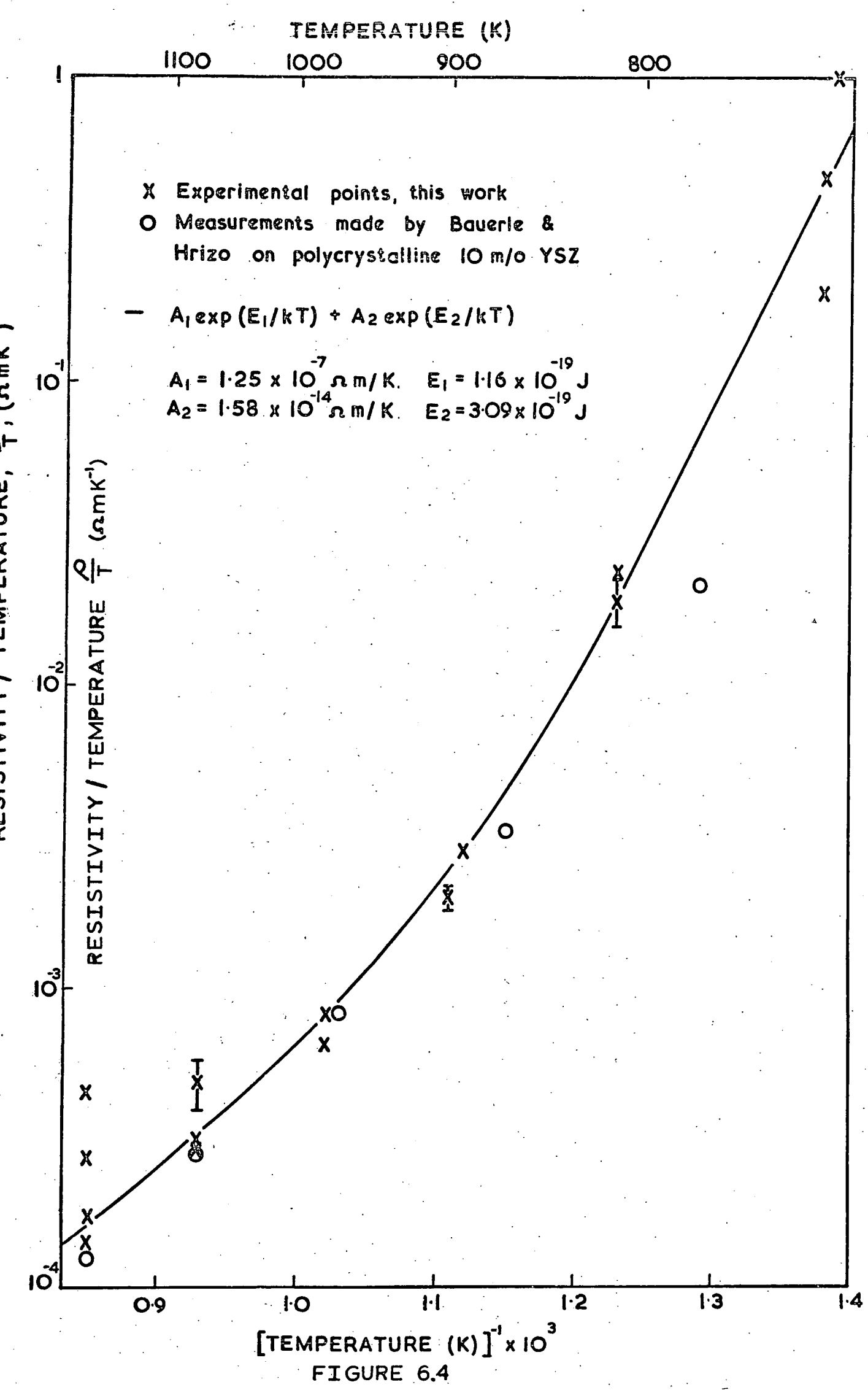

FIGURE 6.4

Resistivity - temperature behaviour for single crystal YSZ

9.3×10^{-4} K^{-1} are taken, to obtain a fit E_1 must be reduced to 1.9×10^{-20} J. Although such a selection of results is unjustified, it does show the need for more reproducibility and accuracy). Such a variation of resistivity with temperature can be explained in terms of two mechanisms which dominate in different temperature regions. As the temperature increases, first the liberation of vacancies from traps (i.e. the increase in carrier concentration) is dominant, then the increase in mobility of the oxygen vacancies takes over. This interpretation gives an activation energy for vacancy motion of 1.16×10^{-19} J (i.e. 0.725 eV compared with 0.682 eV obtained by Bauerle and Hrizo and 0.7 eV by Strickler and Carlson, both for 10 m/o YSZ) and a complex association energy of 1.93×10^{-19} J (1.20 eV compared with 0.486 eV obtained by Bauerle and Hrizo). Under the circumstances this agreement on the 'basic' line is pleasing and the disagreement on the detailed curvature not surprising.

It could be argued that since the atmosphere must have a low partial pressure of oxygen if the crystal is not to disintegrate, an Argon atmosphere should be used in conjunction with A.C. techniques. The latter would prevent electrolysis and the build up of vacancy concentration which is believed to be the basis of the blackening. (There is no guarantee that it would not cause "whitening"). More recently J.E. Bauerle (34) has made A.C. measurements of polycrystalline YSZ using a range of temperatures, frequencies and Oxygen partial pressures and used complex admittance diagrams to analysis his results. He identified contributions from 1) electrode polarization 2) a capacitive, resistive electrolyte polarization 3) a pure ohmic electrolyte polarization. This shows both the power of the technique and the effort and care that must go into its interpretation.

Summary

Preventing YSZ single crystals disintegrating while measuring the temperature variation of their conductivity is a major problem. This can be overcome by using an Air, Argon atmosphere but the problem then becomes one of preventing blackening. The results obtained tend to confirm Bauerle and Hrizo's trapping model (i.e. that the Oxygen vacancies which are the charge carriers in YSZ can be trapped).

Chapter 7.

Current Blackening and "High Field" Conduction

7.1 This chapter will be concerned with the changes that take place when such a high electric current is passed through (hot) YSZ that the supply of oxygen at the cathode is not sufficient. (See equation 6.1).

The sample (originally white (if polycrystalline) or amber (if single crystal)) turns black. This process takes the form of a blackened zone or 'tongue' growing from the cathode. The mechanical strength of the sample is destroyed and it tends to break up. There are changes in the electrical properties, but these are masked by the formation of a conducting layer on blackened material in the presence of traces of air. The bulk conductivity becomes electronic. Under "heavy blackening conditions" some of the oxide can be reduced to zirconium through electrolysis. Some of the observations and measurements made while single crystal samples of YSZ were being blackened will be given. These were partially done for their own sake and partially to prepare specimens for other experiments.

7.2 Survey

"Highfield" conduction is of interest because of the potential uses of YSZ electrodes (in an air atmosphere) for magneto-hydrodynamic power generation. The current densities required (many A/cm^2) are sufficient to cause "blackening" under normal operating conditions. The result is cracking and shattering of the cathode. (The anode also tends to crack, but not as badly since only the cathode "blackens"). This can be avoided by limiting the current. (The critical current for a given electrode in a particular environment can be determined from its current,potential difference characteristics. (Ya.P. Gokhstein & A.A. Sofonov 1970 (35)).

An oxide-metal junction is needed to carry the current to the external circuit and it is from here that the trouble originates. The situation can be improved by drilling holes in the metal to increase the supply of Oxygen to the junction. (R.E.W. Casselton & M.D.S. Watson 1968 (36)). The disintegration is not due to the formation of a monoclinic phase. (S.K. Adams and R.E.W. Casselton 1970 (37)).

If electric current is passed through YSZ in an Oxygen-free atmosphere ionic conduction cannot persist, because it requires Oxygen to be liberated from the solid at the anode and atmospheric Oxygen is needed at the cathode to maintain the supply. (Equation 6.1). Thus the conductivity must either fall to zero or become electronic (possibly due to the oxide being reduced electrolytically to form metal). In fact the material turns black and becomes an electronic conductor without becoming metallic. (Metallic Zirconium has been detected in blackened YSZ (36) but often it is not). This also happens to some extent if Oxygen is present but in insufficient quantities. In this case a black "tongue" comes out from the cathode and grows to an equilibrium size determined by the Oxygen supply and the current.

M. Jacquin, M. Guillou and J. Millet 1967 (38) continuously weighed a sample of Calcia stabilized Zirconia while they passed a constant current through it in an inert atmosphere. At first there was a loss of mass which correlated with the evolution of Oxygen, but the mass became constant and the evolution of Oxygen stopped, although the current continued, indicating electron conduction. Calcia stabilized Zirconia is, like YSZ, an ionic conductor in air; so presumably YSZ would behave similarly. Reference 36 quotes a loss of mass about 0.65% on blackening for the most blackened parts of their (YSZ) samples. This paper also notes that compacted polycrystalline YSZ is much less resistant to thermal shock than porous material, and presumably single crystal material is even less

resistant. Although there is no evidence to suggest that the disintegration of YSZ on blackening is due to thermal shock, this suggests an explanation for our not detecting mass losses on blackening single crystal material; namely that the crystals disintegrate before the electrolysis has gone far enough to be detected. The size limitation on single crystals is an additional obstacle.

When YSZ is blackened in the presence of air a gold-coloured phase, which is highly electrically conducting, forms on the surface (and as inclusions in polycrystalline material). This has been reported by J.P. Loup, Z. Mihailoric and P. Morvan 1965 (39) and A. Wilcockson and R.E.W. Casselton 1970 (40). It has been identified, from x-ray powder photographs, as a solid solution based on zirconium nitride (ZrN), the other component being probably zirconium monoxide (ZrO) (which does not exist by itself in the solid state). The zirconium oxynitride can be re-oxidised by heating in air, to leave a white substance with the same lattice parameter as the starting material (YSZ). The oxynitride only forms if the current passage leads to blackening.

In order to make conductivity measurements on blackened material which was free from oxynitride. Casselton and Watson (36) rigorously excluded Nitrogen from the atmosphere around their samples. The samples were in a double walled alumina tube and a stream of Argon (purified of Nitrogen and Oxygen by being passed over hot Zirconium turnings) was passed through both chambers of the tube. No oxynitride formation was detected. These authors have shown that when a blackened zone is formed the potential difference across the zone is depressed and so the potential distribution is non-linear. Thus the term "conductivity of blackened YSZ" must be treated with caution. (In unblackened material, the potential gradient is constant except near the electrodes). However the distribution depends on the current density and the Oxygen partial pressure in the atmosphere, and high

currents and low pressures give roughly linear distributions. The conductivity of YSZ blackened in Argon is reported to be independent of current density above a certain limit (3 A/cm^{-2} and up to at least 20 A/cm^{2}) (See reference 30). (Below the limit, conductivity increased non-reproducibly with current density). The resulting conductivity at 1400°C is roughly an order of magnitude higher than that of unblackened material, and its temperature variation corresponds to an activation energy of 3×10^{-20} J (i.e. 0.2 eV c.f. 0.7 eV for unblackened material). Casselton suspects that this conduction is due to electron hopping. Finally it is worth noting that the measurements of Casselton et. al. show that much of the potential drop across a sample of YSZ, blackened or not, occurs near the electrodes (i.e. is due to polarization). (In heavily blackened YSZ there is a negative space charge next to the cathode).

7.3 Current Blackening Procedure with Observations and Measurements made

The apparatus used for blackening has been shown in Figure 6.1a together with the sample holders for thick (6.1bi) and thin (6.1bii) samples. Usually current was supplied by a Farnell L30B power supply which has not only a simple voltage control but also an adjustable current limiter. The limiter was used to reduce the applied voltage automatically so as to keep the current down to the set limit. (If a current greater than 1A was required, it was supplied by the 24 V D.C. wall supply in conjunction with a simple potentiometer). The normal procedure was to mount the sample in the apparatus and set the Argon flowing. The main furnace was set at 800°C and switched on. It usually took about one hour to reach 800°C. After the desired current had been passed for the required time the sample was quenched. The rubber tube "R" was disconnected and the silica tube was sealed with Q-compound. This was repeated with joint "J" and the

tube was lifted out of the furnace. The temperature of the sample dropped to 400°C in 2 minutes.

The procedure usually gave blackened crystals whose surfaces were coated in a silvery conducting layer. This caused no concern since it was removed by either polishing (optical samples) or etching (E.S.R. samples) or, for ultrasonics samples, was left since a conducting surface layer was advantageous. If the blackening had not gone completely through the sample it appeared as an opaque "tongue" coming out of the cathode (see Figures 7.1 and 7.2). These could easily be seen if the sample was illuminated from behind, but proved difficult to photograph. When oxynitride was present in such a case it could be detected with an Avometer and was found to remain within the boundaries of the tongue. (There was one exception to this, the surface of R11f which had been in contact with the holder was conducting well beyond the blackened region). Figures 7.1 and 7.2 illustrate the results of an experiment to compare the blackening process in the two compositions (8.3 m/o and 12 m/o). For each part of the experiment a 1 x 4 x 10 mm^3 sample of each composition was used. Both samples were treated by either the same current (Figure 7.1) or the same voltage (Figure 7.2). No consistent difference was observed in blackening between the two compositions.

In Figure 7.2 crystal R2 is shown after it has been blackened by passage of 100 mA for 1 hour (bottom negative) then by passage of 100 mA for 8 minutes (top negative). The second passage seems to have flattened the tongue which the first passage had been observed to produce.

The graphs on these figures show how the blackening process can be detected by a fall in the total resistance of the sample. (Note that the flat portions on the current graphs are due to the operation of the current limiter, which reduced the applied voltage from 30 V, and not to the achievement of a new equilibrium. (This takes about an hour)). Figure 7.1 shows some correlation between growth of blackened tongue and fall in

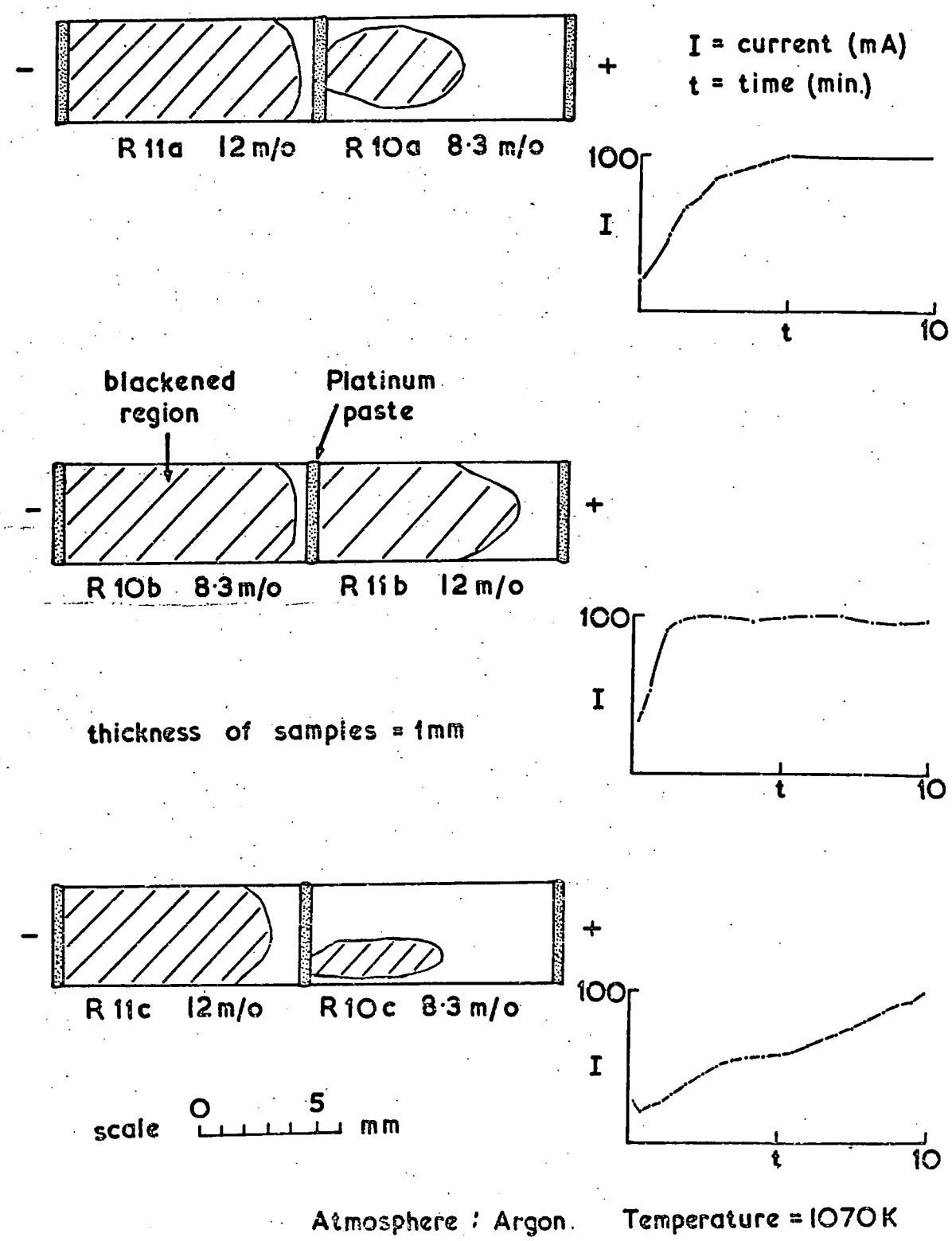

FIG. 7.1 Comparison of current blackened tongues in 8·3 and 12 m/o single crystal yttria stabilised zirconia; equal current conditions.

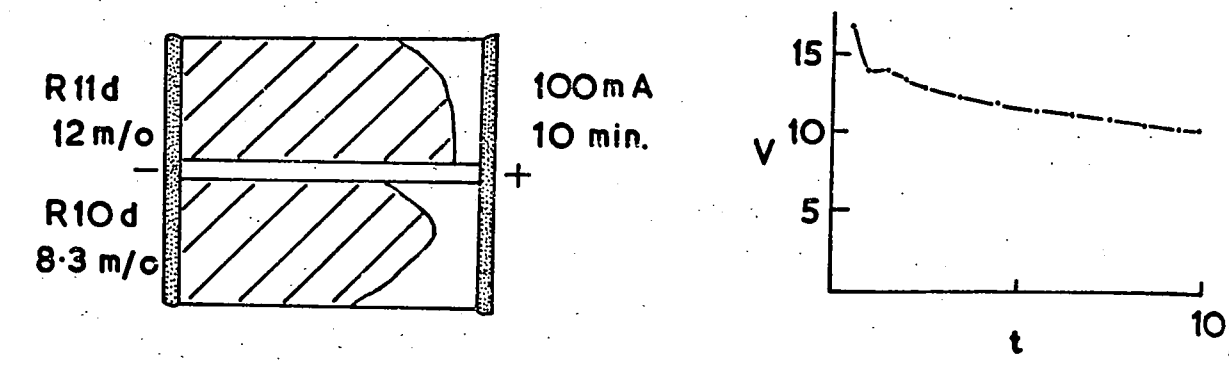

V = applied potential difference (V)
t = time (min)

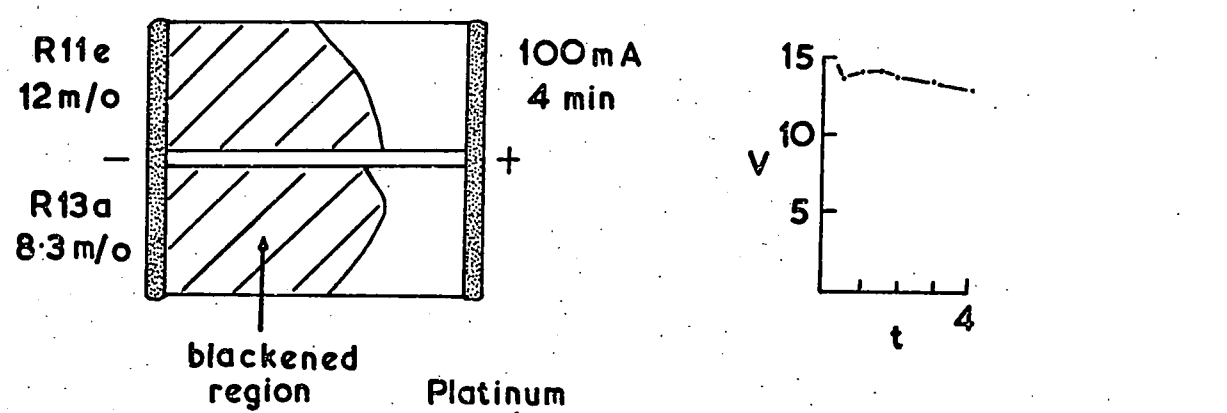

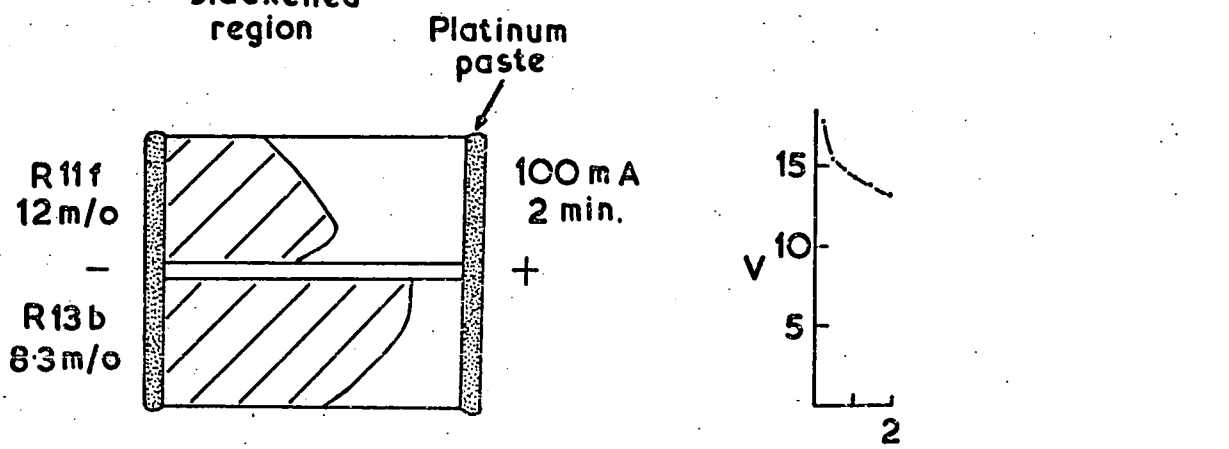

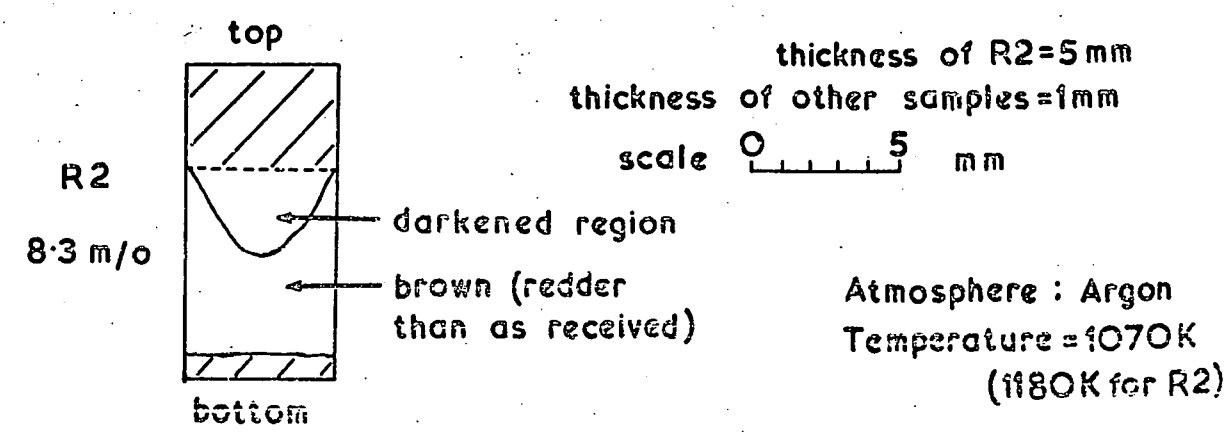

Atmosphere : Argon
Temperature = 1070 K
(1180 K for R2)

FIG. 7.2 Comparison of current blackened tongues in 8·3 and 12 m/o single crystal yttria stabilised zirconia ; equal voltage conditions.

resistance. (The current rises most quickly in the case where the tongue grows most). Figure 7.2 shows that while much of the change takes place within the first minute it does continue at a slower rate. Using the fall in resistance, the importance of Oxygen partial pressure in blackening was demonstrated when sample 1A10r (a $(1\ mm)^2$ rod of 8.3 m/o crystal) was blackened at 600° C. At first the atmosphere was air. When 30 V was applied, for 7 minutes the current fluctuated between 15 and 18 mA. Then the Argon flow was turned on, and immediately the current began to rise, reaching 250 mA in 3 minutes.

It proved possible to 'unblacken' a crystal by heating in what was nominally an Argon atmosphere. For example : after the situation shown in Figure 7.2, R2 was blackened throughout by further passage of current (100 mA for 50 minutes). Then heating it in "Argon" at 910°C for 3 hours 15 minutes resulted in a crystal which was brown and transparent. It only differed in appearance from an as-received crystal in having some small bulk cracks and a slightly mottled surface. (See also Figure 6.2 and Section 6.3). It was for this reason that we quenched our samples.

7.4 Degree of Blackening

It can be seen from the above that a full specification of the blackening a crystal had received would include the parameters : current density, Oxygen partial pressure, time for which current was passed (unless equilibrium had been reached), annealing treatment, and probably sample (and in particular cathode) geometry. Thus it might be wise to measure the change in the crystal rather than record the treatment. The sample is not necessarily uniformly blackened. The loss in mass is small and difficult to measure. The optical absorption is so high that it is difficult to transmit visible light even through a thin sample. Blackened YSZ absorbs microwaves more heavily than does as received material but

attempts to measure these losses were not very fruitful. No significant change in lattice parameter was measured and the only change detected by ultrasonics was bulk cracks. In short we lacked a satisfactory parameter for "degree of blackening ". More recent optical work has suggested that it might be possible to use the absorption coefficient at the wavelength of the absorption peak responsible for blackening as a measure of the "degree of blackening". This involves 'diluting' a powdered sample in a transparent medium.

REFERENCES

1. "Investigations of Structural Transformations in Refractories above 2000°C"
M. Foex. Science of Ceramics 4.P. 217 to 231. 1967
Proceedings of the fourth international conference on the Science of Ceramics.

2. "The Crystal Structure of Baddeleyite (Monochlinic ZrO_2) and its Relation to the Polymorphism of ZrO_2". D.K. Smith and H.W. Newkirk. Acta. Cryst. 18.P. 983.1965.

3. "The Zirconia - Yttria System". P. Duvez, F.H. Brown and F. Odell. J. Electro-chem Soc. 98.P. 356 to 362. 1951

4. "Electrical Conductivity in the ZrO_2 - Rich Region of Several M_2O_3 - ZrO_2 Systems". D.W. Strickler and W.G. Carlson. J. Am. Ceram. Soc. 48.P. 286 to 289. 1965.

5. "The Influence of Additions of Rare-earth Oxides on the Polymorphism of Zirconia and Hafnia". E.K. Kohler and V.B. Glushkova. Science of Ceramics 4. P. 233 to 245.

6. "The Electrical Resistivities of some Castable Zirconias". D.B. Meadowcroft. J. Mat. Sci. P. 768 Sept. 1969.

7. "The Mechanism of Electrical Conduction in the Nerst Glower" C. Wagner. Naturwissen 31. P. 265 to 268. 1943.

8. "Compositional Analysis of Twenty-Six Zirconias". R.E. Heffelfinger, E.R. Blosser, W.M. Henry. J. Amer. Ceram. Soc. 47(12).P. 646. 1964.

9. "Optical Absorption in Current Blackened YSZ".
D.A. Wright, J.S. Thorp, A. Aypar, H.P. Buckley. J. Mat. Sci. 8
P. 876. 1973.

10. "The Dielectric Constants of Current Blackened Single Crystal YSZ." J.S. Thorp and H.P. Buckley. J. Mat. Sci. 1973.

11. "Anomalous Solid Solutions in the System Zirconia - Yttria. Crystal Structure of Nerst Glowers". F. Hund. Z. Elektrocham. 55.
P. 363 to 366. 1951.

12. "Pyrochlore-Type Compounds Containing Double Oxides of Trivalent and Tetravalent Ions". R.S. Roth. J. Res. Natl. Bur . Std. 56
[1] . P. 17 to 25. 1956.

13. "Phase Relationships in the Y_2O_3 - ZrO_2 System". Fan Fu K'ang, A.K. Kuznetov and E.K. Keler. Bulletin of the Academy of Sciences of the U.S.S.R. Division of Chemical Science 1962. P. 1071 to 1075 and 1963. P. 542 to 549 translated from Otdelenie Khimicheskikh Nauk N.4 P. 601 to 610 April 1963 and N.7 P. 1141 to 1146 July 1962.

14. "The Nonexistance of Yttrium Zirconate". D.K. Smith. J. Am. Ceram. Soc. 49. P. 625 to 626. 1966.

15. "Some structural Modifications of Fluorite - Type Phases in Systems Based on Zirconia or Hafnium Oxide". J. Lefevre. Annls. Chim. (Paris) 8. P. 117 to 149. 1963.

16. "The Elastic Constants and Interatomic Bonding in Yttria - Stabilised Zirconia". N.G. Pace, G.A. Saunders, Z. Sümengen, J.S. Thorp. J. Mat. Sci. 4. P. 1106 to 1110. 1969.

17. "CaO - ZrO_2 Anion Vacancy Model". A.H. Diness and R. Roy. Solid State Comm. 3. P. 123. 1965.

18. "Ionic Crystals, Lattice defects and non-stoichiometry". Greenwood U.D.C. 548.7 Butterworth, 1968.

19. "Electronic Processes in Materials". L.V. Azároff and J.J. Brophy. McGraw-Hill. 1963.

20. "Defect Structures in Ceramic Materials". L.E.J. Roberts. Proceedings of the fourth international conference on science of ceramics. 23-27 April 1967 (British Ceramic Society 1968) P. 329 - 347.

21. J.J. Markham S.S. Physics 8.P. 261 1966.

22. M. Caillet Rev. Int. Temp. et Refract. 5. P. 173. 1968.

23. "The Nature and Consequences of Current Blackening in Stabilized Zirconia". R.E.W. Casselton. Electricity from M.H.D. 1968 Vol. V International Atomic Energy Agency.

24. J.R. O'Connor and J.E. Chen. Phys. Rev. 130 P. 1790. 1963.

25. "Principles of Optics". Born and Wolf. Pergamon. 3rd Ed. 1965.

26. "Dielectrics" J.C. Anderson, Chapman & Hall Ltd. (p. 16) 1964.

27. "Measure de la conductibilité électrique de ZrO_2 stabilisée a 10% Y_2O_3 entre 1000 K et 2400 K".
A.M. Anthony.C.R. Acad. Sci. (Paris) V.260.P. 1396. 1965.

28. "Interpretation of the Resistivity Temperature Dependence of High Purity $(ZrO_2)_{0.90}$ $(Y_2O_3)_{0.10}$" J.E. Bauerle & J. Hrizo J. Phys. Chem. Solids V.30.P. 565 - 570. 1969.

29. "Low Field d.c. Conduction in Yttria Stabilized Zirconia". R.E.W. Casselton. Phys. Status Solidi A (Germany) V.2.N.3. P. 571 - 585.16 July 1970.

30. "Electrical Conduction in Yttria Stabilized Zirconia" R.E.W. Casselton, J.S. Thorp & D.A. Wright. Brit. Ceram. Soc. Conference. "Mass Transport in Non-Metallic Solids" 17 / 18 December 1969.

31. "Ionic Conductivities of Cubic Solid Solutions in the System $CaO - Y_2O_3 - ZrO_2$" D.W. Strickler and W.G. Carlson. 1964. J. Am. Ceram. Soc. V.47.N.3. P.122

32. "Transport Numbers in Stabilized Zirconia". D.T. Bray and U. Merten. J. Electrochem. Soc. 111 (4). P. 447 - 452. 1964.

33. "Conduction Mechanism in Yttria Stabilized Zirconia" R.E.W. Casselton and J.C. Scott. Phys. Letters 25A (3). P. 264 14 August 1967.

34. "Study of Solid Electrolyte Polarization by a Complex Admittance Method" J.E. Bauerle. J. Phys. Chem. Solids 30.2657.1969.

35. "Critical Current Density through electrodes of an M.H.D. generator, made of a $ZrO_2 - Y_2O_3$ ceramic" Ya. P. Gokhstein and A.A. Sofonov High. Temp. USA V.8.N.2.P. 368 - 371 1970.

36. "High Temperature Electrodes using Stabilized Zirconia" R.E.W. Casselton & M.D.S. Watson.Science of Ceramics 4.P. 349 1968.

37. "Destabilization of the Yttria:Zirconia Fluorite Phase by Electrolysis".S.K. Adams and R.E.W. Casselton.J. Am. Ceram. Soc. P. 117.February 1970.

38. "Électrochemie Étude thermogravimétrique de l' électrolyse des zircones à conduction ionic". M. Jacquin. M. Guillou and J. Millet. C.R. Acad. Sci (Paris) 264 (series C) 2101.26 June 1967.

39. "Formation of ZrN by passage of continuous D.C. current at 1300°C in Yttria Stabilized Zirconia".
J.P. Loup, Z. Mihailovic and P. Morvan C.R. Acad. Sci (Paris) 261.109.5 July 1965.

40. "Zirconium Oxynitride formation during electrolysis of Stabilized Zirconia" A. Wilcockson and R.E.W. Casselton J. Am. Ceram. Soc. V.53.N.5 P. 293.21 May 1970.

41. E.G. Nice thesis P. 10.

42. "The dielectric constant of zirconia". P.J. Harrop & J.N. Wanklyn. Brit. J. Appl. Phys. 18 739 1967

APPENDIX i.

JOURNAL OF MATERIALS SCIENCE 7 (1972) 729–734

Electron spin resonance in single crystal yttria stabilized zirconia

J. S. THORP, A. AYPAR, J. S. ROSS
Department of Applied Physics and Electronics, University of Durham, UK

Electron spin resonance has been observed at 35 GHz in 8 and 12 mol% yttria stabilized zirconia single crystals before and after blackening by current passage. Measurements were made between 293 and 77K. In both as-grown and blackened crystals the spectra showed anisotropic lines (type A) characterized by $g_{\parallel} = 2.003 \pm 0.002$ and $g_{\perp} = 1.880 \pm 0.002$ with respect to a [111] symmetry axis and a broader, slightly anisotropic line (type B) centred near $g = 1.993$. In current blackened crystals a weak isotropic line (type C) was also found near $g = 1.986$. The type A lines are attributed to a charged complex formed by an electron trapped at an oxygen vacancy and associated with an yttrium ion. Tentative models are suggested to explain the type-B and type-C lines.

1. Introduction

Yttria stabilized zirconia (YSZ) is zirconium oxide (ZrO_2) stabilized by the addition of more than about 7 mol% of yttrium oxide (Y_2O_3). Pure zirconia exhibits a phase change between a monoclinic and a tetragonal structure at about 1400K and therefore, due to the associated volume change, is unsatisfactory as a ceramic [1]. However, the addition of yttria enables the refractory properties of zirconia to be used since yttria stabilized zirconia adopts a cubic structure between room temperature and its melting point, about 2800K [2]. For yttria concentrations between about 7 and 50 mol% the fluorite structure is adopted [3]. The cation sites lie on a face centred cubic lattice and the oxygen sites lie at the centres of the small cubes formed by dividing the unit cell into eight (Fig. 1). There are two oxygen sites to one cation site. Thus the presence of the yttria implies that there must be defects, either oxygen vacancies or cation interstitials. The existence of oxygen vacancies in YSZ has been generally accepted since they were proposed by Wagner [4]; this has subsequently been substantiated by the correlation of X-ray and density measurements [5]. Since the vacancies are mobile at elevated temperatures, the material is valuable as a refractory conductor, e.g. in MHD electrode and fuel cell applications. (At 1400K the conductivity of $(Y_2O_3)_{0.08}$ $(ZrO_2)_{0.92}$ is about 1.2 Ω^{-1} m^{-1}). When an electric field is applied the vacancies migrate to the cathode. However, if there is not sufficient oxygen to fill them as they arrive, a black zone starts to spread from the cathode and eventually the material crumbles. Preliminary electron spin resonance studies on single crystal YSZ have been reported previously [6] and the present work was undertaken in an attempt to examine the defect structure more closely.

2. Experimental details

Single crystals of $(Y_2O_3)_{0.08}$ $(ZrO_2)_{0.92}$ and $(Y_2O_3)_{0.12}$ $(ZrO_2)_{0.88}$, made by electrofusing mixtures of the pure powdered oxides [7], were obtained from W. & C. Spicer Ltd. The as-received crystals varied in appearance from transparent amber to dark and almost opaque. Their orientation was determined by X-ray back reflection methods. They were robust and hard and were cut using a diamond wheel, without difficulties due to fragmentation or cracking. Samples treated in several ways were investigated. Some were studied in the as-received state; some were examined after current blackening; others after being heated in argon, air or oxygen, without having current passed through them. Current blackened samples were prepared by passing direct current through as-received material (using platinum paste contacts) in an argon atmosphere at 1070K. (This temperature was low enough to be reached easily yet high enough to make the material sufficiently conducting.) Currents between 10 and 250 mA were

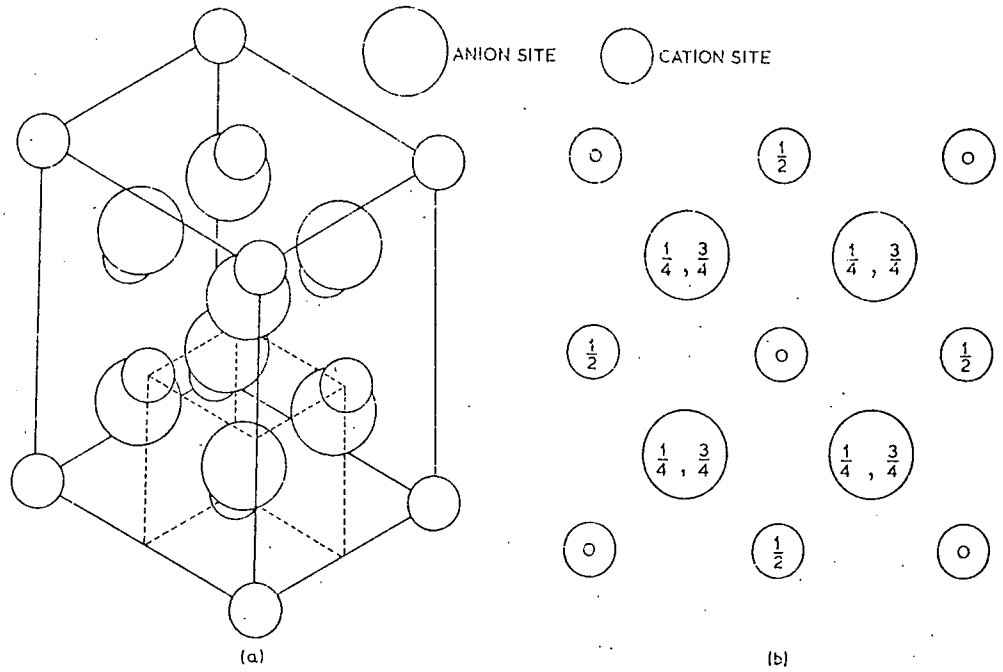

Figure 1 The unit cell of yttria stabilized zirconia: (*a*) general view, (*b*) plan view in which the numbers give the heights of the sites above the base in terms of the lattice parameter.

passed, for times ranging from 3 min to 1 h through rods of 1 mm^2 cross-section. Immediately after current passage the sample holder was withdrawn from the furnace allowing the sample to cool under argon to 670 K in 2 min and subsequently to room temperature. This made the rods very friable. It also left them with a silvery, highly conducting surface layer. The occurrence of conducting surface layers has been reported previously [8, 9], and here they were thought to arise from impurities in the dried argon supply. The layer was easily removed by dipping the sample into hot phosphoric acid (typically for 5 sec at 200° C). The removal of the layer was indicated by appearance, by the high value of the surface resistance and especially by the reduced effect of the sample on the cavity damping. Etching was repeated until there was no further improvement. For comparison purposes some samples were prepared under the same conditions of atmosphere and temperature but without passing current; their colour became paler.

As-received material heated in air or oxygen turned white and translucent and showed signs of cracking. Treatments ranged from heating in air at 1020 K for 6 h (which only whitened a sample to a depth of a few mm) to heating in oxygen at 1275 K for 50 h (which whitened a sample throughout). No change in weight greater than the experimental sensitivity (1 part in 10^4) was observed.

To resolve the lines more clearly than had been possible in the previous study at 9.3 GHz, measurements were made at 35.5 GHz. A cavity spectrometer employing phase sensitive detection at 160 KHz was used. The coupling and tuning of the cavity were adjustable. A ruby sample (with which the cavity Q-factor was $\approx$ 2000) was used to estimate the spectrometer sensitivity. From this it was deduced that the spectrometer could detect 10^{12} spins per millitesla linewidth at room temperature, working at a power level of 1 mW with a time constant of 1 sec. The introduction of yttria stabilized zirconia samples into the cavity affected the coupling. Furthermore, current blackened samples degraded the cavity Q-factor seriously making spectra difficult to observe. Accordingly the sample volume was chosen, at about 1 mm^3, to give a sufficient number of spins in the sample while retaining an adequate Q-factor. With as-received samples Q $\approx$ 900. Most measurements were made at 290 K and some at 77 K. The magnetic field was

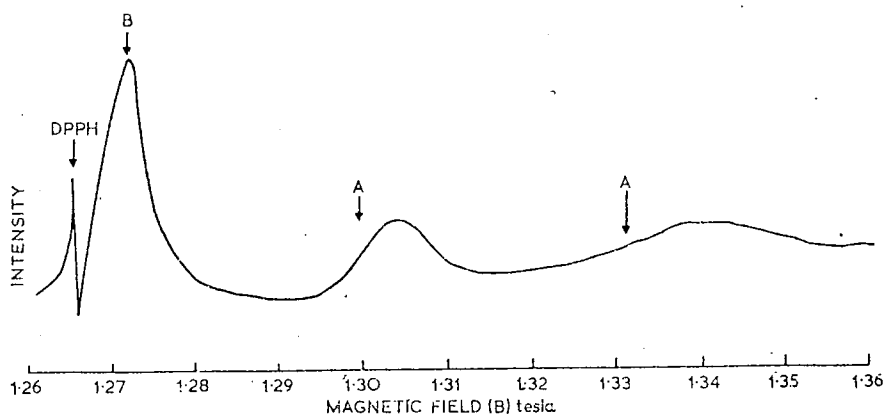

Figure 2 Spectra observed in as-received 8 mol % yttria stabilized zirconia. Magnetic field 16 degrees from [100] direction in (001) plane; 35.5 GHz, 290K.

measured using a calibrated sweep and a DPPH marker. (1 millitesla ≡ 10 gauss.)

3. Results

Spectra were seen in all samples. They were characterized by three types of line of different shape, intensity and variation with polar angle.

In 8 mol % YSZ the lines from the as-received samples were deduced to be of two types, which will be referred to as type A and type B (Fig. 2). The two lines labelled "A" seen when the magnetic field lay in the (100) plane, were believed to be due to one type of site because of their similarity in shape and intensity and especially because of their g-value variation with polar angle (Fig. 3). The peak-to-peak width of an A-type line varied according to the field value at which it occurred from 20 mT at 1.32 T to 8 mT at 1.27 T in the (100) plane, reducing further to 5 mT at 1.26 T in the (111) plane. In the (111) plane three apparently symmetrical lines were clearly seen near this range of g-values, and a fourth was just detectable. Over a matter of months crystals kept at room temperature lost their type-A lines.

The single type-B line was asymmetrical and of higher intensity. Its slightly anisotropic behaviour and the change in the width with polar angle were observed. The width changed periodically between 10 ± 1 mT and 6 ± 1 mT corresponding to the $\langle 110 \rangle$ and $\langle 100 \rangle$ directions of the unit cell. The g-values were 1.990 and 1.997 along the $\langle 110 \rangle$ and $\langle 100 \rangle$ directions respectively.

In samples which were heat treated without current passage no type-A lines were observed,

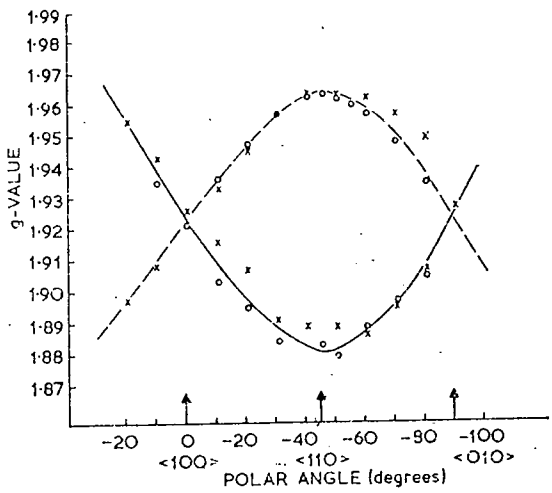

Figure 3 Variation of g-value for two A-type lines with polar angle. (Key: open circles, measured in (001) plane; crosses, measured in (100) plane.)

but the type-B line seemed unchanged. The room temperature ESR spectrum appeared to be independent of the atmosphere (air, oxygen or argon) used for the heat treatment. Current blackened samples exhibited both type-A and type-B lines and also an additional peak (designated type-C) close to the type-B line (Fig. 4). The type-C line was isotropic and so at some polar angles was obscured by the type-B line. The variations with polar angle of the resonance field values for the type-A, -B and -C lines are given in Fig. 5. There was some indication that the intensity of the type-C line increased with increased current density. The position of

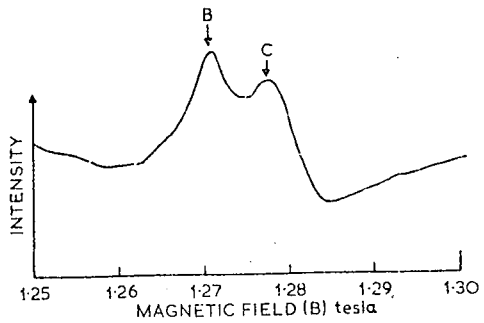

Figure 4 Spectra observed in current blackened 8 mol % yttria stabilized zirconia. Magnetic field 5 degrees from [100] direction in (001) plane; 35.5 GHz, 290K.

the peak of the type-C line corresponded to a g-value of 1.986.

The information is summarized in Table I. Only samples known to exhibit type-A lines before treatment were used.

Preliminary measurements have been made at lower temperatures. For as-received 8 mol % YSZ samples the spectra recorded at 77K were similar to those obtained at 290K and no extra lines were seen. With current blackened 8 mol % samples the type-C line was also present down to 148K, the lowest temperature at which measurements were made. The relative intensities of the type-A, -B and -C lines were approximately

TABLE I

Description of sample	Type of line present (room temperature)	Result of treatment (compared with 1)
(1) As-received (new)	A, B	Reference standard (type-A and type-B present)
(2) As-received (old)	B	Type-A not present
(3) Heated in argon without current passage	B	Type-A not present
(4). Current blackened (while heating in argon)	A, B, C	Type-C is weak. (N.B. Type-A present)
(5) Heated in air or oxygen without current passage	B	Type-A not present
(6) As (5), subsequently heated in vacuum at 1100°C for 3.5 h	B	Faint trace of Type-A lines

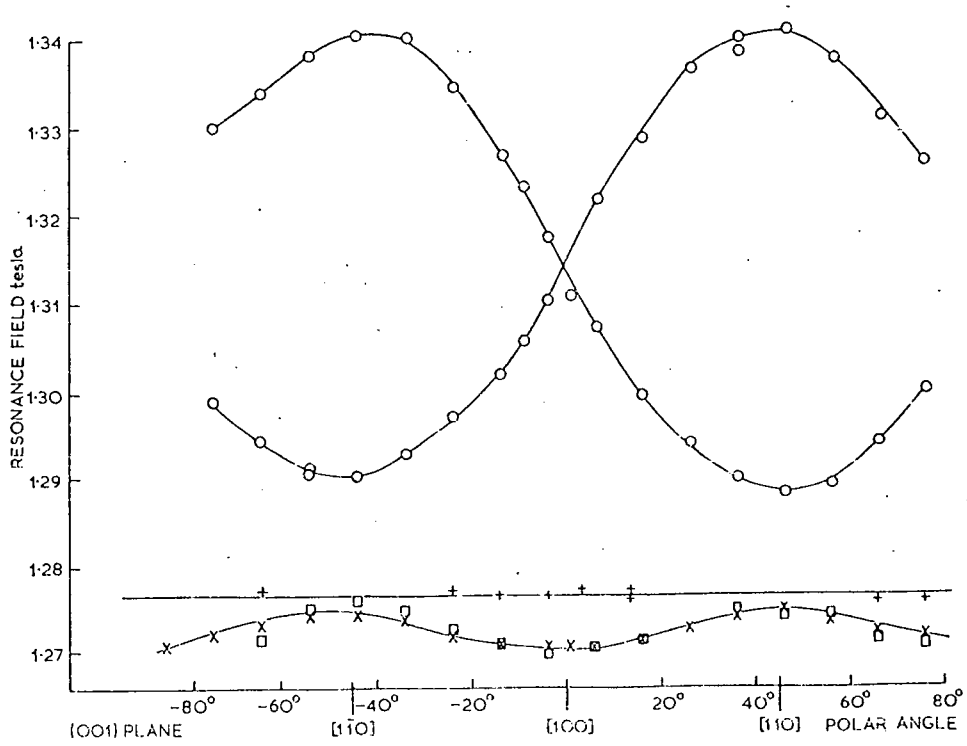

Figure 5 Variation with polar angle of line peak positions in as-received and current blackened YSZ. (Key: open circles, A-type line in as-received sample; crosses, B-type line in as-received sample; open square, B-type line in current blackened sample; addition signs, C-type line in current blackened sample.)

the same at room temperature and low temperature.

In as-received and current blackened 12 mol % YSZ similar results were obtained.

4. Discussion

4.1. Type-A lines

The results shown in Fig. 3 suggest that each type-A site must have a principal axis along one of the [1 1 1] directions. This would mean that there were four alternative A-type sites corresponding to the four three-fold axes. Thus, for certain orientations of the magnetic field four type-A lines should be seen. Observations in the (1 1 1) plane supported this postulate. The intensities of the lines indicated that all four sites were occupied by roughly equal populations. The g-value of a given site was a maximum, (2.003 ± 0.002), parallel to one of the [1 1 1] directions and a minimum (1.880 ± 0.002) perpendicular to it.

A model for this centre can be proposed on the basis of two associated point defects, the first containing a free spin and the second creating an additional component of crystal field. A trapped electron in an oxygen vacancy would provide a free spin on an oxygen site. This process is likely to occur in YSZ as it contains oxygen vacancies. The electron paramagnetic resonance properties of F-centres in alkali halides, reviewed by Markham [10] show g-values between 1.987 and 2.0029 with linewidths of more than 5 mT. The correspondence between these results and the behaviour of the type-A lines (coupled with their time and temperature dependence) supports the assignment of the line to a complex.

To explain the temperature variation of the conductivity of unblackened YSZ, Caillet [11] has proposed a model based on "free" and "trapped" oxygen vacancies. The vacancies were trapped by forming a complex with either one or two Y^{3+} ions. The model suggested here corresponds to Caillet's first "trapped" vacancy with the addition of an electron. With regard to blackened YSZ, Casselton [12] postulated that the onset of current blackening and an enhanced conductivity is accompanied by the injection of electrons from the cathode. Using the model suggested this would be consistent with the reappearance of type-A lines after current blackening since the complexes would act as electron traps.

The required axial symmetry could be obtained if an yttrium ion was on a cation site with the other three nearest cation sites occupied by zirconium ions.

4.2. Type-B line

The type-B line was seen in all samples irrespective of treatment. The symmetry of the variation of resonance field with polar angle showed that the most likely location for this defect centre would be a cation site. The normal occupants of these sites, Zr^{4+} and Y^{3+}, are diamagnetic and consequently would give no spin resonance spectra. The defect has not yet been positively identified.

A possible explanation may be valency changes of the cations. Ionization energy considerations indicate that the ions most likely to be formed would be Zr^{3+} and Y^{2+}. This may apply in the reducing conditions created during crystal growth by electrofusion. No resonance data on Zr^{3+} has been reported in the literature. However, O'Connor [13] has reported electron spin resonance of Y^{2+} in CaF_2 at 4.2 K and quotes a g-value of 1.994 ± 0.005. This is similar to the mean g-value, (1.993), found for the type-B line. The observed intensity of the type-B line corresponded to a spin density of about 10^{15} mm^{-3}. On the assumption that Y^{2+} was responsible this would indicate that about 1 in 10^4 yttrium ions had changed their valency state.

An alternative possibility, that the type-B line might be due to an impurity, cannot be excluded although optical spectrographic analysis showed that the only major impurities present were hafnium (about 2.2%), titanium (300 ppm), calcium (100 ppm), and tantalum (300 ppm).

4.3. Type-C lines

The type-C lines only appeared after current passage. The line was isotropic, with $g = 1.986$, and its intensity (like those of the type-A and type-B lines) was not strongly temperature dependent over the range studied.

A possible model for this site is an F-centre consisting of an oxygen vacancy with a trapped electron surrounded by a tetrahedron of zirconium ions. In as-received material the existence of such a site would be more unlikely than the complex used to explain the type-A lines. The oxygen vacancies occur because yttrium is substituted for zirconium (one vacancy is produced for two yttrium ions), and the cation tetrahedra in which yttrium is not substituted for zirconium would not be expected to have an associated vacancy. During current passage the applied

potential may cause migration of vacancies and the injection of electrons. These electrons may be trapped in vacancies having two different surroundings (i) a tetrahedron of four zirconium ions or, (ii) a tetrahedron of three zirconium ions and one yttrium ion as proposed for the type-A site. The isotropy of the type-C line may be explained because this tetrahedral arrangement of zirconium ions will produce balanced components of crystalline field. This model would be consistent with Caillet's postulate of "free" vacancies.

Acknowledgements

We wish to thank Dr E. G. Nice for much valuable help. One of us (J.S.R.), also wishes to thank the Science Research Council for the award of a research studentship and one (A.A.), the Turkish Atomic Energy Commission for their support.

References

1. P. DUWEZ, F. H. BROWN, and F. ODELL, *J. Electron-Chem. Soc.* 8 (1951) 356.
2. M. FOEX, *Science of Ceramics* 4 (1967) 217.
3. D. K. SMITH, *J. Amer. Ceram. Soc.* 49 (1966) 625.
4. C. WAGNER, *Naturwissen* 31 (1943) 265.
5. F. HUND, *Z. Elektrochem.* 55 (1951) 363.
6. R. E. W. CASSELTON, J. S. THORP, and D. A. WRIGHT, *Proc. Brit. Ceram. Soc.* 19 (1970) 265.
7. R. E. HEFFELFINGER, E. R. BLOSSER, and W. M. HENRY, *J. Amer. Ceram. Soc.* 47 (1964) 646.
8. J. P. LOUP, Z. MILHAILOVIC, and P. MORVAN, *C.R. Acad. Sci.* 261 (1965) 109.
9. A. WILCOCKSON and R. E. W. CASSELTON, *J. Amer. Ceram. Soc.* 53 (1970) 293.
10. J. J. MARKHAM, *S.S. Phys.* 8 (1966) 261.
11. M. CAILLET, *Rev. Int. Temp et Refract.* 5 (1968) 173.
12. R. E. W. CASSELTON, "Electricity from M.H.D." (I.A.E.A., Vienna) 5 (1968) 2951.
13. J. R. O'CONNOR and J. E. CHEN, *Phys. Rev.* 130 (1963) 1790.

Received 1 October 1971 and accepted 7 January 1972.

APPENDIX 2.

Effect of Current-Blackening on the Elastic Constants of Yttria-Stabilised Zirconia

The passage of current through yttria-stabilised zirconia in reducing atmospheres produces visual blackening and leads to an increased friability of the material which restricts its use as a refractory electrode [1, 2]. To assess the effect of current passage on the elastic properties of the material, ultrasound wave velocities have been measured in single crystal, 8 mol % yttria-stabilised zirconia before and after blackening by current passage.

For elastic wave propagation in the [1 1 0] direction of a cubic material three modes can be excited with velocities (v) and particle displacements (q) as follows:

$\rho v^2_1 = (C_{11} + C_{12} + 2C_{44})/2$; q along [1 1 0], longitudinal

$\rho v^2_{s001} = C_{44}$; q along [0 0 1], shear

$\rho v^2_{s1\bar{1}0} = (C_{11} - C_{12})/2$; q along [1 $\bar{1}$ 0], shear

Measurements of the variation of ultrasonic wave transit times with temperature were made by the pulse superposition technique [3] in a conventional cryostat system. Pulse superposition allows an accurate estimation of the variation of the transit time (Δ) with temperature since the ratio

$$\frac{\Delta(0°C)}{\Delta(T)} = \frac{prf(T)}{prf(0°C)}$$

(where $prf(T)$ denotes the repetition frequency of the pulsed rf oscillator required to give superposition of successive echoes at a temperature T) is essentially independent of the properties of the seal and transducer [3].

A crystal, oriented by the symmetry of X-ray back-reflection Laue photographs to $\pm\frac{1}{2}°$, was cut with a diamond wheel and polished to yield a sample 10 × 8 × 4.7 mm thick with faces (parallel to within 3 × 10^{-5} radians) perpendicular to the [1 1 0] axis and edges parallel to the [1 $\bar{1}$ 0] and [0 0 1] axes. Quartz X- and Y- cut transducers, 5 mm in diameter, were used to generate the ultrasound at a carrier frequency of 15 MHz. "Nonaq" stop-cock grease formed a satisfactory transducer-to-specimen seal from about 283 to 77 K. To excite each of the shear modes, the vibration direction (x-axis) of a Y-cut transducer was very carefully aligned in turn parallel to each of the requisite particle displacement directions. After measurements had been made on the crystal in the as-grown state, it was blackened by current passage in dry argon at 2.5 A/cm² and 800°C for 10 min; this treatment was sufficient to produce marked visual blackening without causing fragmentation.

In the as-grown state the velocities at 0°C calculated from the ultrasonic data are:

$v_1 = 7.05$, $v_{s001} = 3.05$, $v_{s1\bar{1}0} = 5.02$
(Units 10^5 cm/sec, accuracy, ±1%)

Comparison with the data reported previously [4] shows that in the earlier work the modes designated fast and slow were incorrectly identified and must be interchanged. This also applies to the data given for 12 mol % yttria-stabilised zirconia. When this alteration is made, the velocities from the previous and present work agree to within the experimental error of ±1%. The corrected values of the elastic constants, using the measured density of 5.99 g/cm^{-3}, are listed in table I. From these the lattice energy per mole U_0 has been recalculated, assuming ionic binding, from [4]

$$U_0 = \frac{\alpha^2 e^2 N A_{\delta_0}}{\delta_0}\left(1 - \frac{1}{n}\right)$$

Here δ_0 is the cube root of the molecular volume, A_{δ_0} is the Madelung constant (7.33058 for the fluorite lattice) and α is the largest common factor in the valencies of the ions (2 in the present instance). The repulsive exponent n can be obtained directly from the bulk modulus by

$$n = 1 + \frac{9\delta_0^4 K}{\alpha^2 e^2 A_{\delta_0}}$$

TABLE I Elastic constant data for 8 mol % yttria-stabilised zirconia. (As-grown single crystal material.)

Elastic-stiffness constants Units 10^{12} dyn cm^{-2}		Elastic-compliance constants Units 10^{-13} cm^2 dyn^{-1}	
C_{11}	3.94	s_{11}	2.78
C_{12}	0.91	s_{12}	−0.52
C_{44}	0.56	s_{44}	18.0

Bulk modulus, K Units 10^{12} dyn cm^{-2}	Anisotropy ratio
$\frac{C_{11} + 2C_{12}}{3} = 1.9$	$\frac{2C_{44}}{(C_{11} - C_{12})} = 0.37$

Cauchy relation $\frac{C_{12}}{C_{44}} = 1.6$

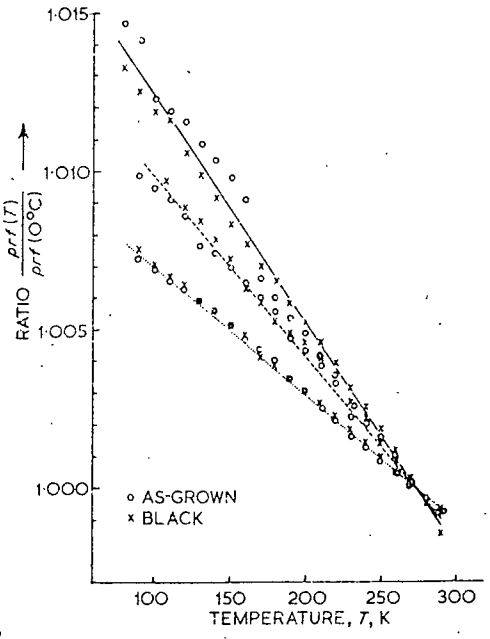

Figure 1 Comparison of temperature dependencies in as-grown and current-blackened 8 mol % YSZ single crystals. Key: open circles, as-grown; crosses, blackened Full line, shear mode with q along [001]. Chain line shear mode with q along [1$\bar{1}$0]. Dotted line, longitudinal mode.

and is 12.0 for this solid solution. The Madelung attractive energy U_M has been calculated as -2945 kcal/mol and the repulsive energy U_n as 245 kcal/mol. Thus the total binding energy $U_0 (= U_M + U_n)$ is -2700 kcal/mol. The elastic stiffness constants were also used to estimate the isotropic Young's modulus; the value obtained (2.1×10^{12} dyn cm^{-2}) can be compared with that (1.5×10^{12} dyn cm^{-2}) for polycrystalline sintered non-stabilised zirconia [5].

A comparison of results before and after blackening is made in fig. 1. It can be seen that the temperature dependencies are substantially the same. Within the experimental error the velocities are unaltered; the elastic constants in the as-grown and blackened states, and thus the lattice stabilities, are the same. This correlates with X-ray evidence [1] that the lattice parameter remains unaltered after blackening at low current densities. In the blackened crystal there was a marked deterioration of echo quality and some intermediate echoes also appeared: the blackened crystal shows the characteristics expected in an inhomogeneous material.

References

1. R. E. W. CASSELTON, J. S. THORP, and D. A. WRIGHT, *Proc. Brit. Ceram. Soc.* 19 (1970) 265.
2. R. E. W. CASSELTON, "Electricity from M.H.D." 5 (1968) 2951 (Atomic Energy Agency, Vienna).
3. H. J. MCSKIMIN and P. ANDREATCH, *J. Acoust. Soc. Amer.* 34 (1962) 609.
4. N. G. PACE, G. A. SAUNDERS, Z. SÜMENGEN, and J. S. THORP, *J. Mater. Sci.* 4 (1969) 1106.
5. S. C. CARNIGLIA, S. D. BROWN, and T. F. SCHROEDER, *J. Amer. Ceram. Soc.* 54 (1971) 13.

Received 24 November
and accepted 2 December 1971

J. M. FARLEY
J. S. THORP
J. S. ROSS
G. A. SAUNDERS
Department of Applied Physics and Electronics
University of Durham, UK

APPENDIX 3.

Use of the E.G. Nice calculator to find the setting on the magnet scale which makes the magnetic field parallel to a crystal face, when using the E.S.R. cavity mentioned in Chapter 4.

The calculator consists of a white scale calibrated in degrees running anticlockwise and a black scale calibrated in degrees running clockwise. The scales are pivoted about a common axis on which an arm is also pivoted. Two fixed cursors (D' and D") are at opposite sides of the white scale and a third (M') is at the side of the black scale. The procedure is as follows.

1. The white scale is rotated to set the first datum line position under the D' line. The scale is then adjusted to halve the angle between the D" line and the second datum line position. (This corrects for the datum line not running directly under the centre of the cavity scale).
2. The arm is rotated so that the lines at the ends are over the "crystal side positions" on the white scale. (correcting as in 1)).
3. Without moving the arm the black scale is rotated to position the broad red triangles under the arm lines.
4. The required setting on the magnet scale is then opposite the M' line.

See also A. Aypar thesis Appendix 3, page 152

APPENDIX 4.

Calculation of the principal g - values and the directions along which they apply.

In E.S.R. an experimental g - value (g_{exp}) is calculated from the formula :

$$g_{exp} = \frac{h \nu}{\beta B}$$

where h is Planck's constant, ν is the frequency of the radiation used, β is the Bohr magneton and B is the resonant field of the E.S.R. line. g_{exp} varies with the orientation of B. This is expressed in vector notation by making g a symmetrical tensor (g_{ij}). A "g^2 - tensor" can be defined by the equation

$$g^2_{ik} = g_{ij}\, g_{jk} \,. \qquad \text{(reference 41)}$$

If x,y,z is an orthogonal co-ordinate system and B lies in the xy plane at angle ϕ from the x - axis :

$$g^2_{exp} = g^2_{xx} \cos^2\phi + g^2_{yy} \sin^2\phi + g^2_{xy} \sin\phi \cos\phi$$

Hence the 6 independent components of the g^2-tensor can be found from 6 experimental g-values taken with B in the xy, yz, and zx planes, at least one value coming from one plane and two from each of the others. A transformation exists which diagonalises both the g^2-tensor and the g-tensor. The principal values of the g^2-tensor are the squares of the principal values of the g-tensor. The new set of axes correspond to the principal values. Computer program DAP 13I carries out these procedures.

FORTRAN IV G COMPILER MAIN PAGE 0001

```
   ELECTRON SPIN RESONANCE G-TENSOR.
THIS PROGRAM CALCULATES THE PRINCIPAL G-VALUES AND PRINCIPAL AXES WITH
RESPECT TO AN IMPLIED SET OF ORTHOGONAL AXES.6 EXPERIMENTAL G-VALUES ,COMING
FROM THE (100) PLANES IN THE IMPLIED AXES,ARE REQUIRED (AT LEAST 1 VALUE
COMING FROM EACH PLANE).SEE E.G.NICE THESIS PAGE 10
DATA CARD1) 6 EXPERIMENTAL VALUES (F6.4),2) CORRESPONDING 6 ANGLES BETWEEN
B AND IMPLIED AXES (F6.1),3) A 6-DIGIT NUMBER,EACH DIGIT BEING THE NUMBER OF
THE PLANE CONTAINING THE MAGNETIC FIELD FOR THE CORRESPONDING VALUE
(PLANE1=(100),2=(010),3=(001)).
USED IN CONJUNCTION WITH *SSP.
   DIMENSION AA(6,6),G(6),V(3,3),A(6),S(6),IP(6)                        0001
   READ (5,1) G,A,IP                                                    0002
 1 FORMAT (6F6.4,6F6.1,6I1)                                             0003
   WRITE (6,2) G,A,IP                                                   0004
 2 FORMAT (11X,'EXPERIMENTAL G-VALUES',6F7.4 ,/,' ANGLE BETWEEN B AND   0005
  1 CHOSEN AXES',6F7.1,/,27X,'PLANE    ',6(I1,6X))
   DO 4 I=1,6                                                           0006
   DO 4 J=1,6                                                           0007
 4 AA(I,J)=0.0                                                          0008
   DO 12 I=1,6                                                          0009
   G(I)=G(I)*G(I)                                                       0010
   A(I)=0.0174533*A(I)                                                  0011
   S(I)=SIN(A(I))                                                       0012
 3 A(I)=COS(A(I))                                                       0013
   IF (IP(I)-2) 5,6,7                                                   0014
 5 AA(I,3)=S(I)*S(I)                                                    0015
   AA(I,1)=A(I)*A(I)                                                    0016
   AA(I,2)=2.0*A(I)*S(I)                                                0017
   GO TO 12                                                             0018
 6 AA(I,6)=S(I)*S(I)                                                    0019
   AA(I,3)=A(I)*A(I)                                                    0020
   AA(I,5)=2.0*A(I)*S(I)                                                0021
   GO TO 12                                                             0022
 7 AA(I,6)=A(I)*A(I)                                                    0023
   AA(I,1)=S(I)*S(I)                                                    0024
   AA(I,4)=2.0*S(I)*A(I)                                                0025
12 CONTINUE                                                             0026
   CALL SIMQ(AA,G,6,KS)                                                 0027
   IF (KS.NE.0) GO TO 9                                                 0028
   CALL EIGEN(G,V,3,0)                                                  0029
   G(1)=SQRT(G(1))                                                      0030
   G(3)=SQRT(G(3))                                                      0031
   G(6)=SQRT(G(6))                                                      0032
   WRITE (6,8) G(1),G(3),G(6),((V(I,J),J=1,3),I=1,3)                    0033
 8 FORMAT (/,14X,'PRINCIPAL G-VALUES   ',3(4X,F7.4),//,18X,'PRINCIPAL   0034
  1 AXES    ' ,3(4X,F7.3),/,2(35X,3(4X,F7.3),/))
   GO TO 11                                                             0035
 9 WRITE (6,10)                                                         0036
10 FORMAT (' THE SIMULTANEOUS EQUATIONS ARE SINGULAR')                  0037
11 STOP                                                                 0038
   END                                                                  0039
```

TOTAL MEMORY REQUIREMENTS 00069A BYTES
EXECUTION TERMINATED

APPENDIX 5

To find the conductivity of a slice of germanium (thickness x) which filled the complete cross-section of a waveguide, the fraction (ρ) of the incident microwave power that the slice reflected and the fraction (T) that it transmitted were measured. Then r, the power reflection coefficient from the surface of the sample, was calculated from the formulae

$$r^2 \left(2^{-2\eta x} (2-\rho)\right) - r (1-e^{-\eta x}) + \rho = 0 \qquad 1$$

$$-r^2(Te^{-2\eta x} + e^{-\eta x}) + 2re^{-\eta x} + T-e^{-\eta x} = 0 \qquad 2$$

by assuming a value for η, the power attenuation coefficient. η was changed until the appropriate roots of 1 and 2 were equal. Then the conductivity (σ) of the sample was calculated from

$$\sigma = \sqrt{(\eta^2 (\eta^2 + 4 w^2 \mu_o \epsilon)/4 w^2 \mu_o^2)} \qquad 3$$

where w is 2 π # microwave frequency, μ_o is the permeability of free space and ϵ is the permittivity of the sample.

This was moderately successful when the attenuation in germanium prevented multiple reflections in the sample, but in this case simpler versions of equations 1 and 2 apply. The defect was that equations 1 and 2 really only apply to incoherent waves. Correcting for this produced a far greater increase in the complication of the method than in the reliability of the answers. Indeed in some cases negative values for η were obtained. The exercise was therefore abandoned.

APPENDIX 6

Program DAP 13P fits a set of n points (X_i, Y_i) to a curve of the type

$$Y = Ae^{Ex} + Be^{Fx}$$

as described in section 6.3 (where for the example given $x = \frac{1}{T}$) A, E, B and F are adjusted in turn by multiplying A by TA and B by TB and adding SE to E and SF to F. This procedure is repeated NCYCLE times, while TA, TB, SE and SF are modified to ensure an increasingly accurate fit. The program requires the following data

1) n and NCYCLE (format I3, I5)

2) all the Y_i (format 8E 10.3)

3) all the X_i (" " ")

4) starting values for A, E, B, F, TA, SE, TB, and SF (format 8E 10.3)

It prints out each set of A,E,B and F it tries and the best set, which it calls AM, EM, BM and FM and uses to calculate values for $Y(X_i)$ (which are listed under R), the corresponding value of $\sum_i (\ln Y(X_i) - \ln Y_i)^2$ which it calls SQMIN, and other data.

N.B. You will get more than 4 * NCYCLE lines of output; so it might be best to keep NCYCLE small and use the program a second time if the first printout shows that the sufficient convergence has not been achieved.

DAPI3P

```
ORTRAN
V G COMPILER        MAIN            08-11-72        12:18.20        PAGE 0001

0001        DIMENSION Y(100),X(100),Z(100)
0002        READ(5,1) N,NCYCLE
0003      1 FORMAT(I3,I5)
0004        WRITE(6,4) N,NCYCLE
0005      4 FORMAT('  N=',I3,'  CYCLES=',I5)
0006        READ(5,2)(Y(I),I=1,N)
0007        READ(5,2)(X(I),I=1,N)
0008        WRITE(6,6)
0009        DO 103 I=1,N
0010        WRITE(6,9) Y(I),X(I)
0011      9 FORMAT(1X,2F12.3)
0012    103 Z(I)=ALOG(Y(I))
0013      2 FORMAT(8F10.3)
0014        READ(5,3) A, E,B,F,TA,SE,TB,SF
0015      3 FORMAT(8F10.3)
0016        WRITE(6,10) A,E,B,F,TA,SE,TB,SF
0017     10 FORMAT('  A=',1PE10.3,'  E=',E10.3,'  B=',E10.3,'  F=',E10.3/'  TA
          1=',E10.3,'  SE=',E10.3,'  TB=',E10.3,'  SF=',E10.3)
0018        CALL CHECK(A,E,B,F,SUMSQ,X,Z,OLDSUM,N)
0019        SQMIN=SUMSQ
0020        DO 102 J=1,NCYCLE
0021        E=E+SE
0022        CALL CHECK(A,E,B,F,SUMSQ,X,Z,OLDSUM,N)
0023        IF (SUMSQ.GT.OLDSUM) SE=-0.5*SE
0024        IF (SUMSQ.LT.SQMIN) CALL BEST(A,E,B,F,AM,EM,BM,FM,SUMSQ,SQMIN)
0025        E=E+SE
0026        CALL CHECK(A,E,B,F,SUMSQ,X,Z,OLDSUM,N)
0027        IF (SUMSQ.GT.OLDSUM) SE=-0.5*SE
0028        IF (SUMSQ.LT.SQMIN) CALL BEST(A,E,B,F,AM,EM,BM,FM,SUMSQ,SQMIN)
0029        A=A*TA
0030        CALL CHECK(A,E,B,F,SUMSQ,X,Z,OLDSUM,N)
0031        IF (SUMSQ.GT.OLDSUM) TA=1.0/SQRT(TA)
0032        IF (SUMSQ.LT.SQMIN) CALL BEST(A,E,B,F,AM,EM,BM,FM,SUMSQ,SQMIN)
0033        B=B*TB
0034        CALL CHECK(A,E,B,F,SUMSQ,X,Z,OLDSUM,N)
0035        IF (SUMSQ.LT.SQMIN) CALL BEST(A,E,B,F,AM,EM,BM,FM,SUMSQ,SQMIN)
0036    102 IF (SUMSQ.GT.OLDSUM) TB=1.0/SQRT(TB)
0037        WRITE(6,8) AM,EM,BM,FM,SQMIN
0038      8 FORMAT('  AM=',1PE12.5,'  EM=',E12.5,'  BM=',E12.5,'  FM=',E12.5,'
          1  SQMIN=',E10.3)
0039        WRITE(6,6)
0040      6 FORMAT(8X,'Y',11X,'X',11X,'R')
0041        DO 101 I=1,N
0042        R=AM*EXP(EM*X(I))+BM*EXP(FM*X(I))
0043      5 FORMAT(1X,3E12.3)
0044    101 WRITE(6,5) Y(I),X(I),R
0045        STOP
0046        END
```

```
FORTRAN
V G COMPILER        CHECK          08-11-72        12:18.23        PAGE 0001

0001        SUBROUTINE CHECK(A,E,B,F,SUMSQ,X,Z,OLDSUM,N)
0002        DIMENSION Z(100),X(100)
0003        OLDSUM=SUMSQ
0004        SUMSQ=0.0
0005        DO 100 I=1,N
0006        R=A*EXP(E*X(I))+B*EXP(F*X(I))
0007        G=ALOG(R)
0008        S=G-Z(I)
0009   100  SUMSQ=SUMSQ+S*S
0010  1100  WRITE(6,7) A,E,B,F,SUMSQ
0011     7  FORMAT(' A=',E10.3,'  E=',E10.3,'  B=',E10.3,'  F=',E10.3,'  SUMS
           1Q=',E10.3)
0012        RETURN
0013        END

                    TOTAL MEMORY REQUIREMENTS 000324 BYTES
```

```
FORTRAN IV G COMPILER        BEST          08-11-72        12:18.24

0001          SUBROUTINE BEST(A,E,B,F,AM,EM,BM,FM,SUMSQ,SQMIN)
0002          SQMIN=SUMSQ
0003          AM=A
0004          EM=E
0005          BM=B
0006          FM=F
0007          RETURN
0008          END
```

DAP 13P' calculates Y (called, for historical reasons, R) given A, E, B, F, for NSTEP values of x increasing from XMIN in steps of STEP.

```
FORTRAN
IV G COMPILER          MAIN              08-21-72        10:56.12        PAGE 0001

0001          READ(5,1) A,E,B,F,XMIN,STEP,NSTEPS
0002        1 FORMAT(6E10.3,I10)
0003          WRITE(6,2) A,E,B,F,XMIN,STEP,NSTEPS
0004        2 FORMAT(//'  A=',1PE10.3,'  E=',E10.3,'  B=',E10.3,'  F=',E10.3/'
             1XMIN=',E10.3,'  STEP=',F10.3,'  NUMBER OF STEPS=',I3//8X,'X',11X,'
             2R')
0005          X=XMIN
0006          DO 100 I=0,NSTEPS
0007          R=A*EXP(E*X)+B*EXP(F*X)
0008   1100   WRITE(6,2) X,R
0009        3 FORMAT(1X,2E12.3)
0010    100   X=X+STEP
0011          STOP
0012          END

                    TOTAL MEMORY REQUIREMENTS 002E6 BYTES
```